Iron metabolism in the *Drosophila* mutants *fumble* and *malvolio*.

Submitted to the College of Graduate Studies and

Research in partial fulfillment of the requirements for

the

Degree of Master of Science

in the

Department of Anatomy and Cell Biology

University of Saskatchewan

Saskatoon, Saskatchewan

by

Akela Hanson

PERMISSION TO USE

In presenting this thesis in partial fulfillment of the requirements for a Postgraduate degree from the University of Saskatchewan, I agree that the Libraries of this University may make it freely available for inspection. I further agree that permission for copying of this thesis in any manner, in whole or in part, for scholarly purposes may be granted by the professor or professors who supervised my thesis work or, in their absence, by the Head of the Department or the Dean of the College in which my thesis work was done. It is understood that any copying or publication or use of this thesis or parts thereof for financial gain shall not be allowed without my written permission. It is also understood that due recognition shall be given to me and to the University of Saskatchewan in any scholarly use which may be made of any material in my thesis.

Requests for permission to copy or to make other use of material in this thesis in whole or part should be addressed to:

Head of the Department of Anatomy and Cell Biology
University of Saskatchewan
Saskatoon, Saskatchewan S7N 5E5

ABSTRACT

The *Drosophila* mutant *fumble* has a defect in mitochondrially targeted pantothenate kinase (PANK) and exhibits a movement disorder in the females. The human disease pantothenate kinase associated neurodegeneration (PKAN) has the same genetic defect and a neurodegenerative phenotype as well as iron accumulation in the brain. We have found that *fumble* females accumulate almost 2 fold more iron in the heads than wildtype. Dietary iron supplementation increases the iron accumulation in the heads further. The small isoform of malvolio (MVL), a homologue of mammalian NRAMP iron transporters, is expressed in the heads of flies. Its expression is upregulated in the *fumble* females, as well as in dietary iron supplemented wildtype flies. Unlike in the wildtype, dietary iron supplementation leads to a downregulation of MVL in the *fumble* flies. Although iron levels were elevated in *fumble*, ferritin expression was relatively unchanged and remained unchanged in the heads of *fumble* and wildtype with dietary iron supplementation.

The *Drosophila* mutant *malvolio* was used to determine how iron metabolism is affected when the MVL gene is defective. Iron levels were unchanged in *malvolio* relative to its parental strain (w1118) with or without dietary iron supplementation. Despite similar iron levels, a small decrease in ferritin expression was found in *malvolio* relative to w1118, and dietary iron increased ferritin expression in *malvolio*. However ferritin expression decreased in the parental strain of *malvolio* after iron supplementation.

Most of the iron in the *Drosophila* heads was in the form of goethite and ferrihydrite. The presence of iron oxides implies that this iron is in a mineralized storage form, likely ferritin. Dietary iron supplementation induced the appearance of ferric phosphates in *fumble*, *malvolio*, and wildtype. The subcellular location of this iron is unknown. It may be non-transferrin bound iron in the hemolymph, or a cytosolic intermediate in the labile iron pool. Also of note was the presence of transferrin-bound iron in wildtype heads on normal diet that was not seen after iron supplementation or in the heads of the fumble mutant. The presence in *fumble* of the kind of ferrihydrite characteristic of the mitochondrial protein frataxin may indicate that iron is accumulating in mitochondria.

The upregulation of MVL in the *fumble* mutant is of significant interest because it is the first protein involved in iron metabolism found to be altered with mitochondrial PANK deficiency. A disruption in MVL could be relevant to the brain iron accumulation in *fumble* and could be a treatment target for human PKAN.

ACKNOWLEDGEMENTS

I would like to thank my supervisor Dr. Helen Nichol for all the help and guidance she provided in my project. I would also like to thank all the members of the Nichol lab. I would like to thank Bogdan Popescu for help with XAS models, data acquisition and advice. I would like to thank Stephanie Roach and Carmen Mircea for taking care of my flies when I was away. I would like to thank Dr. Konstantin Ignatyev (SSRL) and Dr. Ingrid Pickering for help and advice with XAS imaging. Thanks to Dr. Graham George and Dr. Ingrid Pickering for help with EXAFSPAK and data analysis as well as training at SSRL. I would like to thank Dr. Ovsenek, Dr. Kulyk, and Dr. Harkness and their lab groups for equipment, antibodies, and advice. I would like to thank Tonya McGowen for help and advice with figures. I would like to thank Dr. Boris Dunkov (University of Arizona) for the ferritin antibodies, Dr. Ovsenek for the PCNA and GAPDH antibodies, and Dr. Kulyk for actin antibody. I would like to thank my committee members Dr. Ingrid Pickering, Dr. Nick Ovsenek, and Dr. Bernie Juurlink for thoughtful advice and ideas. Thanks to Dr. G. Boulianne (Hospital for Sick Children, Toronto) for providing wildtype flies. Thanks to Dr. G. Isaya (Mayo Clinic) for the human frataxin model and Dr. G. Brown (Stanford University) for some of the iron models used in the data analysis. Thanks to Dr. B. Hedman (SSRL), Dr. M. Adams (University of Georgia), Dr. Graham George, and Dr. Ingrid Pickering for providing model spectra. Thanks to Drs. Uwe Bergman, Katharina Luening, Sean Brennan and Konstantin Ignatyev for beamline support at SSRL. Thanks to Dr. Sam Webb for the SMAK program.

I would like to thank the Department of Anatomy and the College of Graduate Studies for scholarships and funding. I would like to thank the Saskatchewan Synchrotron Institute for travel grants. Funding for this research was provided by Saskatchewan Health Research Foundation (SHRF).

Portions of this research were carried out at Stanford Synchrotron Radiation Laboratory (SSRL), a national user facility operated by Stanford University on behalf of U.S. Department of Energy, Office of Basic Energy Sciences. The SSRL Structural Molecular Biology Program is supported by the Department of Energy, Office of Biological and Environmental Research and by the National Institutes of Health, National Center for Research Resources, Biomedical Technology Program.

TABLE OF CONTENTS

LIST OF FIGURES

LIST OF FIGURES - CONTINUED

LIST OF FIGURES - CONTINUED

LIST OF FIGURES - CONTINUED

LIST OF TABLES

LIST OF ABBREVIATIONS AND SYMBOLS

aa	amino acid
A-P	anterior-posterior
ARE	antioxidant response element
C	Celsius
CoA	coenzyme A
Dcytb	duodenal cytochrome b
DMT1	divalent metal transporter 1
DNA	deoxyribonucleic acid
D-V	dorsal-ventral
ER	endoplasmic reticulum
eV	electron volts
FBL	fumble protein
fbl	fumble gene
Fe-S	iron-sulfur
FPN1	ferroportin
g	gram
GAPDH	glyceraldehyde-3-phosphate dehydrogenase
GeV	giga electron volts
HCH	heavy chain homologue
HCP-1	heme carrier protein-1
HFE	hemochromatosis gene

HIF-1	hypoxia-inducible factor-1
HJV	hemojuvelin
HO-1	heme oxygenase-1
Hp	hephaestin
HRP	horse radish peroxidase
ICP-MS	inductively coupled plasma mass spectrometry
IDL	interactive data language
IRE	iron response element
IRP	iron regulatory protein
K	Kelvin
kDa	kilodaltons
keV	kiloelectron volts
L	liter
LCH	light chain homologue
LIP	labile iron pool
M	molar
mA	milliamps
MARE	maf-recognition element
mg	milligram
mL	milliliter
mM	millimolar
mm	millimeter
mRNA	messenger RNA

MtF	mitochondrial ferritin
MVL	malvolio protein
mvl	malvolio gene
NBIA	neurodegeneration with brain iron accumulation
ng	nanogram
NMDA	N-methyl-D-aspartic acid
nNOS	nitric oxide synthetase
NRAMP1	natural resistance associated macrophage protein 1
NRAMP2	natural resistance associated macrophage protein 2
PAGE	polyacrylamide gel electrophoresis
PANK	pantothenate kinase
PAP7	peripheral benzodiazapine receptor-associated protein
PKAN	pantothenate kinase associated neurodegeration
ppb	parts per billion
RER	rough endoplasmic reticulum
ROS	reactive oxygen species
SDS	sodium dodecyl sulfate
SMAK	Sam's microprobe analysis kit
SRC	Saskatchewan Research Council
SSRL	Stanford Synchrotron Radiation Laboratory
TBS	Tris buffered saline
Tf	transferrin
TfR	transferrin receptor

TNF-α	tumour necrosis factor-alpha
Tsf	*Drosophila* transferrins 1-3
UTR	untranslated region
V	volts
XAS	x-ray absorption spectroscopy
XRF	x-ray fluorescence
μg	microgram
μL	microliter
μM	micromolar
μm	micron

1.0 Introduction.

1.1 Iron in mammals.

Iron is an essential trace element but can also be toxic in excess. Cycling between Fe^{3+} and Fe^{2+} states of iron can result in the production of free hydroxyl radicals that can cause oxidative damage to lipids, proteins, and nucleic acids through the iron-catalyzed Fenton reaction. The Fenton reaction forms a hydroxyl radical and a hydroxyl anion through homolytic cleavage of hydrogen peroxide. This reaction cycles as the Fe^{3+} ion is reduced back to Fe^{2+} by the superoxide anion and the Fe^{2+} is there to act on H_2O_2 again (Crichton et al 2002, Winterbourn 1995). Damage to cell membranes through lipid peroxidation can lead to disruption of cell function and cell death. Iron can also cause direct oxidation of sulfhydryl compounds, ascorbic acid, and biogenic amines (Lubec 1996). Ferric iron is virtually insoluble at physiological pH and forms precipitates (Cornell 1989), but becomes soluble in the low pH of the stomach (Wienk et al 1999).

A quarter of total body iron is stored in macrophages and hepatocytes and can be used for erythropoiesis if needed. Depletion of these iron stores leads to restricted erythropoiesis and can lead to iron deficiency and anaemia, resulting in decreased transport of oxygen to tissues. Iron overload occurs when iron uptake is greater than iron usage and iron excretion. Excess iron is eventually deposited in the liver, pancreas,

heart, and pituitary gland and can cause organ dysfunction (reviewed by Ganz & Nemeth 2006).

Iron is required for many cellular functions, including energy metabolism. Heme and iron-sulfur clusters are synthesized in the mitochondria (Lill et al 1999, Lill & Kispal 2000, Ponka 1997). Iron participates in electron transfer in the mitochondria (Drysdale et al 2002). Heme is required for catalase, cytochrome p450, hemoglobin, mitochondrial complexes, cytochrome oxidases, nitric oxide synthetase, and other enzymes. Iron-sulfur clusters are part of many proteins, including iron regulatory protein, ferrochelatase, and aconitase (Lill & Muhlenhoff 2005).

1.2 Iron in neurodegeneration.

Iron has been implicated to play a role in many neurodegenerative diseases, including Parkinson's, Alzheimer's, and Huntington's among others (Asenjo 1968, Bonilla et al 1991, LeVine 1997, Youdim & Riederer 1993, Zecca et al 2004).

Neurodegeneration with brain iron accumulation (NBIA) is a family of diseases sharing iron accumulation in the brain and a neurodegenerative phenotype. NBIA is characterized by iron accumulation in the globus pallidus, dystonia, and Parkinsonism (Hayflick 2003). One type of NBIA is referred to as Pantothenate Kinase Associated Neurodegeneration (PKAN) and is caused by a mutation in PANK2, a mitochondrially targeted pantothenate kinase (PANK) (Hortnagel et al 2003, Johnson et al 2004). PANK catalyzes the rate-limiting step in coenzyme A biosynthesis and is key in

regulating CoA metabolism in mitochondria (Leonardi et al 2007, Rock et al 2000, Zhang et al 2006). It has been suggested that iron accumulates after cysteine accumulation in the mitochondria, but cysteine-iron chelates have not been identified (Zhou et al 2001). A mouse knock-out lacking PANK2 shows growth retardation, azoospermia, and retinal degeneration (Kuo et al 2005). This mouse does not show the brain iron accumulation characteristic of human PKAN, but when deprived of pantothenate it shows a movement disorder that is corrected by restoring dietary pantothenate levels to normal (Kuo et al 2007). The *Drosophila* mutant, *fumble*, also has a deficiency in PANK, and this mutant shows a movement disorder in the females (Afshar et al 2001). *Fumble* has been used to screen compounds for possible dietary supplementation strategies for human PKAN, but pantothenate did not result in an effective treatment in this mutant (Yang et al 2005).

1.3 Iron storage in mammals.

Ferritin is a polymer consisting of 24 subunits. One ferritin polymer, which is referred to as holoferritin, can store ~4500 atoms of iron as ferrihydrite and this iron is visible by electron microscopy. Ferrihydrite ($5Fe_2O_3 \cdot 9H_2O$) is a ferric oxide that is formed when ferrous iron is taken into the cavity of the ferritin polymer, oxidized to ferric iron and then converted to ferrihydrite (Harrison & Arosio 1996). Ferritin polymers with little iron stored in them are referred to as apoferritin. Most isolated ferritins contain approximately 2000 iron atoms (Crichton & Charloteaux-Wauters 1987). Storage of iron in ferritin allows for iron to remain in a soluble and non-reactive form in the cell, while it is still bioavailable if needed for cellular functions (Crichton &

Charloteaux-Wauters 1987). In mammals, most ferritin is in the cytosol, some is found in mitochondria, and a small amount is found circulating in the serum.

Ferritin polymers are made of H and L subunits (see section 1.3.1). Isoferritins are ferritin polymers isolated from specific tissues and have different H:L subunit ratios (Worwood 1990). H-subunit rich ferritins are more acidic and generally found in tissues with high iron requirements, such as heart, erythrocytes, and monocytes. L-subunit isoferritins are more basic and found in tissues used for iron storage, such as liver, spleen, and placenta (Worwood 1990). H-isoferritins take up iron faster than L-isoferritins (Wagstaff et al 1978). The H-subunit has ferroxidase activity, while the L-subunit does not catalyze iron uptake (Levi et al 1989, Levi et al 1994, Levi et al 1992).

1.3.1 Cytosolic ferritin.

The cytosolic ferritin polymer is made up of 24-subunits of 2 kinds. The H-chain subunit has ferroxidase activity that allows for conversion of ferrous iron (Fe^{2+}) to ferric iron (Fe^{3+}), while the L-chain subunits promote nucleation of ferrihydrite (Chasteen 1998, Chasteen & Harrison 1999, Drysdale et al 1991, Harrison & Arosio 1996, Lawson et al 1989, Levi et al 1994, Levi et al 1992). Expression of the H-chain and L-chain subunits is regulated at both the transcriptional and translational level. Both H and L-chain mRNA contains an iron response element (IRE), to which iron regulatory proteins (IRPs) bind to repress translation of ferritin when iron levels are low in the cell (Casey et al 1988, Caughman et al 1988, Hentze et al 1987, Mikulits et al 1997, Rouault et al 1988). Expression of the subunits is also regulated by oxidative

stress at the level of transcription. An antioxidant response element (ARE) as well as a Maf recognition element (MARE) are found in the promoter regions of both H and L chain genes of mice. These elements mediate response to oxidative stress by increasing expression of genes involved in redox homeostasis (Hintze & Theil 2005, Iwasaki et al 2006, Theil 2006, Theil 2007, Tsuji 2005). The L-chain subunit is regulated by hemin and hemin also regulates heme oxygenase 1 and β-globin, suggesting a role in cellular dioxygen metabolism (Hintze & Theil 2005). The H-chain subunit is also induced by tumor necrosis factor (TNF)-α and c-Myc. (Kwak et al 1995, Miller et al 1991, Wu et al 1999). Deletion of the H-ferritin gene is lethal in mice (Ferreira et al 2000). Mutations in L-chain ferritin are associated with neuroferritinopathy in humans. Neuroferritinopathy is an inherited neurodegenerative disease characterized by a movement disorder and low serum ferritin (Cozzi et al 2006, Crompton et al 2005, Crompton et al 2002, Curtis et al 2001, Levi et al 2005, Levi et al 1998, Mancuso et al 2005).

1.3.2. Mitochondrial ferritin.

Mammals also have a mitochondrial ferritin (MtF) that can sequester iron inside of the mitochondrial matrix. Human MtF is also important in regulating mitochondrial heme synthesis (Levi & Arosio 2004). MtF, unlike cytosolic ferritin is a 24-subunit homopolymer formed entirely of H-type subunits. These subunits assemble after cleavage of the mitochondrial-targeting peptide from the 30 kDa pre-protein. The ferroxidase activity of these subunits reduces free iron in the mitochondria and thus decreases the toxicity of iron (Levi et al 2001). The MtF sequence shares 55%

sequence identity with the L-chain subunit and 80% sequence identity with the H-chain subunit (Galatro & Puntarulo 2007). The aa residues responsible for the ferroxidase activity of H-chain are conserved in MtF (Levi & Arosio 2004).

Patients with sideroblastic anemia show high levels of MtF in erythroblasts, which is not seen in control erythroblasts suggesting MtF can be induced in diseases characterized by abnormal hemoglobin synthesis and high mitochondrial iron. Sideroblasts, abnormal erythrocytes having a ring of iron loaded mitochondria around the nucleus, expressing MtF are able to survive the stress caused by excess iron in the mitochondria (Cazzola et al 2003).

MtF has also been shown to decrease oxidative stress when overexpressed in HeLa cells, probably through sequestration of mitochondrial free iron (Drysdale et al 2002). The accumulation of toxic iron in mitochondria resulting from frataxin, a mitochondrial iron storage protein, deficiency leading to decreased respiratory activity is partially recovered in yeast expressing human MtF (Campanella et al 2004). MtF overexpression leads to cytosolic iron deficiency and induces iron uptake in cell culture (Nie et al 2005). MtF is present in neurons and spermatozoa, cells with high respiratory activity, and therefore MtF likely protects mitochondria from Fenton chemistry (Levi & Arosio 2004). There is no IRE found in the mRNA of mice or human MtF, however little is known about its regulation (Levi & Arosio 2004).

1.3.3 Serum ferritin.

Serum ferritin is used clinically to assess iron stores, but remains poorly understood. Ferritin is secreted from the liver and lymphocytes, likely derived from cytosolic H and L ferritins (Dorner et al 1980, Ghosh et al 2004, Tran et al 1997). Human serum ferritin is mostly L ferritin with some glycosylated L ferritin (G ferritin) and a small amount of H ferritin (Cragg et al 1981). Overexpression of L ferritin leads to secretion of G ferritin and L ferritin, and G ferritin is derived from L ferritin (Cazzola et al 1997, Ghosh et al 2004). Serum ferritin is secreted through the ER-Golgi pathway although no signal sequence targeting it to the ER has been found, and the mechanism of entering the secretory pathway for ferritin is not known (Ghosh et al 2004). Secretion of ferritin is inhibited during translation by an unidentified serum factor (Ghosh et al 2004).

Hyperferritinemia with cataract syndrome is caused by mutations in the IRE of L ferritin that inhibits binding of IRP to the IRE resulting in increased expression of L ferritin (Arosio et al 1999, Cazzola et al 2002, Girelli et al 1997). Symptoms include cataracts and hyperferritinemia with low serum iron, and cataracts contain ferritin crystals (Brooks et al 2002). The high level of serum ferritin is suggested to result from overexpression of L ferritin, which may or may not be glycosylated prior to its secretion (Cazzola et al 1997, Ghosh et al 2004).

1.4 Regulation of ferritin expression.

The synthesis of ferritin subunits is regulated at both DNA and mRNA levels. Once in the cell the iron can interact with RNA-binding iron regulatory proteins (IRPs) in the cytosol. When iron levels are low IRP can bind to iron response elements (IREs), hairpin structures in the untranslated regions of the mRNA (Hentze et al 1988). IRP binding of IREs in the 5'UTR blocks transcription of proteins, while binding in the 3'UTR increases mRNA stability (Koeller et al 1989, Kuhn & Hentze 1992, Theil 1993). IRP1 and IRP2 are iron biosensors. When iron is high IRP1 assembles an iron-sulfur cluster and is converted to its non-RNA-binding form so ferritin can be translated to sequester the increased iron in the cell. When iron is low in the cell the IRP1 is able to bind to mRNA and suppress translation of ferritin. IRP2 works slightly differently than IRP1. When iron is high in the cell IRP2 is ubiquinated and targeted for proteasomal degradation (Rouault 2006). IRP-IRE interactions are also influenced by growth factors, heme, and free radicals, therefore the regulation of translation through this mechanism is complex (reviewed by Theil 2000).

Heme can influence the expression of ferritin in mammals. An ARE in the promoter region of ferritin DNA decreases transcription of ferritin when bound by Bach1 and maf. Heme induces ferritin transcription by disrupting Bach1-maf-binding that occurs in the absence of heme. Heme can also affect IRE-IRP binding, heme binds to IRP1 and IRP2 changing the rate of IRP protein degradation (Goessling et al 1998, Jeong et al 2004, Theil 2006). Hemin, the oxidized form of protoporphyrin IX, induces hemoglobin synthesis in pre-erythroid cells as well as regulates the growth and differentiation of hemopoietic and non-hemopoietic cells (Tsiftsoglou et al 2006). Hemin has been shown to activate transcription of H ferritin through Ref-1-mediated

activation of the b-zip transcription factors to the ARE in mammals (Iwasaki et al 2006). Combined effects of both ARE-DNA and IRE-mRNA activation of the ferritin gene is higher than the activation by each alone (Theil 2006).

1.5 Dietary iron uptake in mammals.

1.5.1 Inorganic iron.

Before absorption, Fe^{3+} must be reduced to Fe^{2+} at the apical surface of enterocytes by ferrireductase. Originally this was attributed to duodenal cytochrome b (Dcytb) but recently the mouse knock-out has shown that it is not required for dietary iron absorption (Gunshin et al 2005b). Once in the Fe^{2+} state, iron can be taken into the cell through natural resistance associated macrophage protein 2 (NRAMP2) (Fleming et al 1997, Gunshin et al 2005a, Tandy et al 2000). NRAMP2 is a divalent metal transporter that acts as a ferrous-proton symporter, best functioning with a positive pH gradient in the direction of iron transport (Gunshin et al 1997). This transporter is required for absorption of inorganic iron in the intestine (Gunshin et al 2005a).

1.5.2 Organic iron (heme).

Heme is believed to be taken in by receptor heme carrier protein (HCP-1). Heme binds to HCP-1 in the duodenum and is internalized by receptor-mediated endocytosis, the endosomal vesicles are believed to translocate to the endoplasmic reticulum (ER) and once there, iron is released from heme by heme oxygenase-1 (HO-1)

on the surface of the reticulum (Rouault 2005, Shayeghi et al 2005). Once liberated from heme, the iron is imported by NRAMP2 into the cytosol of the enterocyte and becomes part of the intracellular labile iron pool (LIP). Little is known about the LIP, but it likely contains low molecular weight chelates and chaperone proteins (Garate & Nunez 2000, Picard et al 2000). Iron is delivered to the basolateral membrane by unknown mechanisms.

1.5.3 Iron Export.

Ferroportin (FPN1) exports Fe^{2+} through the basolateral membrane to the interstitial space, where it is oxidized to Fe^{3+} by hephaestin (Hp) (Chen et al 2003, Han & Kim 2007, Petrak & Vyoral 2005, Vulpe et al 1999). Hepcidin, an iron regulatory protein, binds to and negatively regulates FPN1, which results in its internalization and degradation (Ganz 2005, Nemeth et al 2004). FPN1 is the only known mechanism of iron efflux from mammalian cells (Ganz 2005). Extracellular Fe^{3+} is bound to transferrin (Tf), a serum iron transport protein that can hold 2 ferric iron atoms per molecule (reviewed by Hentze et al 2004).

1.5.4 Regulation of iron homeostasis.

Hepcidin is the key iron regulatory hormone in vertebrates. Hepcidin is a peptide hormone produced in the liver, circulated by plasma, and secreted in urine. Hepcidin controls iron levels by interacting directly with FPN1 when iron levels are

high (De Domenico et al 2007, Nemeth et al 2004, Oates 2007). It blocks the release of iron from macrophages, hepatocytes, and enterocytes. NRAMP2 and Dcytb are also negatively regulated by hepcidin. Hemojuvelin (HJV), transferrin receptor 2 (TfR2), and haemochromatosis gene (HFE) all affect hepcidin expression and form an intricate signaling network to control iron homeostasis (Lin et al 2005, Nemeth et al 2005). Overexpression of hepcidin leads to iron deficiency anemia, while down-regulation of hepcidin leads to iron overload (Nicolas et al 2001, Nicolas et al 2002, Viatte et al 2005, Viatte et al 2006). HFE is the gene mutated in haemochromatosis, and is known to interact with the transferrin receptor (TfR). A mutation in HFE leads to iron overload, but the role of HFE in the hepcidin-regulation of iron homeostasis remains unclear (Petrak et al 2007).

1.6 Cellular iron uptake.

1.6.1 Transferrin-dependant uptake.

The diferric-transferrin (Tf) binds the TfR and the iron is taken into the cell by receptor-mediated endocytosis (reviewed by Dunn et al 2007, Hentze et al 2004)). Acidification of the endosome frees iron from Tf (Levy et al 1999, Touret et al 2003). The iron is exported from the endosome by NRAMP2, that suggests a ferrireductase, possibly Steap3, must be present in the endosome to reduce the Fe^{3+} to Fe^{2+}. Steap3 is a ferrireductase localized to Tf-TfR1 containing endosomes (Ohgami et al 2005, Ohgami et al 2006). There may be other ferrireductases in the endosome but Steap3 is the only one found thus far (Dunn et al 2007).

In reticulocytes there is no unbound iron in the cytosol as a LIP but rather iron is directly transported from protein to protein or compartment to compartment (Sheftel et al 2007). Sheftel et al (2007) reported intracellular trafficking of iron directly from Tf-containing endosomes to the mitochondria. There are also reports of Tf-TFR-containing endosomes moving to Golgi complexes, ER, and perinuclear structures and this is likely related to iron delivery to these organelles (Maxfield & McGraw 2004, Ponka 1999). The endosome is acidified by lowering vesicular pH, done by the v-ATPase proton pump (Levy et al 1999, Touret et al 2003), then iron is transported through the endosomal membrane by NRAMP2 as Fe^{2+}, after being reduced by Steap3. It remains unknown what happens to the iron at this point, but some must be utilized or stored in the cytosol, some goes to various organelles, and most iron goes to mitochondria (Dunn et al 2007). Iron must be transported through both outer and inner mitochondrial membranes to the matrix where ferrochelatase can insert ferrous iron into the protoporphyrin IX ring so heme can be synthesized (reviewed by Dunn et al 2007). Iron transport is suggested to occur through mitoferrin, into the mitochondria where it can be used for heme synthesis and Fe-S cluster assembly (Shaw et al 2006). The presence of the LIP has been disputed in reticulocytes since iron seems to be transported directly from the endosome to the mitochondria (Sheftel et al 2007), but it is possible that there is a LIP in other cell types. It is also possible that the endosome transports iron directly to other compartments in all cells, reducing the free iron in the cytosol, and thus reducing oxidative stress.

1.6.1.1 Regulation of Transferrin-Receptor Dependant Iron Uptake.

Ferric iron binds to extracellular Tf. Diferric-Tf then binds to the TfR and is taken into the cell by receptor mediated endocytosis (reviewed by Hentze et al 2004). TfR is a homodimeric glycoprotein that binds 2 molecules of Tf (reviewed by Richardson & Ponka 1997). TfR1 is required for development, and TfR1 knockout mice die in utero (Levy et al 1999). TfR2 mutations lead to iron overload, suggesting a role in iron homeostasis. TfR1 has a higher affinity for Tf than TfR2, but both bind in a pH dependant manner (Kawabata et al 2001, Kawabata et al 1999, Trinder & Baker 2003). Acidification of the Tf-TfR containing endosome releases iron from Tf.

TfR1 contains IREs in the 3'UTR that stabilizes the mRNA when IRP is bound when cytosolic iron levels are low (Casey et al 1988, Lok & Loh 1998). By stabilizing the mRNA, more TfR1 is synthesized and cellular iron uptake is increased. TfR2 does not contain an IRE (Fleming et al 2000).

The TFR1 promoter region contains a hypoxia response element and transcription is induced by hypoxia-inducible factor-1 (HIF-1) (Kawabata et al 2001, Lok & Ponka 1999, Tong, 2002 #783). HFE competitively binds to TfR, blocking the TfR-Tf-Fe interaction (Feder et al 1998, Lebron et al 1999, West et al 2000, West et al 2001). Mutations in HFE dysregulate TfR, leading to haemochromatosis by a poorly characterized mechanism.

Mutations in TfR2 lead to non-HFE linked haemochromatosis (Camaschella et al 2000, Fleming et al 2002, Parkkila et al 2001, Roetto et al 2001). Unlike TfR1, TfR2 is not downregulated in conditions of iron overload (Fleming et al 2000). Rather, TfR2 is stabilized by binding to iron-loaded Tf. TfR2 may provide information to liver cells

on Tf saturation status so that the liver cells can regulate hepcidin expression (Johnson et al 2007).

The role of glyceraldehyde -3-phosphate dehydrogenase (GAPDH) as a novel transferrin receptor has recently been reported (Raje et al 2007). Surface GAPDH expression is modulated by iron. Iron deficient mice showed a 2.3 fold increase in liver GAPDH mRNA. *In vitro* binding assays showed a GAPDH-Tf interaction and *in vivo* assays showed co-localization and co-immuno-precipitation of GAPDH and Tf. There is no homology between GAPDH and TfR1 or TfR2. The affinity of Tf for GAPDH is 120-fold lower than for TfR1, suggesting TFR1 is the major transferrin uptake pathway, but GAPDH may function as a low affinity receptor for Tf. This study also showed the GAPDH-Tf complex traffics to the endosome, like the other TfRs (Raje et al 2007). GAPDH is speculated to be the low affinity, pronase-sensitive non-TfR dependant mechanism involved in Tf uptake previously reported by Ikuta and Trinder (Ikuta et al 2004, Raje et al 2007, Trinder et al 1996).

1.6.2 NRAMP1 and NRAMP2 iron transport.

Mammals have several iron uptake pathways. The natural resistance associated macrophage protein 2 or NRAMP2 is expressed in the plasma membrane as well as recycling endosomes of most cells (Gruenheid et al 1999). Although its original name implies that it is localized to macrophages, this was later found to be incorrect and so the transporter was renamed, divalent metal transporter 1 (DMT1). However, for the purposes of this thesis the older name has been retained.

Most cells in the body acquire iron from serum Tf through the TfR. When Tf binds to the TfR it triggers endocytosis. Acidification of the endosome releases the iron from Tf. Iron then crosses the endosomal membrane via NRAMP2 (Lam-Yuk-Tseung et al 2003, Picard et al 2000, Touret et al 2003). NRAMP2 is a proton-coupled metal uptake system that can take up Fe, Mn, Cu, and Ni (Garrick et al 2006). Some studies suggest it may transport Zn, Co, Pb, and Cd as well (Bannon 2003, Gunshin et al 1997, Okubo et al 2003, Tabuchi et al 2000). This transporter is also responsible for absorption of inorganic iron in the gut (see section 1.5.1) (Fleming et al 1997, Gunshin et al 2005a, Tandy et al 2000).

There are 4 isoforms of NRAMP2 in mammals due to alternative splicing in the 5'UTR and the 3'UTR (Hubert & Hentze 2002). An IRE is present in the 3' end that can be spliced out of the message (Canonne-Hergaux et al 2000, Canonne-Hergaux et al 2001, Gunshin et al 2001, Lee et al 1998). Of the 4 isoforms of NRAMP2, two contain an IRE (1A-IRE and 1B-IRE); isoforms 1A-non-IRE and 1B-non-IRE do not contain an IRE. The IRE containing isoform has recently been found to be targeted to late endosomes and lysosomes; while the non-IRE containing isoform has been associated with recycling endosomes (Lam-Yuk-Tseung & Gros 2006). Upregulation of the IRE containing isoform is seen in the duodenum of iron deficient animals, suggesting that the IRE in the 3'UTR promotes mRNA stability as is seen with TfR, (Canonne-Hergaux et al 1999, Gunshin et al 1997). NRAMP2 expression is therefore likely regulated by iron at both the transcriptional and translational levels (Hubert & Hentze 2002).

A mutation of one amino acid in (G185R) NRAMP2 of mice (*mk*) and rats (Belgrade) leads to microcytic anemia (Canonne-Hergaux et al 2000, Canonne-Hergaux & Gros 2002, Fleming et al 1998, Su et al 1998, Touret et al 2004). G185R mutants are unable to transfer iron from the endosome to the cytoplasm (Fleming et al 1998). This same mutation leads to Ca^{2+} transport rather than iron transport by NRAMP2 (Xu et al 2004). NRAMP2 does not usually transport calcium (Gunshin et al 1997). The use of an L-type calcium channel blocker, nifedipine, leads to mobilization of iron from the liver and increased excretion of iron by the kidneys by prolonging the activation of NRAMP2 in primary and secondary iron overload murine models, but the mechanism is not known (Ludwiczek et al 2007). An increase in dietary iron decreases NRAMP2 expression in the kidneys, probably to decrease re-uptake of iron at the brush border (Canonne-Hergaux & Gros 2002, Ferguson et al 2001, Wareing et al 2003). Recently, NRAMP2 has been found to be expressed in late endosomes/lysosomes, and is suggested to be involved in reabsorption of Tf-Fe in the proximal tubule (Abouhamed et al 2006). Plasma membrane NRAMP2 is upregulated in the liver of haemochromatosis patients and could account for non-transferrin bound iron uptake from plasma in iron overload disorders (Mackenzie et al 2006).

NRAMP2 has also been implicated in iron influx in N-methyl-D-aspartic acid (NMDA) -mediated neurotoxicity. NRAMP2 is activated through stimulation of the NMDA-receptor, which activates nitric oxide synthase (nNOS). S-nitrosylation leads to Dexras1 (a G-protein in the Ras subfamily that is induced by dexamethasone) activation which activates peripheral benzodiazepine receptor-associated protein (PAP7). PAP7

binds NRAMP2 and increases iron uptake in the neurons through this transporter (Cheah et al 2006).

Mammals also have natural resistance associated macrophage protein 1, NRAMP 1, a paralog of NRAMP2, which is expressed in the phagosomal membrane of macrophages, neutrophils, and neurons (Evans et al 2001, Forbes & Gros 2003). NRAMP1 may be capable of transport of different cations in both directions against a proton gradient (Nevo & Nelson 2006). NRAMP1 is involved in innate immunity. Mutations in NRAMP1 are associated with susceptibility to infection as well as autoimmune diseases and diabetes (Blackwell 1998, Blackwell et al 2003). In its role to fight infection, the direction of transport of NRAMP1 has been disputed. Studies suggest that NRAMP1 contributes to defense against infection by extrusion of divalent cations from the phagosome to starve microbes of iron required for growth (Jabado et al 2000). Other studies suggest that NRAMP1 transports divalent cations into the phagosome, inhibiting pathogenic growth by generating toxic hydroxyl radicals (Zwilling et al 1999).

The membrane topology and transport properties of NRAMP1 and NRAMP2 are indistinguishable, which suggests that the divalent-metal transport of NRAMP1 is mechanistically similar to that of NRAMP2 at the membrane of acidified endosomes (Forbes & Gros 2003). NRAMP1 has been localized to late endosomes and lysosomes and is a proton/divalent metal antiporter, transporting metals from the phagosome into the cytoplasm (Lam-Yuk-Tseung et al 2006). NRAMP1 may play a key role in metal ion homeostasis in the brain (Evans et al 2001). NRAMP1 is implicated in stress-induced immunosuppression. In NRAMP1 mutant mice, less corticotrophin releasing

hormone (CRH) is induced in neurons in response to stress than wildtype (Evans et al 2001). Transcription of NRAMP1 can be increased by oxidative stress and NRAMP1 expression can be protective against oxidative stress. This protective effect is suggested to be a result of NRAMP1 removing the divalent cations from the cytosolic pool (Yeung et al 2004).

1.7 Iron Metabolism in Insects.

1.7.1 Iron storage in Drosophila.

While both insects and vertebrates have three ferritin genes, there are important differences in ferritin protein targeting. *Drosophila* assembles ferritin heteropolymers in the ER, and some tissues that are suspended in the hemolymph secrete ferritin into the hemolymph. The midgut excretes ferritin with high iron into the gut lumen to compensate for iron overload somewhat by getting rid of some excess iron in the feces. The midgut secretes ferritin that is iron rich, and the fat body secretes iron poor ferritin. Holoferritin has been observed in the ER and secretory pathway in all insects surveyed so far (Nichol & Locke 1990). The presence of holoferritin in any compartment implies that iron is transported across the membrane. Little is known about intracellular iron transport in *Drosophila*. In addition to being secreted into the hemolymph, some holoferritin seems to be retained in the rough endoplasmic reticulum (RER) to act as an iron buffer. Retention or secretion of ferritin seems to be regulated by cycles of acylation that temporarily bind the protein to the lumen of the RER (Nichol & Locke 1999). No cytosolic ferritin gene has been found in the *Drosophila* genome, and

holoferritin has not been observed in the cytosol (Nichol et al 2002, Nichol & Locke 1990).

In *Drosophila*, the genes encoding the secreted subunits, Ferritin 1 Heavy Chain Homologue (Fer1HCH) and Ferritin 2 Light Chain Homologue (Fer2LCH), are closely clustered on position 99F on the third chromosome and their transcriptional regulation appears to be coordinated (Charlesworth et al 1997, Dunkov & Georgieva 1999). The Fer1HCH gene produces 2 subunits (HCH) with molecular weights of 25 and 26 kDa. The Fer2LCH gene produces the 28 kDa LCH subunit. The LCH has no IRE in the message, while the HCH subunit has an IRE in an intron that may be spliced out of or left in the message. This suggests that control of ferritin synthesis in *Drosophila* is complex and unusual (Georgieva et al 2002, Georgieva et al 1999, Lind et al 1998). Ferritins are made in the endoplasmic reticulum and can be glycosylated. The LCH subunit is larger and glycosylated, while the HCH subunit is smaller and non-glycosylated (Nichol & Locke 1999). The lack of cytosolic ferritin and the presence of secreted ferritin suggest a unique role for ferritins in iron homeostasis in *Drosophila*. Ferritin has been shown to be upregulated in oxidative stress, which suggests it has a similar antioxidant role in insects to that of mammals (Hentze & Kuhn 1996, Kwak et al 1995, Landis et al 2004, Pantopoulos et al 1997, Tsuji et al 2000, Zou et al 2000). Upregulation of ferritin in mosquitoes after blood-feeding suggests that ferritin sequesters excess iron, therefore having an antioxidant effect (Dunkov et al 2002, Geiser et al 2003, Pham et al 2005). Differential expression of both HCH and LCH subunits after infection suggest that ferritins are involved in the insect immune response (Dunkov & Georgieva 2006, Levy et al 2004, Vierstraete et al 2004). Fungal infection

was found to decrease the expression of both LCH and HCH, while bacterial infection lead to an increase in HCH expression (Levy et al 2004). An NF-κB-like binding site is present in the shared promoter region of the Fer1HCH and Fer2LCH genes of *Drosophila* suggesting it may be activated by NF-κB transcription factors which are involved in the insect immune response (Dunkov & Georgieva 1999, Kappler et al 1993).

The LCH subunit of *Drosophila* is very similar to that of other insect LCH, but has a very low degree of similarity to human H and L chains. The LCH subunit is designated LCH because it lacks the ferroxidase center residues of vertebrate H chain. All LCH proteins in insects known so far lack the glutamate residues of vertebrate L chain which are thought to be involved in nucleation of the crystalline iron oxyhydroxide mineral core (Chasteen & Harrison 1999, Dunkov & Georgieva 2006, Georgieva et al 2002). The LCH subunit predominates in all life stages in the Oregon R strain of *Drosophila* suggesting LCH is important in these flies (Georgieva et al 2002).

Ferritin in adults consists of almost exclusively LCH subunits, and occurs abundantly in the hemolymph and ovaries. Iron feeding dramatically increases the amount of ferritin in the gut, but has a lesser effect in other tissues. Since insect ferritins store large amounts of iron, it is likely that at least one HCH subunit is present in each polymer.

Drosophila has a homologue of mitochondrial ferritin as well, Ferritin 3 Heavy Chain Homologue (Fer3HCH). Similar to mammalian MtF, Fer3HCH is expressed

mainly in the testis (Drysdale et al 2002, Missirlis et al 2006). The residues responsible for the ferroxidase activity of ferritin are conserved in Fer3HCH (Missirlis et al 2006). Over-expression of Fer3HCH in *Drosophila* does not affect total body iron or levels of LCH and HCH subunits (Missirlis et al 2006). Overexpression of Fer3HCH decreases viability of female flies when raised under iron deficient conditions, suggesting that this protein may sequester iron in mitochondria at the expense of other cellular functions (Missirlis et al 2006). This was not seen in male flies, suggesting that females have a higher iron requirement than males. Since ferritin is expressed in the ovary, iron is likely sequestered in eggs and the iron is lost when eggs are laid. This is similar to effects of overexpression of MtF in HeLa cells; iron is sequestered in the MtF and leads to cytosolic iron depletion (Corsi et al 2002, Nie et al 2005). The Fer3HCH was localized to mitochondria using an epitope-tagged version in transfected cells (Missirlis et al 2006).

1.7.2 Regulation of ferritin expression.

When put on an iron-rich diet, ferritin synthesis is strongly increased, especially in the midgut, and holoferritin is seen in the Golgi complex (Nichol & Locke 1990). This allows for excretion of iron-loaded ferritin into the gut lumen. Regulation of ferritin synthesis in *Drosophila* is under transcriptional control as well as translational control (Dunkov & Georgieva 1999). IREs have been found in *Drosophila* mRNA of HCH and aconitases (Charlesworth et al 1997, Gray et al 1996, Muckenthaler et al 1998). *Drosophila melanogaster* has 2 homologues of IRP1 (IRP1A and IRP1B), but

no homologue of IRP2 (Muckenthaler et al 1998). Only IRP1A can bind to IREs, although both homologs have aconitase activity (Lind et al 2006). Regulation of protein expression by IRE/IRP was previously discussed (see section 1.4).

In vertebrates, it is proposed that increasing ferritin expression is the first line of defense against chemically induced oxidative stress. Oxidants induce the transcription of both H and L chain (Theil 2007, Tsuji et al 2000) and this would decrease free iron in the cell to limit oxidative stress. In *Drosophila*, iron treatment induces expression of both HCH and LCH messages and subunits. HCH has 4 isoforms, one containing an IRE in an intron that may be spliced out of the message (Lind et al 1998). LCH does not have an IRE and is not regulated at the level of translation by iron levels in the cell. A 2-fold larger increase in LCH message levels than in LCH protein levels in both larvae and adults fed on iron supplemented diet compared to control insects was observed by Georgieva et al (Georgieva et al 2002). This may be due to transcription and translation becoming uncoupled when iron levels are high. Since LCH subunits are already abundant, the message level increase caused by gene activation by iron does not lead to LCH subunit synthesis (Georgieva et al 2002). The lack of change in LCH expression is more likely due to secretion of ferritin into the hemolymph and excretion of ferritin into the gut lumen. There is no evidence of an IRE in Fer3HCH, the mitochondrially targeted *Drosophila* ferritin.

1.7.3 Iron Transport in Drosophila.

The *Drosophila* homologue of NRAMP1 and NRAMP2 is *malvolio (mvl)* (Folwell et al 2006, Rodrigues et al 1995). NRAMP iron transport has been previously discussed (see section 1.6.2). Localization of *mvl* expression was determined with beta-galactosidase reporter gene assay and expression was seen in both the peripheral and central nervous system as well as some cells of the haematopoietic system, mainly macrophages (Rodrigues et al 1995). In recent findings, expression of *mvl* was observed in macrophage-like cells, malpighian tubules, testis, brain, amnioserosa of embryos, and the alimentary canal by immunolocalization (Folwell et al 2006). The expression in malpighian tubules suggests involvement in divalent cation reabsorption, similar to the proposed role of NRAMP2 in iron re-uptake at the brush border of the kidney. Expression in the alimentary canal suggests the possibility of an IRE to modulate function and a role in dietary iron uptake, like NRAMP2 in the duodenum (Folwell et al 2006). There is no evidence of an IRE in *mvl* (see section 1.10), but insect IREs are found in non-canonical positions in the 5'UTR of ferritins (Nichol & Winzerling 2002).

Drosophila differs from mammals in that it only has a single copy of the NRAMP gene family. This could mean that *mvl* is a bifunctional NRAMP gene (Folwell et al 2006, Nevo & Nelson 2006). The effect of dietary iron supplementation on *mvl* expression would be of significant interest because it could show a similar function to that of NRAMP2 for iron uptake in the gut. Since NRAMP1 transcription is induced by oxidative stress (Yeung et al 2004), it is possible that *mvl* transcription could

be induced by reactive oxygen species (ROS) generated in the Fenton reaction, after iron loading, rather than by IRP translational control.

Deficiency in *mvl* results in abnormal taste perception that can be corrected by supplementing the diet with $FeCl_2$ or $MnCl_2$ (Orgad et al 1998). MVL is expressed in and may be responsible for iron uptake in both the brain and the gut. For further discussion of *malvolio* see section 1.10.

1.7.4 Transferrin in Drosophila.

The structure and function of transferrins and ferritins have been conserved between insects and mammals during evolution (Dunkov & Georgieva 2006). *Drosophila* Tf messages are upregulated during infection, possibly to sequester iron from invading pathogens. The Tf message is not detectable in embryos. Iron loading of *Drosophila* decreases the message levels of Tf, unlike iron loading in mammals which does not affect Tf message levels (Basclain & Jeffrey 1999, McKnight et al 1980a, McKnight et al 1980b, Tuil et al 1985, Yoshiga et al 1999). If Tf is involved in iron transport in *Drosophila*, Tf could be down-regulated under high iron conditions to reduce transport of iron to tissues (Nichol et al 2002, Yoshiga et al 1999).

Drosophila Tfs differ from mammalian Tfs in that there is a loss of iron-binding capacity in the C-terminal half of the molecule (Dunkov & Georgieva 2006). The insect Tfs only bind 1 atom of ferric iron, rather than 2 atoms that are bound by mammalian Tf

(Dunkov & Georgieva 2006, Yoshiga et al 1999). Insect Tfs are proposed to play a role in iron transport and also act as an antibiotic agents by with-holding iron from invading pathogens (Nichol et al 2002). *Drosophila* has three Tfs. Tsf1 is abundant in the hemolymph while Tsf2 and Tsf3 are similar to mammalian melanotransferrin, and have a GPi anchor (Dunkov & Georgieva 2006). Vertebrate melanotransferrin does not require a TfR to take up iron, and instead it is taken into the cell by a non-specific process, adsorptive pinocytosis (Dunkov & Georgieva 2006, Food & Richardson 2002, Food et al 2002, Richardson 2000, Yang et al 2004).

Since no TfR has been found in *Drosophila*, the importance of Tf in iron transport to tissues has been questioned (Nichol et al 2002). Recent findings show that GAPDH binds Tf in macrophages. GAPDH does not resemble TFR1 orTFR2, so previous attempts to find homologous sequences in the *Drosophila* may not have recognized novel transferrin receptors (Raje et al 2007). The role of GAPDH as a TfR has not been established in *Drosophila*, but a homologue to GAPDH is present in the fly.

This project looks at the role of MVL, an iron transporter expressed in neurons, in the *Drosophila* mutant *fumble*, which is a model for the human disease PKAN. Iron accumulation in the brain is associated with PKAN, and *fumble* has the same genetic defect as the human disease.

1.8 Using Drosophila to study neurodegeneration.

Cross-species comparisons indicate that more than half of all known human disease genes have homologues in the *Drosophila* genome. *Drosophila* is an ideal system for dissecting the normal functions of genes associated with neurodegenerative disease due to the high degree of evolutionary conservation, ease of generating mutant or transgenic animals, and minimal genetic redundancy. *Drosophila* offers the power of rapid genetic analysis with a generation time 10 times less than mice, flexible ectopic expression, and the ability to perform large-scale mutagenesis screens not yet possible in mammals (Shulman et al 2003). Researchers can create "knock-out" mutants, as well as transgenic mutants and have the ability to regulate expression in specific tissues and at specific times. This allows researchers to develop a series of mutant alleles with a spectrum of severities to study the consequences of varying levels of gene function. The simplicity of the *Drosophila* genome often allows single counterparts of a mammalian gene family to be studied without the complications of genetic redundancy resulting from duplications that have arisen through vertebrate evolution (Restifo 2005). Some mechanisms of neurodegeneration have been shown to be conserved in the fly and could potentially provide mechanistic insight that forms the basis for eventual treatments for human disease. We use two classical *Drosophila* mutants, *fumble* and *malvolio*, to examine the effects of these mutations on expression of proteins involved in iron uptake and storage in the heads of *Drosophila*.

1.9 Background of the fumble mutant.

The *fumble* mutant was selected as a male sterility mutant (Castrillon et al 1993). *Fumble* (*fbl*) codes for the *Drosophila* homologue of PANK which catalyzes the rate-

limiting step in Coenzyme A biosynthesis. The *Drosophila* mutant *fumble* is a hypomorphic mutant with deficient PANK function. Homozygous males are sterile, and heterozygous females (*fbl*/TM6B) are uncoordinated having impaired ability to climb, mate, and fly. FBL has been shown to be required for proper meiosis and mitosis. PANK plays an essential role in both meiosis and mitosis and has a critical function for membrane assembly in cell division (Afshar et al 2001). This is likely due to the shortage of phospholipids since Coenzyme A is required for their synthesis (Afshar et al 2001). As in the fly, mouse PANK2 knock-out males are sterile (Kuo et al 2005).

A ClustalW alignment of amino acid sequences of FBL-PE, the fumble polypeptide isoform E, with that of human PANK2, mouse PANK, and *Arabidopsis* PANK (Figure1a) shows that both the human and *Drosophila* sequences have expansions at the N termini that are not present in *Arabidopsis* and mouse. The N-terminus of human PANK2 has been shown to have a mitochondrial signal sequence while the N-terminus of FBL is predicted to be targeted to mitochondria by MitoProt (Expasy tools) (Claros 1995, Claros & Vincens 1996). However this common function is not reflected in sequence identity in the N termini because mitochondrial signal sequences are diverse (Truscott et al 2003). Those regions of the protein with highest identity between *Drosophila* and human are also highly conserved in the mouse and *Arabidopsis.* *Arabidopsis* and *Drosophila* have a C terminal extension that is conserved between insect and plant. FBL has the greatest overall amino acid identity with mouse (54.6%) and human (53.0%) but also shares 35.6% of amino acids with plants (Figure 1 b). Phylogenetic analysis using percent identity shows the human and mouse PANK

Figure 1: a) ClustalW alignment of amino acid sequences for *Drosophila* FBL (Genbank accession number AAF34653), human PANK2 (AAN32907), mouse PANK2 (AAI06185), and *Arabidopsis* PANK (NP_176247). Amino acid residues identical to FBL are shaded in yellow.

Figure 1a

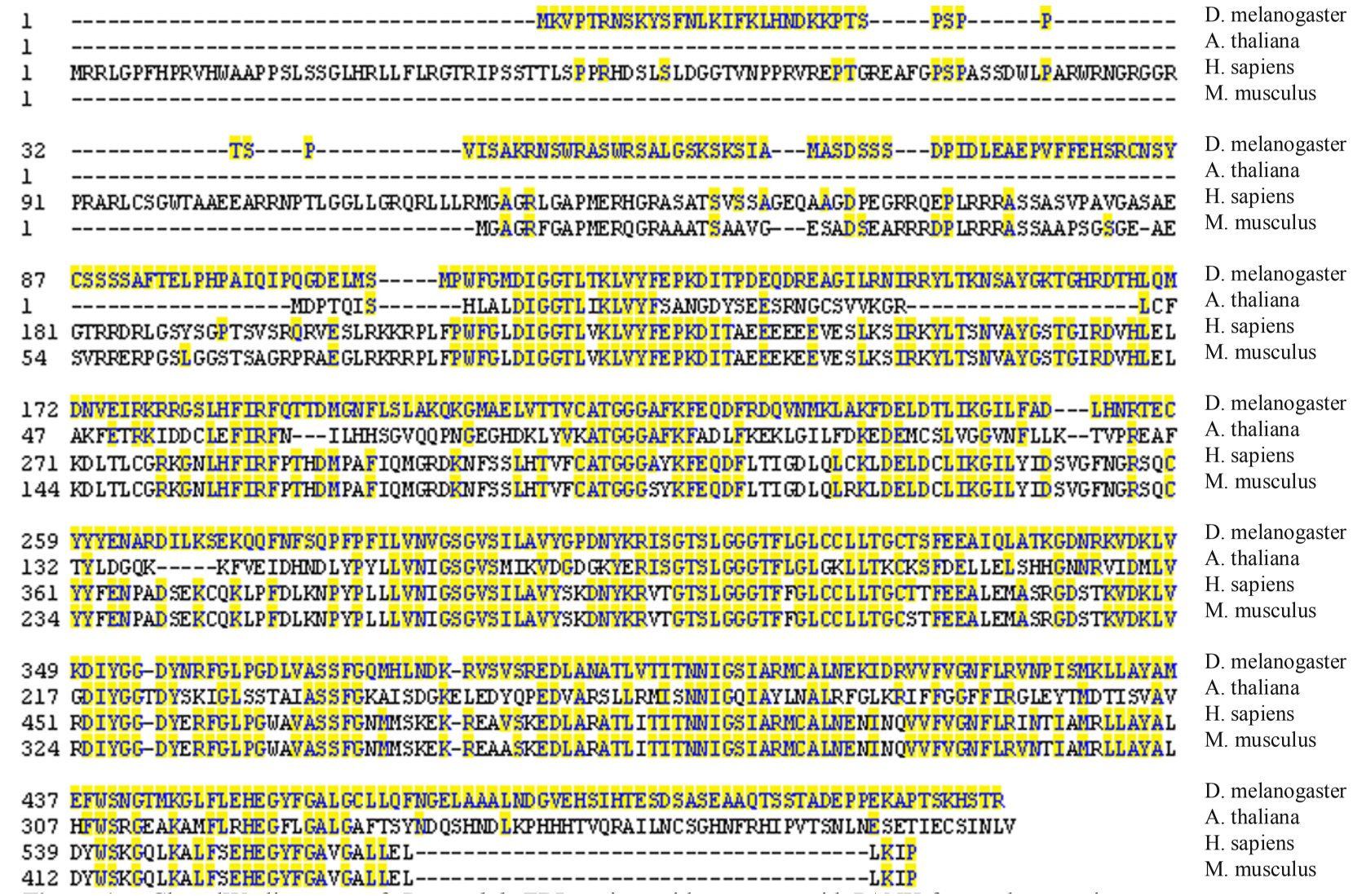
1 ----------MKVPTRNSKYSFNLKIFKLHNDKKPTS-----PSP------P---------- D. melanogaster
1 ---------- A. thaliana
1 MRRLGPFHPRVHWAAPPSLSSGLHRLLFLRGTRIPSSTTLSPPRHDSLSLDGGTVNPPRVREPTGREAFGPSPASSDWLPARWRNGRGGR H. sapiens
1 ---------- M. musculus
32 ----------TS----P----------VISAKRNSWRASWRSALGSKSKSIA---MASDSSS---DPIDLEAEPVFFEHSRCNSY D. melanogaster
1 ---------- A. thaliana
91 PRARLCSGWTAAEEARRNPTLGGLLGRQRLLLRMGAGRLGAPMERHGRASATSVSSAGEQAAGDPEGRRQEPLRRRASSASVPAVGASAE H. sapiens
1 ----------MGAGRFGAPMERQGRAAATSAAVG---ESADSEARRRDPLRRRASSAAPSGSGE-AE M. musculus
87 CSSSSAFTELPHPAIQIPQGDELMS-----MPWFGMDIGGTLTKLVYFEPKDITPDEQDREAGILRNIRRYLTKNSAYGKTGHRDTHLQM D. melanogaster
1 ----------MDPTQIS-------HLALDIGGTLIKLVYFSANGDYSEESRNGCSVVKGR----------LCF A. thaliana
181 GTRRDRLGSYSGPTSVSRQRVESLRKKRPLFPWFGLDIGGTLVKLVYFEPKDITAEEEEEEVESLKSIRKYLTSNVAYGSTGIRDVHLEL H. sapiens
54 SVRRERPGSLGGSTSAGRPRAEGLRKRRPLFPWFGLDIGGTLVKLVYFEPKDITAEEEKEEVESLKSIRKYLTSNVAYGSTGIRDVHLEL M. musculus
172 DNVEIRKRRGSLHFIRFQTTDMGNFLSLAKQKGMAELVTTVCATGGGAFKFEQDFRDQVNMKLAKFDELDTLIKGILFAD---LHNRTEC D. melanogaster
47 AKFETRKIDDCLEFIRFN---ILHHSGVQQPNGEGHDKLYVKATGGGAFKFADLFKEKLGILFDKEDEMCSLVGGVNFLLK--TVPREAF A. thaliana
271 KDLTLCGRKGNLHFIRFPTHDMPAFIQMGRDKNFSSLHTVFCATGGGAYKFEQDFLTIGDLQLCKLDELDCLIKGILYIDSVGFNGRSQC H. sapiens
144 KDLTLCGRKGNLHFIRFPTHDMPAFIQMGRDKNFSSLHTVFCATGGGSYKFEQDFLTIGDLQLRKLDELDCLIKGILYIDSVGFNGRSQC M. musculus
259 YYYENARDILKSEKQQFNFSQPFPFILVNVGSGVSILAVYGPDNYKRISGTSLGGGTFLGLCCLLTGCTSFEEAIQLATKGDNRKVDKLV D. melanogaster
132 TYLDGQK-----KFVEIDHNDLYPYLLVNIGSGVSMIKVDGDGKYERISGTSLGGGTFLGLGKLLTKCKSFDELLELSHHGNNRVIDMLV A. thaliana
361 YYFENPADSEKCQKLPFDLKNPYPLLLVNIGSGVSILAVYSKDNYKRVTGTSLGGGTFFGLCCLLTGCTTFEEALEMASRGDSTKVDKLV H. sapiens
234 YYFENPADSEKCQKLPFDLKNPYPLLLVNIGSGVSILAVYSKDNYKRVTGTSLGGGTFFGLCCLLTGCSTFEEALEMASRGDSTKVDKLV M. musculus
349 KDIYGG-DYNRFGLPGDLVASSFGQMHLNDK-RVSVSREDLANATLVTITNNIGSIARMCALNEKIDRVVFVGNFLRVNPISMKLLAYAM D. melanogaster
217 GDIYGGTDYSKIGLSSTAIASSFGKAISDGKELEDYQPEDVARSLLRMISNNIGQIAYLNALRFGLKRIFFGGFFIRGLEYTMDTISVAV A. thaliana
451 RDIYGG-DYERFGLPGWAVASSFGNMMSKEK-REAVSKEDLARATLITITNNIGSIARMCALNENINQVVFVGNFLRIMTIAMRLLAYAL H. sapiens
324 RDIYGG-DYERFGLPGWAVASSFGNMMSKEK-REAASKEDLARATLITITNNIGSIARMCALNENINQVVFVGNFLRVMTIAMRLLAYAL M. musculus
437 EFWSNGTMKGLFLEHEGYFGALGCLLQFNGELAAALNDGVEHSIHTESDSASEAAQTSSTADEPPEKAPTSKHSTR D. melanogaster
307 HFWSRGEAKAMFLRHEGFLGALGAFTSYNDQSHNDLKPHHHTVQRAILNCSGHNFRHIPVTSNLNESETIECSINLV A. thaliana
539 DYWSKGQLKALFSEHEGYFGAVGALLEL----------LKIP H. sapiens
412 DYWSKGQLKALFSEHEGYFGAVGALLEL----------LKIP M. musculus

Figure 1: b) Percent identity of each pair of amino acid sequences based on alignment in 1 a). See 1 a) for accession numbers. c) The phylogenetic relationship between the aligned sequences. Scale shows approximate number of amino acid substitutions. See 1(a) for accession numbers.

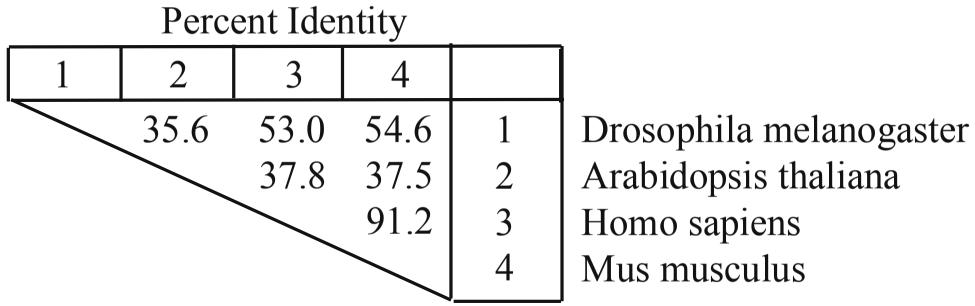

Figure 1b

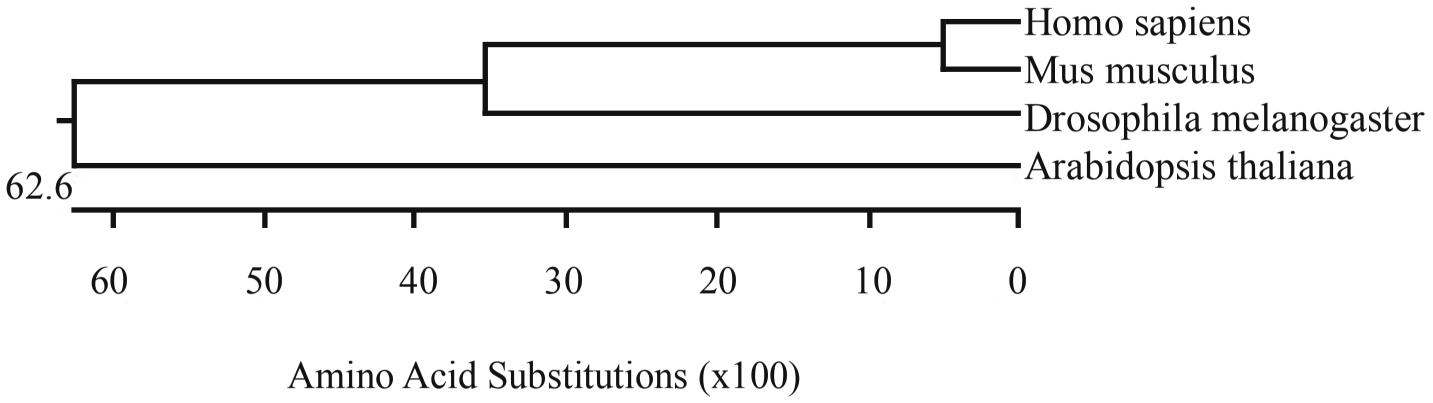

Figure 1c

sequences are most closely related, as would be expected. FBL is more closely related to mammalian than to plant PANK (Figure 1c), as would be expected.

The *fbl* gene is located on the 3L chromosome arm between 77B9 and 77C1. *Drosophila* has only one copy of the *fbl* gene. Alternative splicing results in 5 different transcripts and polypeptides (Figure 1 d). The longest polypeptide, fbl-PE, is the only one predicted to be targeted to mitochondria (Yang et al 2005). The *fumble* mutant has a P-element insertion in the 5' flanking region upstream of the transcription start site as determined by Southern blot analysis and sequence analysis of cDNAs (Afshar et al 2001).

The human disease PKAN is caused by a defective gene that encodes hPANK2, that is localized to mitochondria (Hortnagel et al 2003). This gene is located on chromosome 20. The disease is characterized by accumulation of iron in the brain and neurodegeneration. It has been suggested that iron accumulation occurs due to a build-up of cysteine in the mitochondria (Zhou et al 2001). The affected pathway in Coenzyme A biosynthesis is conserved in humans and *Drosophila* (Yang et al 2005). The *fumble* mutant has been used as a model to screen dietary treatments for the human PKAN (Yang et al 2005) with limited success. Since the *fumble* mutant has a similar genetic defect to that found in human PKAN, as well as a phenotype showing a movement disorder in the female, we sought to determine how iron transport and storage are affected in the fly.

Figure 1: d) Physical Map of *fbl* transcripts and polypeptides. Alternative splicing results in 5 different transcripts (shown in blue). Fbl-RA is 1866 nt, Fbl-RB is 1908 nt, Fbl-RC is 1634 nt, Fbl-RD is 1541 nt, and Fbl-RE is 2502 nt. The blue boxes show positions of exons and the lines between show introns. The polypeptides, shown in green, are Fbl-PA is 419 aa with a predicted molecular weight of 46.5 kDa, Fbl-PB is 417 aa with a predicted molecular weight of 46.3 kDa, Fbl-PC and Fbl-PD are identical and 401 aa with a predicted molecular weight of 44.5 kDa, and Fbl-PE is 512 aa with a predicted molecular weight of 56.7 kDa.

Figure 1d

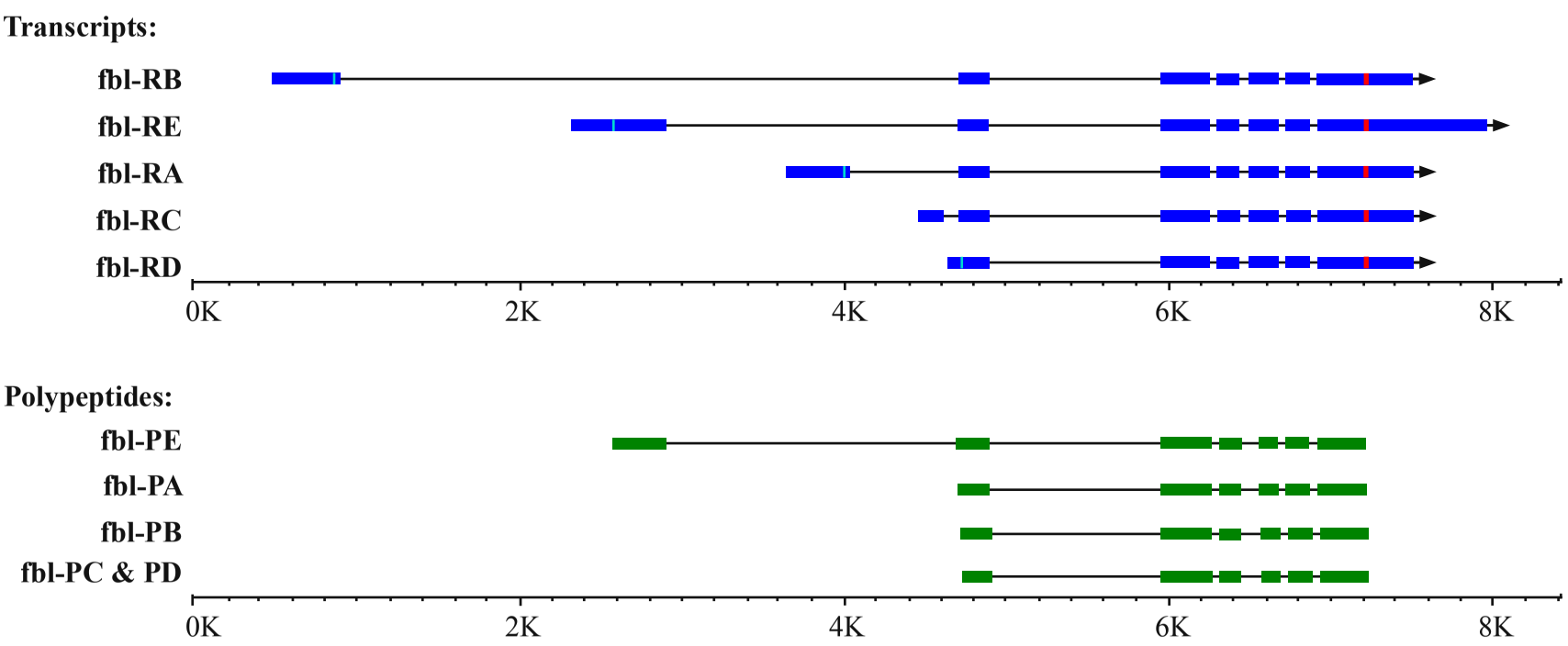

* Figure adapted from *fbl* gene annotation on flybase.

1.10 Background of the malvolio mutant.

The *malvolio* (*mvl*) mutant was found in a screen of mutations that affect taste perception in *Drosophila*. The Mvl^{97f} mutation is a loss of function mutation. Both heterozygous and homozygous *malvolio* mutants show abnormal taste behaviour, a reduced preference for sugars and an increased acceptance of sodium chloride. Homozygotes show a significantly stronger phenotype. Reporter enzyme β-galactosidase assays revealed that *mvl* is expressed in the peripheral and central nervous system, as well as macrophages (Rodrigues et al 1995). Electrophysiological responses of peripheral neurons of the *malvolio* mutant are normal, suggesting this defective taste response is due to defects at the level of information processing rather than the reception of stimulus (Rodrigues et al 1995). *Mvl* is expressed in neurons and macrophages in *Drosophila*, similar to NRAMP1 expression in neurons and macrophages in mammals, suggesting MVL is homologous to NRAMP1 (Evans et al 2001). Dietary supplementation with $FeCl_2$ and $MnCl_2$ suppresses this defective taste behaviour in *malvolio* (Orgad et al 1998), suggesting that MVL functions as a metal transporter and that Mn^{2+} and Fe^{2+} are involved in signal transduction in taste perception in *Drosophila*. The phenotype is corrected after only 2 hours on $FeCl_2$ or $MnCl_2$ supplemented diet, indicating that these ions are not required for the development of the nervous system components involved in taste perception (Orgad et al 1998). The taste defect was also corrected by expression of human NRAMP1 in the *malvolio* mutant (D'Souza et al 1999). Recently, immunolocalisation has revealed MVL expression in malpighian tubules, testis, brain, amnioserosa of embryos, and gut (Folwell et al 2006). Expression in the malpighian tubules suggests involvement in re-

absorption of divalent metals, similar to NRAMP2 function at the brush border of the kidneys in mammals. Another significant finding is MVL expression in the gut of both larvae and adults, suggesting an analogous mechanism for divalent cation uptake from the gut lumen in both flies and mammals (Folwell et al 2006). MVL is also expressed in the fat body where it may participate in iron uptake, storage, and release to the hemolymph (Folwell et al 2006). It has been suggested that MVL may be a bifunctional NRAMP that serves as both NRAMP1 and NRAMP2 in *Drosophila* (Nevo & Nelson 2006). We sought to determine whether iron uptake and storage are altered in the head of the *malvolio* mutant to provide insights into the function of MVL in iron transport in the brain.

The *mvl* gene is found on the 3R chromosome arm. The P(*w*+-*lacZ*) transposon is inserted 313 base pairs upstream of the translational start site within the transcribed, non-translated region of the *mvl* transcription unit (Rodrigues et al 1995). A ClustalW alignment of MVL amino acid sequence with human NRAMP1, mouse NRAMP1, *Arabidopsis* NRAMP, and *Dictyostelium* NRAMP shows residues identical to MVL (Figure 2a). Only one residue substitution is present in the 'binding protein-dependent transport system inner membrane component signature' sequence motif between MVL and human-NRAMP1 (aa 396-415 in MVL). This motif is proposed to lie on the fifth cytoplasmic face of the membrane and mediates interaction between ATP binding subunits serving a role in energy coupling (Rodrigues et al 1995). The motif is identical between human and mouse NRAMP1. The amino terminal domain of MVL does not have any classical signal sequences ((Rodrigues et al 1995) whereas in mammalian NRAMP1, signal sequences are found that target this membrane protein to the

endoplasmic reticulum (Figure 2a). MVL shares 54.6% of amino acids with mouse and 54.5% with human, but shares only 35.9% of amino acids with *Arabidopsis* and 46.3% with *Dictyostelium* (Figure 2 b). Phylogenetic analysis showed that human and mouse NRAMP1 are the most closely related, and MVL is more closely related to the mammalian than the plant NRAMP proteins (Figure 2c). Alternative splicing of the MVL mRNA results in 3 different transcripts and polypeptides (Figure 2d). The UTR of the *mvl* mRNA do not contain the consensus CAGUG of an IRE; there is no evidence that MVL is regulated at the translational level by iron (data not shown).

Figure 2: a) ClustalW alignment of amino acid sequences for *Drosophila* MVL (Genbank accession number AAF55839), human NRAMP1 (AAG15405), mouse NRAMP1 (AAB35205), *Dictyostelium* NRAMP (EAL68988) and *Arabidopsis* NRAMP (AAF36535). Amino acid residues identical to MVL are shaded in yellow. The thick line indicates the 'binding protein-dependent inner membrane component signature' motif.

Figure 2a

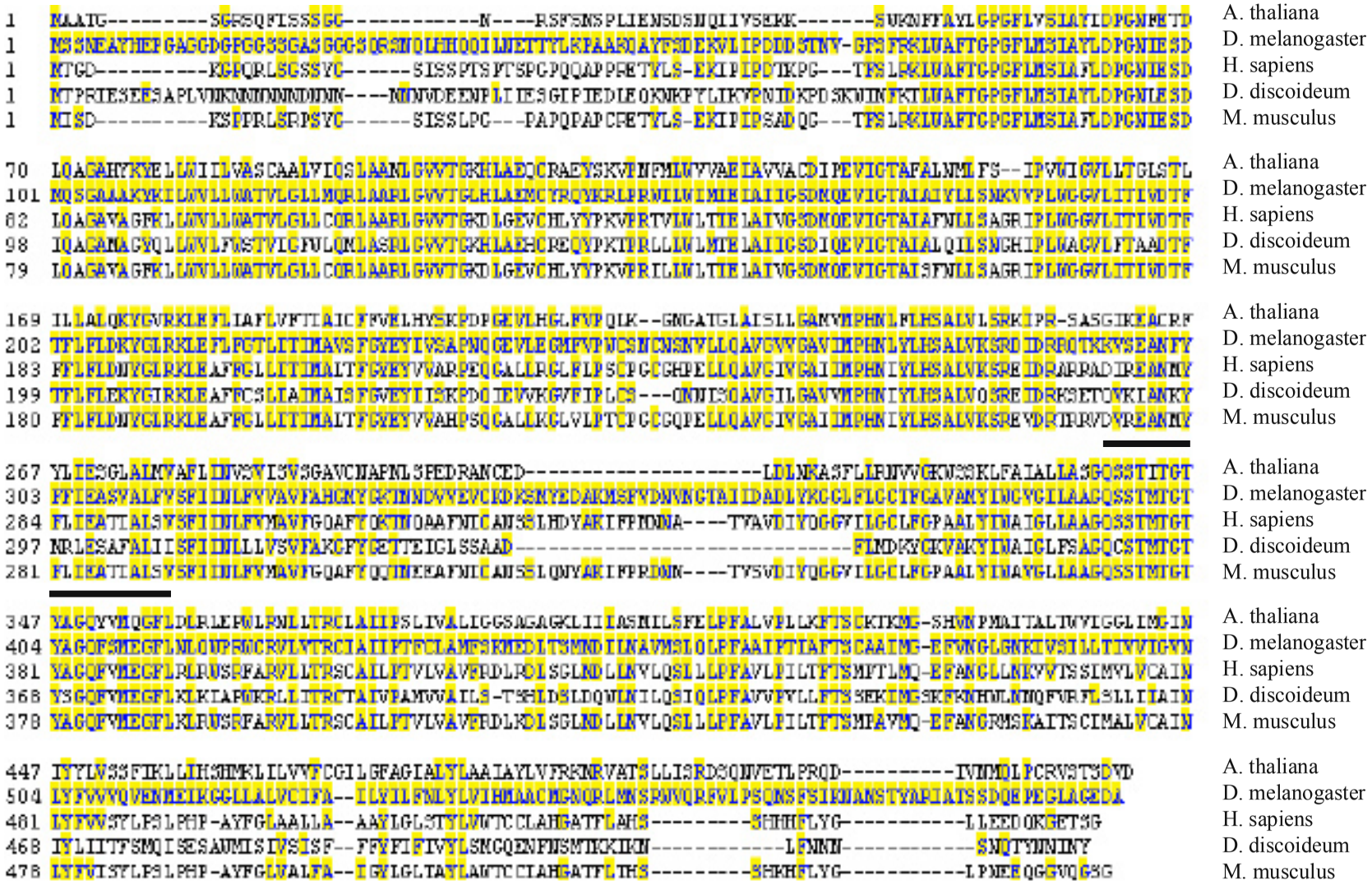
A. thaliana
D. melanogaster
H. sapiens
D. discoideum
M. musculus

Figure 2: b) Percent identity of each pair of amino acid sequences based on alignment in 2 a). See 2(a) for accession numbers. c) The phylogenetic relationship between the aligned sequences. Scale shows approximate number of amino acid substitutions. See 2 a) for accession numbers.

Percent Identity

1	2	3	4	5		
	35.9	37.7	37.3	36.3	1	Arabidopsis thaliana
		54.5	46.3	54.6	2	Drosophila melanogaster
			45.8	87.4	3	Homo sapiens
				46.9	4	Dictyostelium discoideum
					5	Mus musculus

Figure 2b

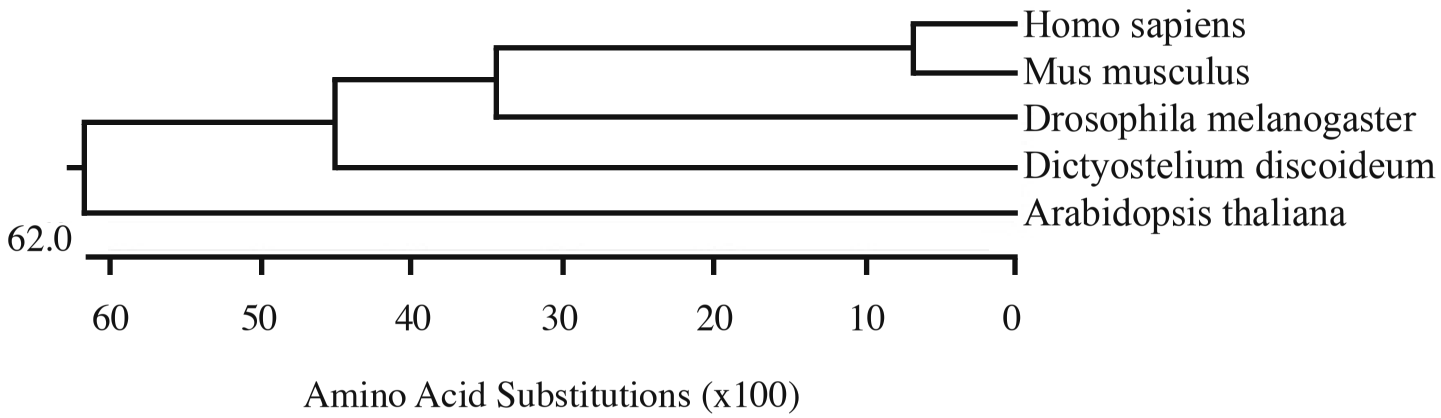

Figure 2c

Figure 2: d) Physical map of *mvl* transcripts and polypeptides. Alternative splicing results in 3 transcripts (shown in blue). Mvl-RA is 2795 nt, Mvl-RB is 2424 nt, and Mvl-RC is 2157 nt. The blue boxes show position of exons and the lines between show introns. The resulting polypeptides are shown in green. Mvl-PA and Mvl-PB are 596 aa with a predicted molecular weight of 65.5 kDa. Mvl-PC is 486 aa with a predicted molecular weight of 53.3 kDa.

Figure 2d

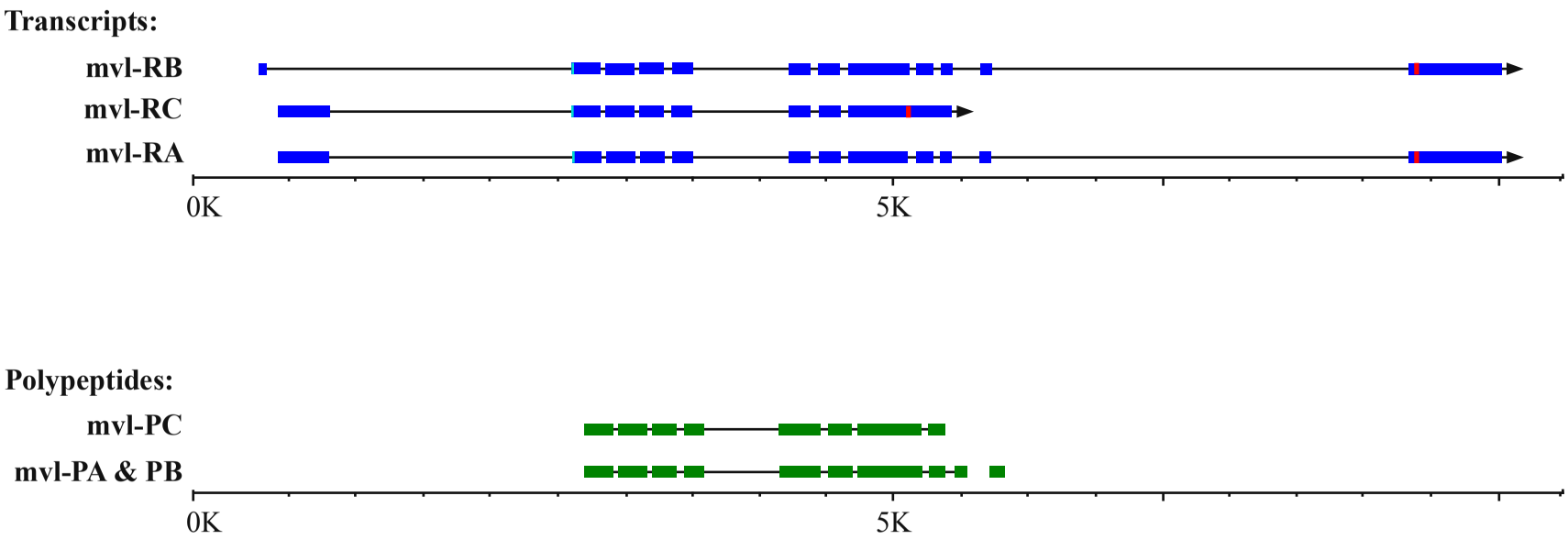

* Figure adapted from *mvl* gene annotation on flybase.

2. Research Objectives and Hypotheses.

2.1 Hypotheses.

The expression of proteins involved in iron uptake and storage are altered in the heads of the *Drosophila* mutants *fumble* and *malvolio*. Dietary iron supplementation will alter the expression of proteins involved in iron uptake and storage in the heads of *Drosophila* mutants and wildtype.

2.2 Research Objectives.

1. Quantify iron in the heads of *Drosophila* and determine if sufficient iron is present for x-ray absorption spectroscopy.
2. Determine if the *malvolio* or *fumble* mutants have altered iron levels in heads.
3. Determine how dietary iron supplementation affects iron levels in the heads of mutants and their respective wildtypes.
4. Determine the chemical form of iron in the heads of the *malvolio* and *fumble* mutants that have altered expression of the MVL and PANK respectively.
5. Determine if dietary iron supplementation affects the chemical form of iron in the heads of *malvolio* and *fumble* mutants and their respective wildtypes.
6. Determine if the mutations or iron supplementation affect the localization of iron in the heads.

7. Determine if the expression of ferritin or MVL protein is altered in the heads of the *fumble* mutant relative to wildtype.
8. Determine if the expression of ferritin protein is altered in the heads of the *malvolio* mutant relative to wildtype.
9. Determine if elevated dietary iron alters the expression of ferritin or MVL protein in the heads of wildtype.
10. Determine if elevated dietary iron alters the expression of ferritin protein in the heads of the *malvolio* mutant.
11. Determine if elevated dietary iron alters the expression of ferritin or MVL protein in the heads of the *fumble* mutant.

3. Materials and Methods.

3.1 Drosophila care.

Drosophila were fed on a standard *Drosophila* diet (9.3 g Bacto Agar (VWR), 61.2 g cornmeal (Purity), 0.7 M anhydrous dextrose (EM Science), 32.4 g yeast (Fleishmann's Traditional Active dry yeast), in 1L of water. The diet was heated to boiling, cooled and 10 mL/ L of 10% Tegosept (Apex) was added. This diet was estimated to contain 50 μM iron based upon data from the United States Department of Agriculture foodstuffs database. Ferric chloride was used to supplement the diet. ICP-MS analysis confirmed that the iron supplemented diet contained about 60 μM iron. This is very close to the iron content of other *Drosophila* diets (Massie et al 1985). Iron supplementation at 20% above that found in the normal diet was judged to be within the normal physiological range of dietary iron to which flies might normally be exposed. Based on previous work by Massie et al (Massie et al 1985, Massie et al 1993) this level of iron should not have a significant effect on lifespan. Flies were reared at a constant temperature of 25° C on a 12 hour day-night cycle. Oregon R, the parental strain of *fumble* and w1118, the parental strain of *malvolio* were kind gifts from G. Boulianne, (Hospital for Sick Children, Toronto). The classical mutants *mvl* 5151 (w[1118];P{w[+mC]=lacW}Mvl97f), and *fbl* 11777 (P{ry[+t7.2]=PZ}fbl[1]

ry[506]/TM3, ry[RK]Sb[1]Ser[1]) were obtained from the Bloomington *Drosophila* Stock Center.

3.2 Sequence Alignment.

Multiple sequence alignments were performed using the ClustalW method (Megalign program, Lasergene 7.1, DNASTAR, Inc.) using the Gonnet series protein weight matrix (Gonnet et al 1994). Percent identity values of each sequence pair were compared directly without accounting for phylogenetic relationships. The phylogenetic tree shows predicted evolutionary relationships based on the ClustalW sequence alignment. The length of each pair of branches represents the distance between sequence pairs, while the units at the bottom of the tree indicate the number of substitution events. Below the tree is a scale indicating the number of "Amino Acid Substitutions" per 100 residues. Megalign uses the Kimura (Kimura 1980) distance formula to calculate distance values, derived from the number of non-gap mismatches and corrected for silent substitutions. The values computed are the mean number of differences per site and the mean falls between 0 and 1. Zero represents complete identity and 1 represents no identity. The phylogenetic tree scale uses these values multiplied by 100 (Lasergene 7.1).

3.3 Inductively Coupled Plasma Mass Spectrometry (ICP-MS).

Flies were anesthetized with CO_2 and kept cold on ice. Flies were sorted into male and female and then decapitated using titanium forceps. Heads were counted and

put into pre-weighed borosilicate glass vials (VWR) and the wet weight of the heads was determined. For each sample 25 heads were completely digested with 200 μL of concentrated high purity nitric acid (EM Sciences) at room temperature. ICP-MS was carried out at the Saskatchewan Research Council (SRC) Analytical Laboratories using an Agilent 7500C ICP-MS. Internal standards used were Sc, Ge, Y, Cs, and Bi. All samples were diluted to 10 mL with 0.2% HNO_3 before analysis. Approximately 4 mL of sample was used per run. Iron was analyzed in hydrogen mode to minimize interference. Iron standards of 250 ppb and 500 ppb as well as a nitric acid blank were used to calibrate. Uptake time was 35 seconds, stabilization time was 25 seconds, washout time was 35 seconds, and integration time was 0.3 seconds/mass with 3 repeats on each mass. Every tenth sample was run in duplicate. A 10 μg/L standard was run every 10 samples and read back within 10% of true value to ensure accuracy. The limit of detection for iron is 0.02 mg/L. These data are accurate to ±20%. Iron concentrations were calculated based on the wet weight of tissue.

3.4 Antibodies.

Polyclonal antibodies to human NRAMP1 were raised in rabbit against a 17 aa highly conserved peptide sequence (Alpha Diagnostics International). This sequence is from 316-332 aa in the 550 aa human NRAMP1 sequence and corresponds to EC4 of the protein. This portion is 25% identical and 82% similar to MVL based on ClustalW alignment.

Polyclonal rabbit antibodies to *Drosophila* ferritin were a gift from Dr. Boris Dunkov, University of Arizona. Ferritin antigen was purified from D. melanogaster (Canton S strain) larvae raised on an iron-rich diet (Georgieva et al 2002).

Mouse monoclonal antibodies to chicken actin (JLA20) were obtained from Developmental Studies Hybridoma Bank, University of Iowa.

HRP linked secondary anti-rabbit and anti-mouse antibodies were from Biorad.

3.5 Gel Electrophoresis and Western Blotting

3.5.1 Sample preparation.

Flies were anesthetized with CO_2; females were decapitated on ice using forceps. Whole heads of female flies were homogenized in 2X sample buffer containing protease inhibitor (1% SDS, 4% 2-mercaptoethanol, 24% glycerol , 0.4 mM Pefabloc SC (Roche Applied Science), 0.1M Tris-HCl, pH 6.8). Samples were sonicated (10 pulses, Sonifer® Cell Disruptor Model W140, Heat Systems – Ultrasonic, Inc.) then boiled for 10 minutes. Samples were centrifuged for 10 minutes at 12,000 x g and the supernatant transferred to fresh tubes. Centrifugation was repeated 3 times.

3.5.2 Gel electrophoresis.

Sodium dodecyl sulfate polyacrylamide gel electrophoresis (SDS-PAGE) was using the method originally described by Laemmli (Laemmli 1970) with the following modifications. Samples were loaded on 4-15% precast gradient gels (Biorad). These gels differ from those of Laemmli in that SDS is not included in the separating gel or stacking gel. SDS is included in the running buffer (25 mM Tris, 192 mM glycine, 0.1% SDS) in addition to the sample buffer (above). Polypeptides were separated for 2 hours at 110 V.

3.5.3 Western blotting.

Immunoblotting was performed using the method of Towbin et al (1979) with the following modifications. Gels were equilibrated for 15 minutes in transfer buffer (25 mM Tris, 192 mM glycine, 20% methanol) and transferred to nitrocellulose (Pall Life Sciences) membrane using the Biorad wet transfer apparatus for 2 hours at 80V with cooling. Membranes were stained with Ponceau S to monitor protein transfer, washed with Tris-buffered saline (TBS) (20 mM Tris-HCl, pH 7.5, 0.5 M NaCl), and then blocked in blocking solution (5% skim milk (Carnation), 0.1% Tween-20 (EM Science) in TBS) for 3 hours. Primary NRAMP1 antibody was used at a dilution of 1:3000 in blocking solution. Primary ferritin antibody was used at a dilution of 1:2000. Membranes were incubated with primary antibodies overnight at 4° C with rocking. Membranes were washed 3 times in blocking solution for 5, 15, and 5 minutes. Secondary goat anti-rabbit-HRP (Biorad) was used at a dilution of 1:4000 and incubated at room temperature for 90 minutes with rocking. Membrane was washed 3 times in blocking solution for 5, 15, and 5 minutes, then washed in TBS containing 0.1% Tween

for 15 minutes followed by a 5 minute wash in TBS. HRP-bound proteins were detected using a chemiluminescence kit (PerkinElmer Life Sciences, Inc.) and x-ray film (Kodak Biomax XAR). After detection, membranes were immersed in an antibody stripping solution (2% SDS, 25mM glycine pH 2) for 30 minutes at room temperature with rocking. Stripped membranes were washed in TBS 3 times for 10 minutes each then blocked in blocking solution for 3 hours. Primary actin antibody was used at a dilution of 1:500 and membranes were incubated for 2 hours at room temperature. Membranes were washed 3 times, 5 minutes each in blocking solution then incubated with secondary anti-mouse-HRP (Biorad) at a dilution of 1:3000 for 90 minutes at room temperature. Membranes were washed 3 times, 5 minutes each in skim milk blocking solution, once in TBS-0.1% Tween for 5 minutes, and once in TBS for 5 minutes. HRP-bound proteins were detected as above. Proteins were quantified using NIH ImageJ software. MVL and ferritin expression was normalized to actin and averaged over 4 independent replicates.

3.6 X-ray Absorption Spectroscopy (XAS).

XAS is a tool that can provide information about the chemical form of a metal in a sample without causing damage. Each element has an absorption edge at a different energy, and thus XAS is element specific. The x-ray beam is scanned over a short range of energies and an absorption spectrum is collected. When the energy specific to iron is reached, a core electron absorbs the x-ray and the electron is ejected. In K-edge fluorescence, the 1s core electron is ejected and a 2p electron moves into its place and an x-ray fluorescent photon is emitted. The energy of the photon emitted is element specific

and the near-edge structure (XANES) of the spectra gives insight to coordination of the molecule. The fluorescence photons are counted by a detector and the number of photons at each energy yields the spectrum. The sample spectrum can then be fitted with edges of model compounds to determine what chemical form of iron makes up the sample (reviewed by Koningsberger & Prins 1988, Lytle 1989).

3.6.1 X-ray Absorption Near Edge Structure (XANES)

3.6.1.1 Sample Preparation for XAS

Flies were chilled then decapitated on ice using titanium forceps. Female and male whole heads were mixed and tightly packed into the center of 1mm path length Lucite sample cells and flash frozen in isopentane chilled with liquid nitrogen. Samples were stored and transported to the Stanford Synchrotron Radiation Laboratory (SSRL) in liquid nitrogen. Iron model compounds were prepared for transmittance measurements by grinding each with boron nitride and pressing it in a 2 mm thick sample holder between Mylar. Protein model compounds were prepared in 20% glycerol and loaded in Lucite sample cells. Dry bovine hemin (Sigma) and human met-hemoglobin (SIGMA) were dissolved in 20% glycerol and used as saturated solutions. Iron loaded human frataxin was a gift from Dr. G. Isaya. Horse spleen holoferritin was obtained from Sigma. The frataxin model has a less ordered ferrihydrite core, while the ferritin has a highly ordered ferrihydrite core (Nichol et al 2003).

3.6.1.2 Bulk XAS

Data from whole heads was acquired on the SPEAR 3 storage ring (85-100 mA at 3.0 GeV) on beamlines 9-3 and 10-2 each equipped with a Silicon (220) double-crystal monochromator. Data from some model compounds were collected on beamline 2-3 and beamline 7-3 with the SPEAR 2 storage ring. The incident and transmitted X-ray intensities were monitored using N_2-filled ionization chambers. The Fe K X-ray absorption near edge spectra of heads were recorded as Kα fluorescence excitation spectra using a 30-element germanium detector. The X-ray energy was calibrated with reference to the lowest K-edge energy inflection point of a metallic iron foil, the energy of which was assumed to be 7111.3 eV. Harmonic rejection was accomplished on beamline 9-3 using an upstream vertical collimating Rh-coated mirror and downstream re-focusing Rh-coated mirror. This was done on beamline 10-2 by detuning one monochromator crystal to approximately 50% off peak. Four sweeps were collected for each sample. In order to reduce X-ray damage, samples were maintained between 5 and 10 K in a liquid helium flow cryostat (Oxford instruments), and each sample was exposed to X-rays for about 1 hour.

3.6.1.3 XAS Data Analysis.

Data analysis was performed using the EXAFSPAK suite of computer programs. Quantitative determination of the different chemical forms of iron present was carried out by least-squares fitting of the near-edge spectra to linear combinations of the spectra of

standards, as previously described (Pickering et al 1998). A library of 21 model compounds was used to fit all of the near edges (Table 1). In this type of analysis the inclusion of the spectrum of a particular compound in a fit is an indication of the presence of a class of species, rather than the presence of the particular compound from which the spectrum was obtained. No smoothing or related data manipulations were performed. Figure 3 shows iron K-edge spectra of model compounds used in the fit of the samples.

3.6.2 Microprobe X-ray Fluorescence Imaging (micro-XRF).

Micro-XRF data collection was done on beamline 6-2 (rear hutch) on the SPEAR 3 storage ring (85-100 mA and 3.0 GeV) at SSRL. Fly heads were imaged using a microprobe with a 10 or 15 micron spot size. This spot size was achieved using Kirkpatrick-Baez mirrors. Flies were decapitated and heads mounted between Mylar on a cardboard frame (for dorsal-posterior view) or whole flies were mounted on a fine quartz capillary (anterior-posterior view). The beam was in a fixed position and the sample was moved in a raster pattern in steps with a count time of 1 or 2 seconds/pixel. The incident energy was set at 10 000 eV. Both scatter and iron K_α fluorescence was collected using a 13-element germanium detector located at 90 ° to the incident beam. Images were produced using interactive data language (IDL) software and the iron was normalized to scatter to account for thickness effects.

3.6.3 Rapid scanning X-ray fluorescence imaging (macro-XRF).

Table 1: Chemical formulas and coordination of model compounds used for near-edge fitting. Models found in the fit are bolded.

Model compounds and metalloproteins	Chemical formula	Coordination
Fe (III)		
1. Holoferritin (*E. callabus*, spleen)	FeOOH	6O
2. Frataxin (*H. sapiens*)	FeOOH	6O
3. Goethite	FeOOH	6O
4. Ferric sulfate	$Fe_2(SO_4)_3$	6O
5. Ferric pyrophosphate	$Fe_4(P_2O_7)_3$	4O
6. Ferric phosphate	$FePO_4$	4O
7. Ferric citrate	$FeC_6H_5O_7$	3O
8. Heme (*H. sapiens*, met-hemoglobin)		5N
9. Hemin (*B. taurus*)		4N, 1Cl
10. Cytochrome c (*B. taurus*)		4N
11. Transferrin (*H. sapiens*)		4N, 2O
12. Frataxin holopolymer (*S. cerevisiae*)	FeOOH	6O
Iron-sulfur cluster		
13. Ferredoxin - oxidized (*Anabaena sp.*)	$[Fe_2\text{-}S_2(SR)_2]^{2-}$	4S
14. Rubredoxin – oxidized (*P. furiosus*)	$[Fe(SR)_4]^{1-}$	4S
15. Iron regulatory protein – oxidized (*M. sexta*)	$[Fe_3\text{-}S_4]^{+}$	4S
16. Rubredoxin – reduced (P. furiosus)	$[Fe(SR)_4]^{2-}$	4S
17. Ferredoxin – reduced (*Anabaena sp.*)	$[Fe_2(SR)_4]^{3-}$	4S
18. Ferrochelatase (*S. cerevisiae*)	$[Fe_2\text{-}S_2]^{+}$	2S
Fe (II)		
19. Ferrous sulfide	FeS	1S
20. Ferrous ammonium sulfate hexahydrate	$[Fe(H_2O)_6](NH_4)_2(SO_4)_2$	6O
21. Ferrous hexaimidazole dichloride	$[Fe(imidazole)_6]Cl_2$	6N

* Spectra from the listed compounds are used in the fit to represent a general class or category of compound rather than of the particular species from which the spectrum was obtained.

Figure 3: Iron K-edge spectra of model compounds used to fit data, (a) holoferritin (*Equus callabus* spleen), (b) frataxin (*Homo sapiens*), (c) goethite, (d) ferric pyrophosphate, (e) ferric phosphate, (f) hemin (*Bos taurus*), (g) transferrin (*Homo sapiens*), (h) rubredoxin – reduced (*Pyrococcus furiosus*), (i) ferrochelatase (*Saccharomyces cerevisiae*), (j) ferrous ammonium sulfate.

Figure 3

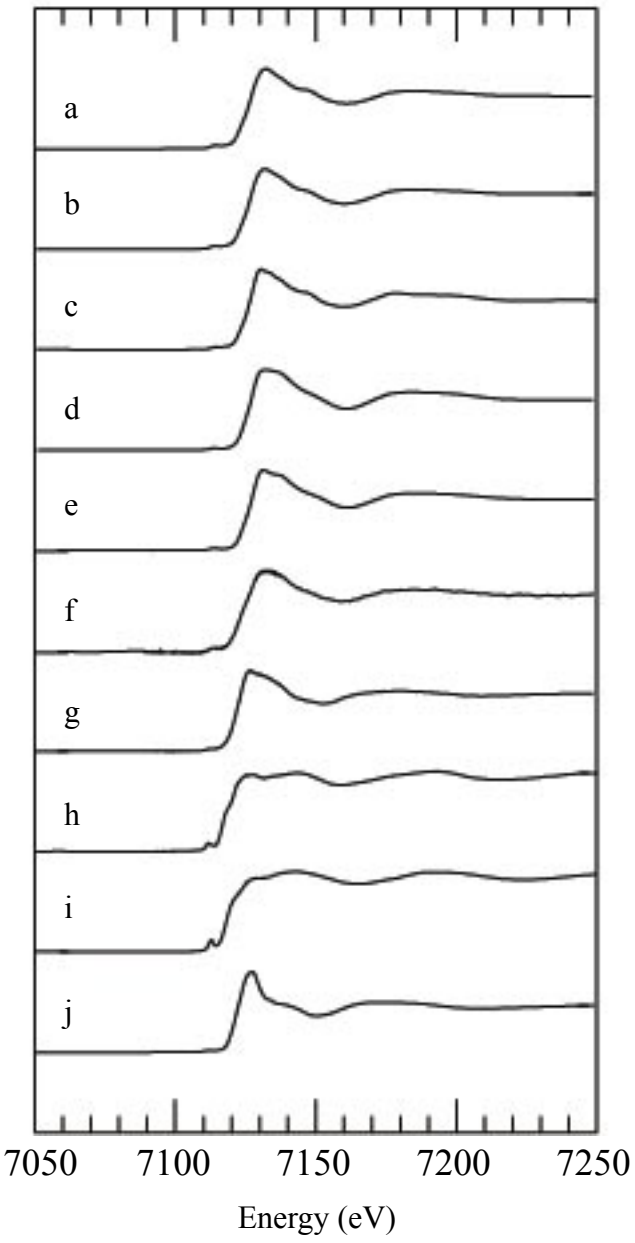

Data from whole flies was acquired on the SPEAR 3 storage ring (85-100 mA at 3.0 GeV) at SSRL. Imaging was done on beamline 6-2 front hutch which is equipped with a Si (111) double crystal monochromator. Whole flies were mounted between metal-free Mylar on a cardboard frame and mounted vertically at a 45 ^{o} angle to the incident beam. Samples were rapidly translated in a raster pattern in continuous collection mode using a count time of 200 msec/pixel. The incident energy was set at 11 keV to excite elements below arsenic. Energy windows were set up to collect K_{α} fluorescence from manganese, iron, copper and zinc using a 13-element germanium detector. The pixel size was measured on a test object and found to be 40 x 40 microns. Since the sample was at a 45 ^{o} angle to the incident beam, a rectangular aperture was used that produced a 40 micron square spot at the sample. Images were normalized using Sam's Microprobe Analysis Kit program (SMAK) written by Dr. Sam Webb, SSRL. Only data for iron is shown.

4.0 Results.

4.1 Rationale for elemental analysis.

Pooled samples of 25 whole adult heads were weighed and dissolved in 200 µL of acid. Heads were used in these studies because the head has a greater ratio of tissue to hemolymph than the body and contamination by dietary iron is less of a factor when the gut is not included. We are also interested in the role of iron in neurodegenerative disease and both MVL and FBL are expressed in neurons. The iron content as determined by ICP-MS has an intrinsic error of +/- 20% (personal communication, SRC laboratories) and values were consistent within each batch but not consistent between batches. The average wet weight of 25 heads was 2.3 mg. Iron ranged from 40 - 200 ng iron/mg wet weight. The amount of iron found in the fly heads was sufficient for bulk XAS. Similar samples in the same batch were compared using ng iron/mg of wet weight and are expressed as fold difference (Figure 4, 7, 9).

4.2 Iron levels in heads of fumble mutant relative to wildtype.

FBL is a PANK that when mutated in humans causes PKAN, a neurodegenerative disorder characterized by massive brain iron overload. The biochemical pathways linking iron metabolism with CoA metabolism are not well understood. If *fumble* is a

model for human PKAN it may exhibit brain iron overload. Males may be more affected than females since females lose iron during egg production. Average iron levels in male or female heads of *fumble* were compared with the parental strain (Oregon R). In both sexes, iron levels in the heads were higher in *fumble* flies than in Oregon R wildtype flies when both were fed on normal diet. The female *fumble* flies had nearly 2 fold more iron than wildtype flies while male *fumble* had 1.6 fold more iron than wildtype (Figure 4 a, b). Female wildtype had 105 ng/mg of iron and *fumble* had 200 ng/mg of iron. Male wildtype had 55 ng/mg of iron and male *fumble* had 85 ng/mg of iron. Female flies had a more severe iron overload in the head than males. Since females lose iron during egg production, this suggests iron uptake in *fumble* females must be much higher than in males, at least in the head.

The increase in iron seen in *fumble* relative to its parental strain was large and a two-fold change in iron is expected to be visible by synchrotron imaging. We therefore compared the quantity and location of iron by XRF mapping of iron for female wildtype compared to *fumble* (Figure 5). The *fumble* fly accumulated iron in the posterior thorax and the head. This agrees with the ICP-MS data that *fumble* accumulates iron in the head. The iron fluorescence image of male wildtype and *fumble* flies fed on normal diet showed more iron in the abdomen of the *fumble* than wildtype (Figure 6). No visible difference was apparent in the heads of *fumble* males.

4.3 Effect of elevated dietary iron on iron levels in fumble heads.

Figure 4: *Fumble* has higher iron levels in the head relative to wildtype (Oregon R) when both are reared on a normal diet. Iron levels in whole adult heads measured by ICP-MS are expressed as the fold difference of *fumble* relative to wildtype. (a) Females; (b) Males. The 1.8 fold difference between *fumble* and Ore R females exceeds the intrinsic error of ICP-MS. The 1.5 fold difference between *fumble* and Ore R males exceeds the intrinsic error of ICP-MS.

Figure 4

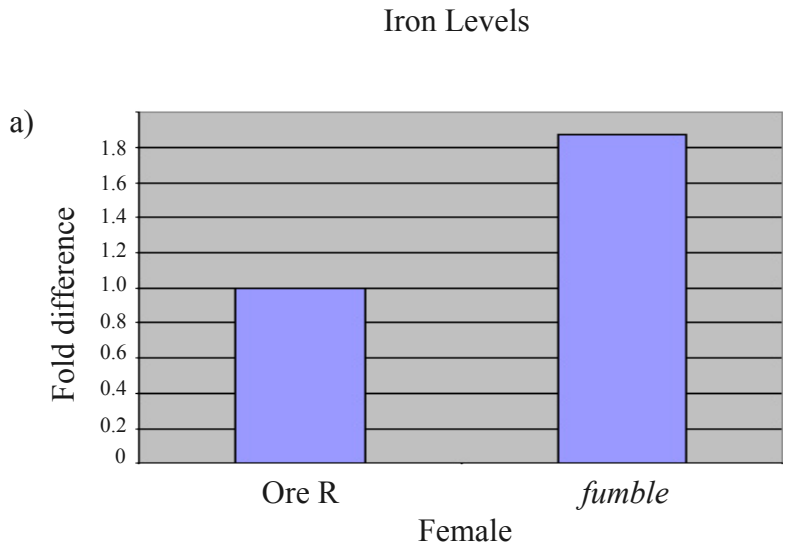
Iron Levels
a)
Fold difference
1.8
1.6
1.4
1.2
1.0
0.8
0.6
0.4
0.2
0
Ore R
fumble
Female

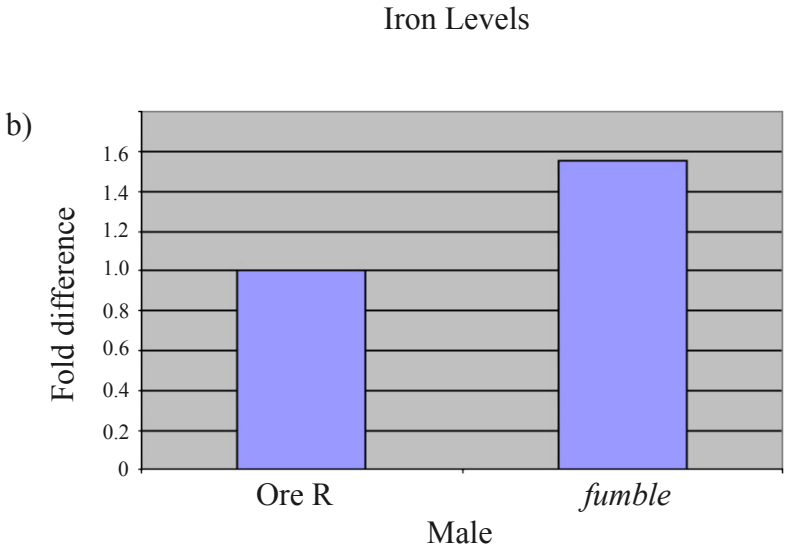
Iron Levels
b)
Fold difference
1.6
1.4
1.2
1.0
0.8
0.6
0.4
0.2
0
Ore R
fumble
Male

Figure 5: Rapid XRF imaging of whole female flies: When fed on a normal diet, *fumble* has visibly elevated iron relative to Oregon R. In *fumble*, iron accumulates in the posterior thorax (green arrow) and head (red arrow). *Limited conclusions can be made from these data due to small sample size resulting from limited beamtime. Left: Optical image, Right: Iron Kα fluorescence, Scale bar: 1mm.

Figure 5

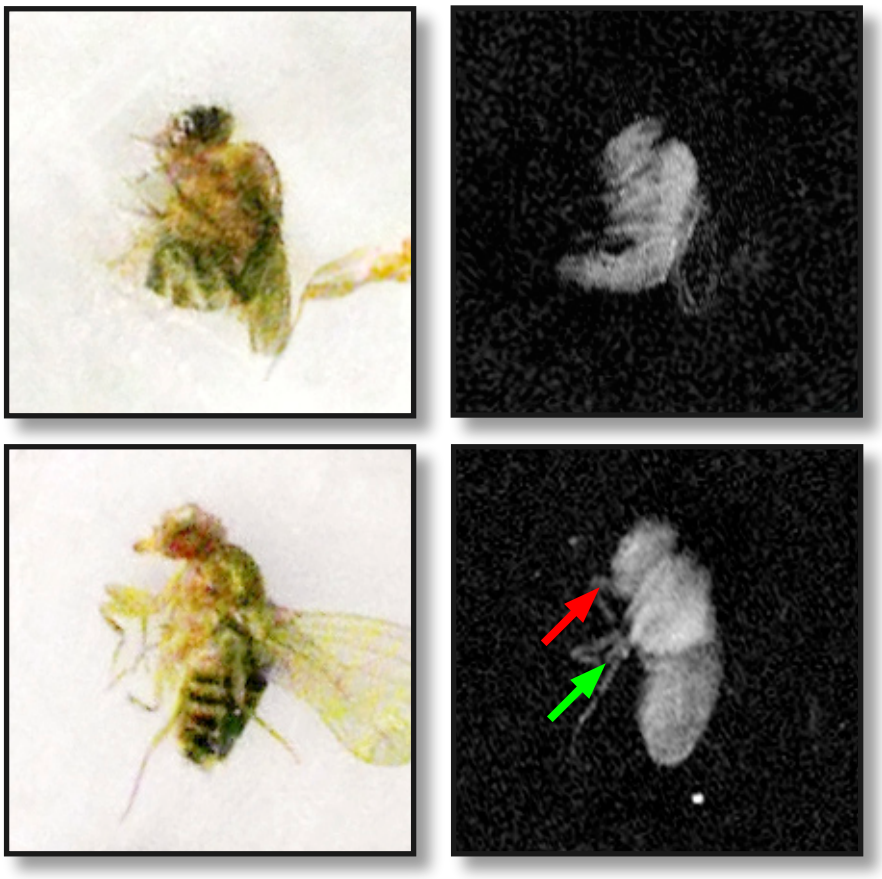
Ore R
fumble
Optical Image
Iron
1 mm
lowest iron
highest iron

Figure 6: Rapid XRF imaging of whole male flies: When fed on normal diet, *fumble* has more iron in the abdomen than Oregon R (red arrows). *Limited conclusions can be made from these data due to small sample size resulting from limited beamtime. Left: Optical image, Right: Iron Kα fluorescence, Scale bar: 1mm.

Figure 6

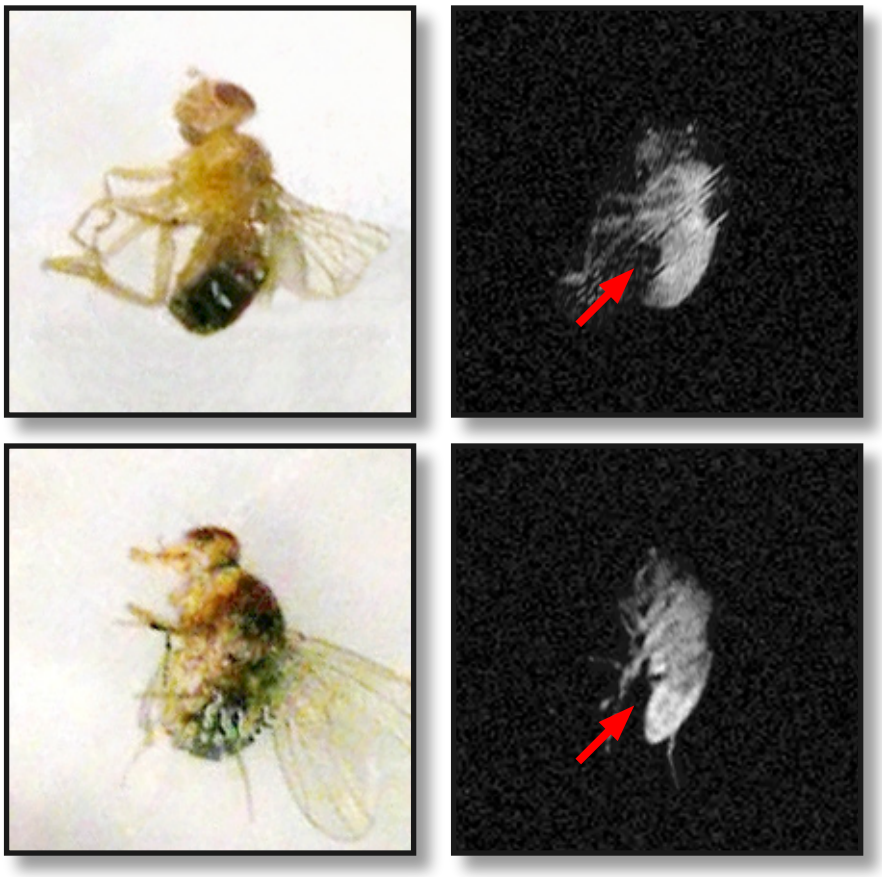
Ore R
fumble
Optical Image
Iron
1 mm
lowest iron
highest iron

Since the *fumble* mutant accumulates iron in the head and has the same genetic defect as the human PKAN disease, it is of interest to see how dietary iron affects the amount of iron in the heads of the *fumble* mutant. Dietary iron supplementation with 9 μM $FeCl_3$ increases the iron content of the normal diet by 20%. This concentration of iron is physiologically relevant and does not affect the lifespan of *Drosophila* (Massie et al 1985, Massie et al 1993). Dietary iron increased iron levels in the heads of both male and female *fumble* flies (Figure 7 a, b) as measured by ICP-MS. The female *fumble* heads on normal diet had 65 ng/mg of iron and the iron-supplemented had 105 ng/mg of iron. The male *fumble* heads on normal diet had 60 ng/mg of iron and the iron-supplemented had 90 ng/mg of iron. Even though *fumble* already has excess iron in the heads it is still able to accumulate additional iron.

XRF mapping was performed to determine if there were visible differences in the amount of iron in the *fumble* normal diet compared to iron fed. The iron fluorescence images of *fumble* females fed on iron-supplemented diet show more iron in the abdomen than the normal diet *fumble* (Figure 8). This could be dietary iron in a fecal pellet in the gut lumen. *Fumble* flies show iron accumulation in the head and thorax of both normal and iron-supplemented diet, but there is no visible increase in iron in the iron-supplemented *fumble*. The resolution of rapid-scanning XRF mapping may not be high enough to distinguish small changes in iron concentration.

4.4 Effect of elevated dietary iron on iron levels in wildtype heads.

Figure 7: Dietary iron supplementation increases iron levels in *fumble* adult heads. Iron levels in whole adult heads measured by ICP-MS are expressed as the fold difference between flies reared on iron supplemented (Fe +) relative to normal diet. (a) Females; (b) Males. The 1.6 fold difference between Fe (+) and normal diet in the females exceeds the intrinsic error of ICP-MS. The 1.5 fold difference between Fe (+) and normal diet in the males exceeds the intrinsic error of ICP-MS.

Figure 7

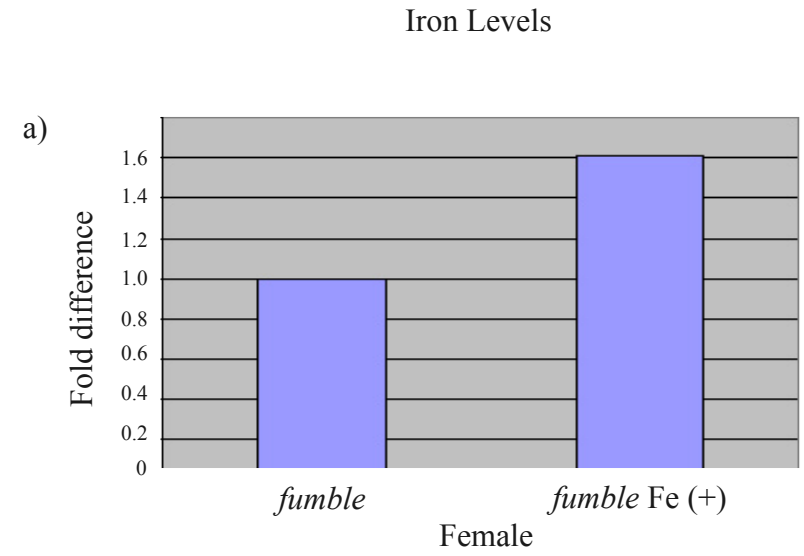
Iron Levels
a)
Fold difference
1.6
1.4
1.2
1.0
0.8
0.6
0.4
0.2
0
fumble
fumble Fe (+)
Female

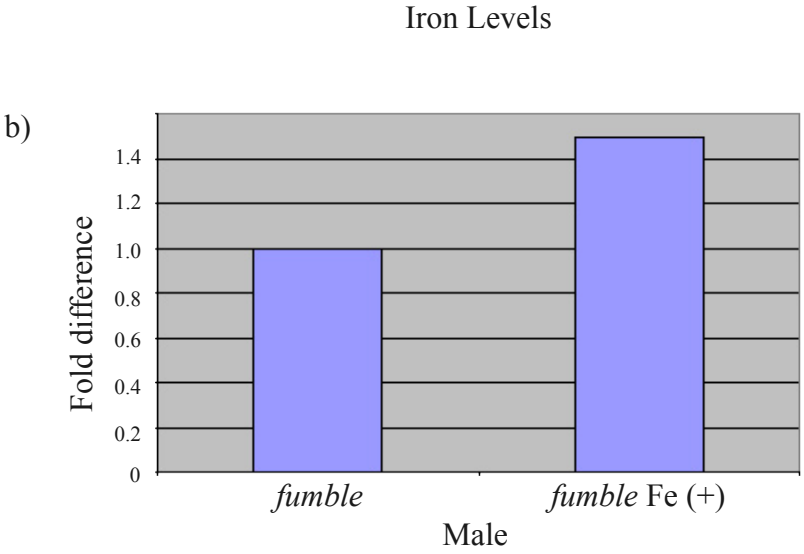
Iron Levels
b)
Fold difference
1.4
1.2
1.0
0.8
0.6
0.4
0.2
0
fumble
fumble Fe (+)
Male

Figure 8: Rapid XRF imaging of whole female flies: Iron can be visualized within the abdomen of *fumble* reared on an iron-supplemented diet (Fe +) but not normal diet. Iron in the abdomen is unevenly distributed (blue arrows). Both iron-supplemented (Fe+) and normal diet *fumble* flies show iron accumulation in the posterior thorax (green arrows) and head (red arrows) but iron supplementation does not visibly increase head or thoracic iron. *Limited conclusions can be made from these data due to small sample size resulting from limited beamtime. Left: Optical image, Right: Iron Kα fluorescence, Scale bar: 1mm.

Figure 8

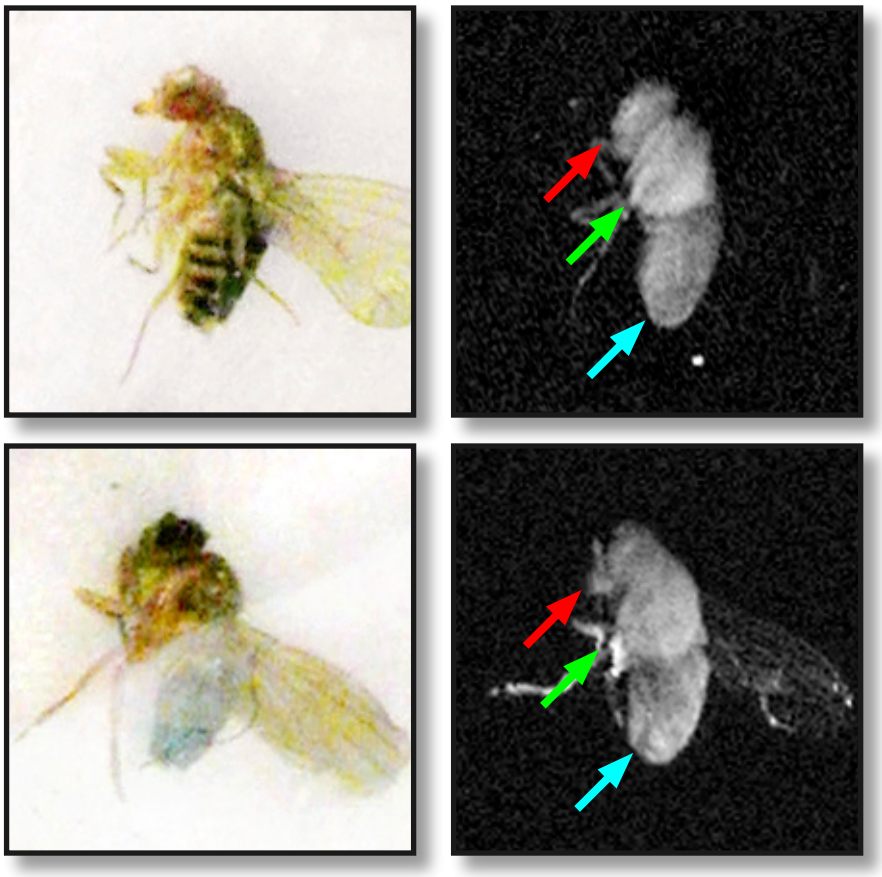
fumble
fumble
Fe (+)
Optical Image
Iron
1 mm
lowest iron
highest iron

Since dietary iron supplementation increases the iron levels in the heads of *fumble* mutants, the effect of dietary iron on Oregon R, the parental strain of *fumble*, was measured by ICP-MS. An increase in dietary iron is expected to lead to increased iron uptake. Iron-supplemented wildtype female flies accumulated two-fold more iron in the heads than those fed a normal diet (Figure 9). The female wildtype heads on normal diet had 45 ng/mg of iron and the iron-supplemented had 90 ng/mg of iron.

The female wildtype flies accumulate iron when reared on the iron supplemented diet relative to those on control diet. The two-fold difference is a large enough difference to be visible with XRF imaging. This was true of both males and females (Figure 10, 11). The iron signal is decreased in the heads of male and female wildtype raised on iron supplemented diet. However, iron was elevated in the abdomen of the iron-supplemented flies. A small number of iron-supplemented flies were observed and iron seemed to localize to the gut lumen.

4.5 MVL expression in the heads of the fumble mutant.

The elevated iron levels in *fumble* led us to examine proteins involved in iron uptake. One of these proteins is the divalent metal transporter MVL. MVL is expressed in neurons and therefore could be involved in iron uptake into the head. Since the *fumble* female has a movement disorder as well as visibly increased iron in the head, Western blots were done on whole female heads. MVL expression was compared in Oregon R and *fumble* flies, both reared on normal diet. The *fumble* mutant shows a nearly

Figure 9: Dietary iron supplementation increases iron levels in wildtype (Ore R) female adult heads. Iron levels in whole adult heads measured by ICP-MS are expressed as the fold difference between flies reared on iron supplemented (Fe +) relative to normal diet. The 1.9 fold difference between Fe (+) and normal diet exceeds the intrinsic error of ICP-MS. This number is the average of 2 replicates.

Figure 9

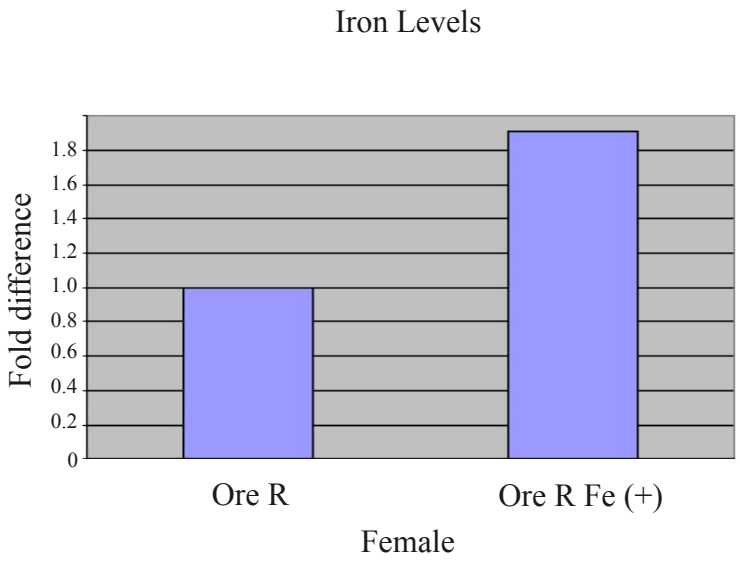
Iron Levels
Fold difference
1.8
1.6
1.4
1.2
1.0
0.8
0.6
0.4
0.2
0
Ore R
Ore R Fe (+)
Female

Figure 10: Rapid XRF imaging of whole female flies: Iron can be visualized within the abdomen of Oregon R reared on an iron-supplemented diet (Fe +) but not normal diet. Iron in the abdomen is unevenly distributed (red arrows). *Limited conclusions can be made from these data due to small sample size resulting from limited beamtime. Left: Optical image, Right: Iron Kα fluorescence, Scale bar: 1mm.

Figure 10

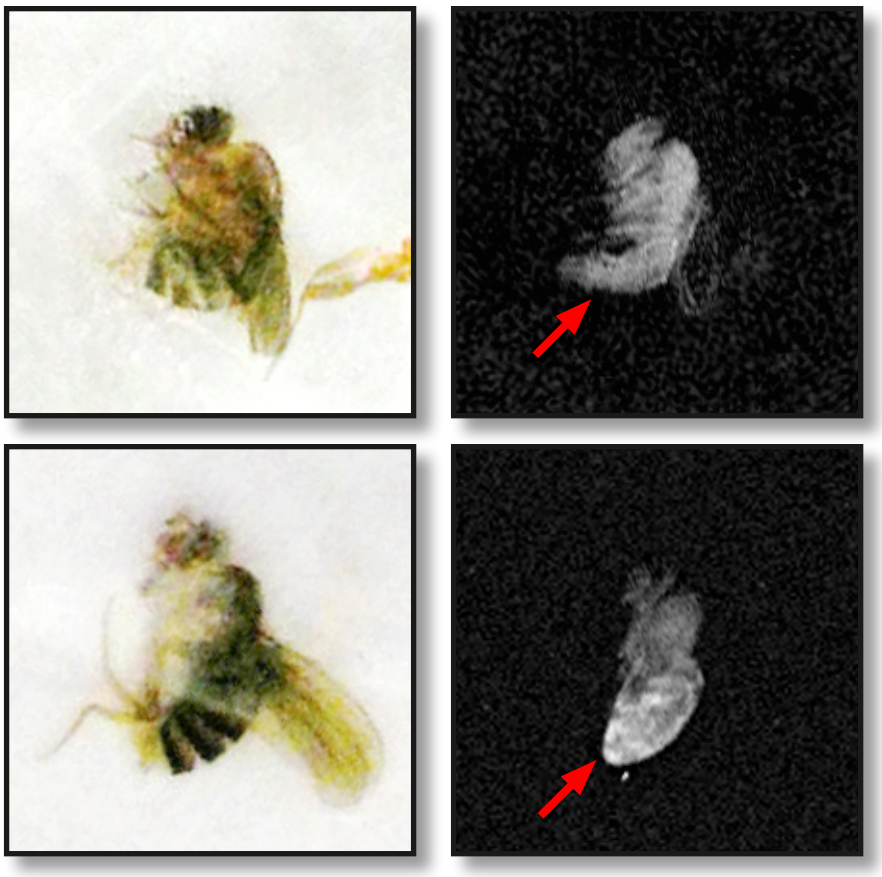
Ore R
Ore R
Fe (+)
Optical Image
Iron
1 mm
lowest iron
highest iron

Figure 11: Rapid XRF imaging of whole male flies: Oregon R fed on iron diet (Fe +) has more iron in the abdomen than Oregon R fed on normal diet (red arrows). *Limited conclusions can be made from these data due to small sample size resulting from limited beamtime. Left: Optical image, Right: Iron Kα fluorescence, Scale bar: 1mm.

Figure 11


Ore R
Ore R
Fe (+)
Optical Image
Iron
1 mm
lowest iron
highest iron

4 fold increase in expression of MVL in the heads compared to wildtype (Figure 12). This very large upregulation of MVL indicates that iron absorption is dysregulated in the *fumble* mutant. This is the first protein involved in iron metabolism shown to have altered expression in PANK deficiency.

4.6 Effect of dietary iron supplementation on MVL expression in fumble heads.

Since the expression of MVL is elevated in the *fumble* mutant, we wanted to know how dietary iron supplementation affects MVL expression in *fumble*. We expected that dietary iron would increase MVL expression, but we found that MVL expression in the iron-supplemented heads was about half (55%) of that seen in *fumble* fed on a normal diet (Figure 13). Dietary iron decreases MVL expression in the *fumble* mutant.

4.7 Effect of dietary iron supplementation on MVL expression in wildtype heads.

Since dietary iron reduced the expression of MVL in the *fumble* mutant we wanted to know if the same was true for wildtype flies. If wildtype and *fumble* respond to iron in a similar way, iron should reduce the expression of MVL. Surprisingly, MVL expression was increased 2.5 fold in female Oregon R iron fed flies compared to flies fed on normal diet (Figure 14). We found that in contrast to *fumble*, dietary iron induces MVL expression in Oregon R. This shows that the normal response to low-level dietary iron supplementation is an upregulation of MVL. In *fumble* iron reduces MVL expression showing that MVL is dysregulated in *fumble*.

Figure 12: MVL expression is elevated in *fumble* female heads relative to parental strain Oregon R. (a)Western blot of protein extracts (15 μg) prepared from whole heads of Oregon R and *fumble* female flies raised on normal diet, probed with polyclonal anti-human NRAMP1. (b) MVL quantification: Four independent replicates were normalized to actin and averaged. Error bars indicate standard error of the mean. ** indicates significant difference, $p<0.01$.

Figure 12

a)

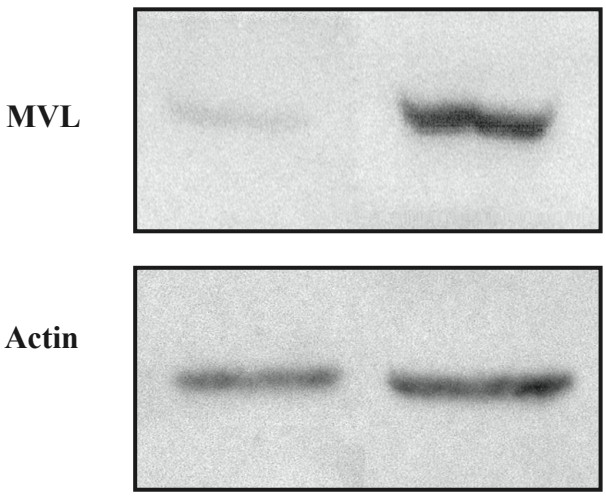
Ore R
fumble
MVL
Actin

b)

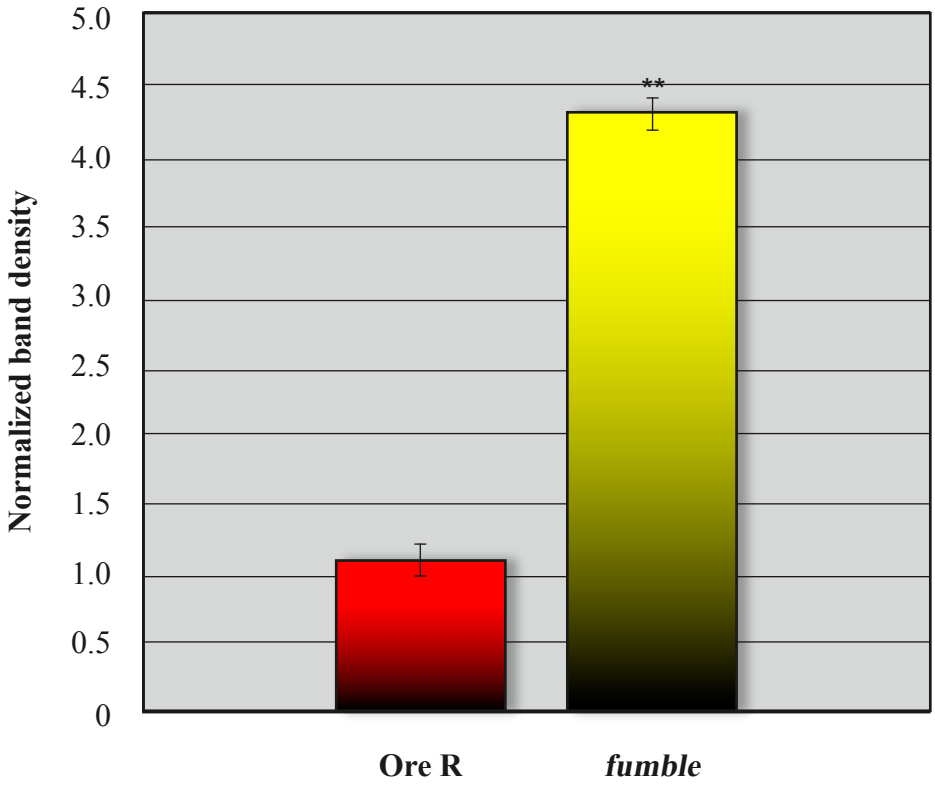
Normalized band density
5.0
4.5
4.0
3.5
3.0
2.5
2.0
1.5
1.0
0.5
0
**
Ore R
fumble

Figure 13: A 20% increase in dietary iron decreases MVL expression in heads of *fumble* female flies. (a)Western blot of protein extracts (15 μg) prepared from whole heads of *fumble* female flies raised on normal or iron-supplemented (Fe +) diet, probed with polyclonal anti-human NRAMP1. (b) MVL quantification: Four independent replicates were normalized to actin and averaged. Error bars indicate standard error of the mean. * indicates significant difference, $p<0.05$.

Figure 13

a)

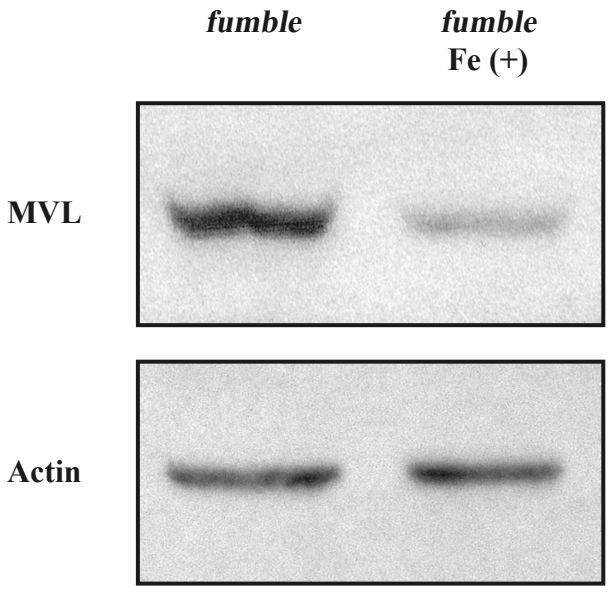
fumble
fumble
Fe (+)
MVL
Actin

b)

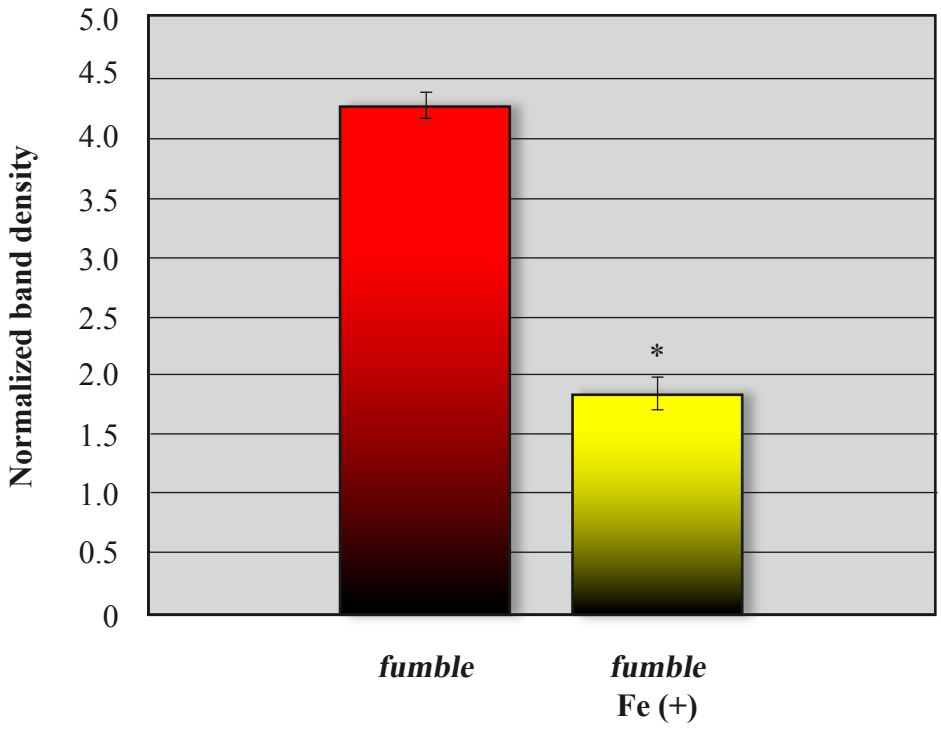
Normalized band density
5.0
4.5
4.0
3.5
3.0
2.5
2.0
1.5
1.0
0.5
0
*
fumble
fumble
Fe (+)

Figure 14: A 20% increase in dietary iron increases MVL expression in heads of Oregon R female flies. (a) Western blot of protein extracts (15 μg) prepared from whole heads of Oregon R female flies raised on normal or iron supplemented (Fe +) diet, probed with polyclonal anti-human NRAMP1. (b) MVL quantification: Four independent replicates were normalized to actin and averaged. Error bars indicate standard error of the mean. * indicates significant difference, $p<0.05$.

Figure 14

a)

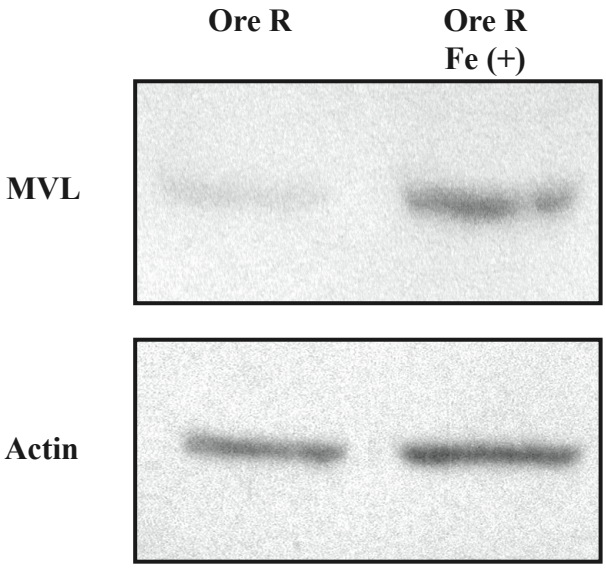
Ore R
Ore R
Fe (+)
MVL
Actin

b)

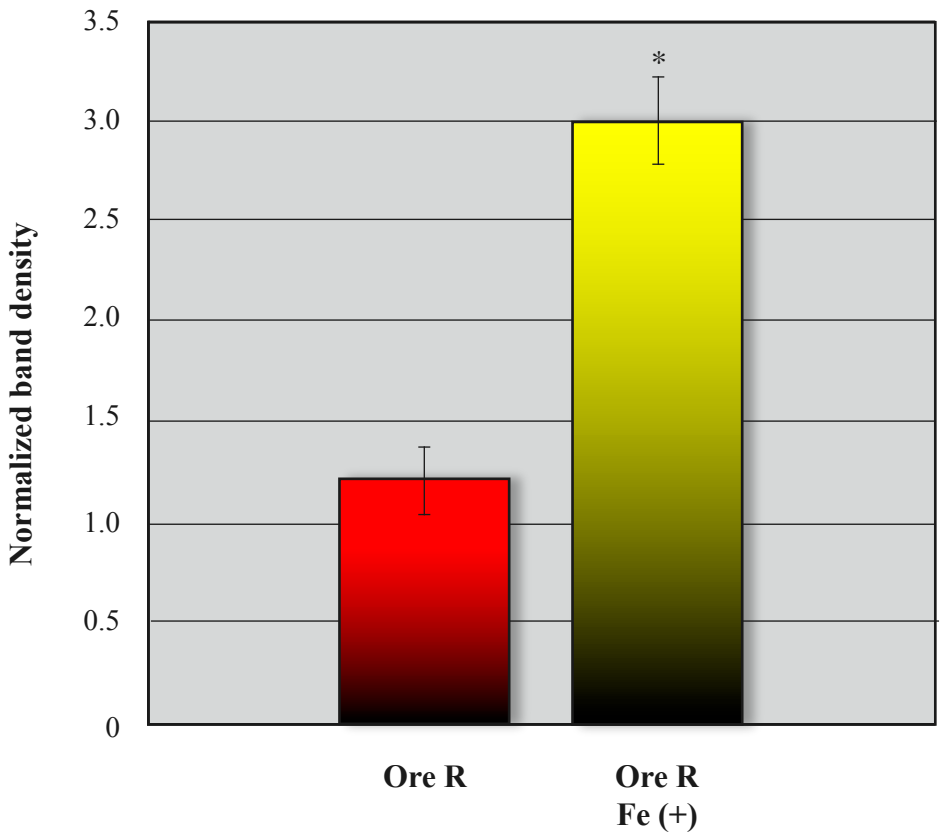
Normalized band density
3.5
3.0
2.5
2.0
1.5
1.0
0.5
0
*
Ore R
Ore R
Fe (+)

4.8 Iron levels in heads of malvolio mutant relative to wildtype.

The *fumble* mutant accumulates iron and has high expression of MVL. To investigate the role of MVL in iron accumulation in the head, iron levels in the *malvolio* mutant were measured. The *malvolio* mutant expresses a non-functional MVL protein. MVL is a divalent metal transporter in flies that is expressed in neurons, macrophages, and the gut. Impaired expression of MVL would be expected to reduce iron uptake in those tissues that express MVL, producing iron deficiency. Pooled samples of 25 whole adult heads were prepared for ICP-MS analysis as previously described (section 4.1). Similar samples were compared using ng iron/mg wet weight and are expressed as fold difference (Figure 15, 18, 21).

The iron requirements of male and female flies may be different since females lose iron when eggs are laid. We found that female *fumble* and Oregon R take up or store more iron than males (section 4.2). Therefore, average iron levels in male or female heads of *malvolio* were compared with the same sex of the parental strain (w1118). Iron levels were similar in *malvolio* and wildtype flies fed on a normal diet and this was true for both males and females (Figure 15 a, b). Wildtype and *malvolio* females had about 80 and 70 ng/mg of iron respectively. Both wildtype and *malvolio* males had about 70 ng/mg of iron.

Although there were no differences in iron levels in the *malvolio* mutant compared to its parental strain, XRF mapping was performed on these flies to see if there were differences in iron concentrations in specific tissues. The iron Kα fluorescence

Figure 15: *Malvolio* and wildtype (w1118) have similar iron levels when both are reared on a normal diet. Iron levels in whole adult heads measured by ICP-MS are expressed as the fold difference of *malvolio* relative to wildtype. (a) Females; (b) Males. Differences do not exceed the intrinsic error of ICP-MS.

Figure 15

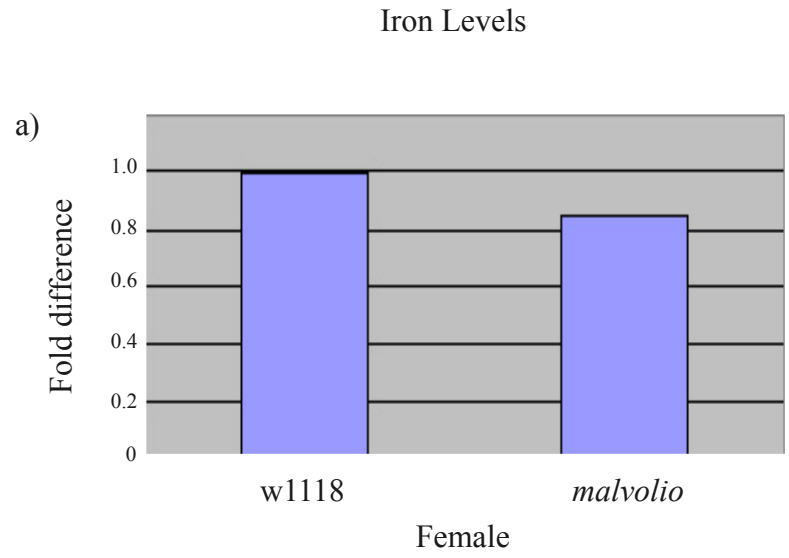
Iron Levels
a)
Fold difference
1.0
0.8
0.6
0.4
0.2
0
w1118
malvolio
Female

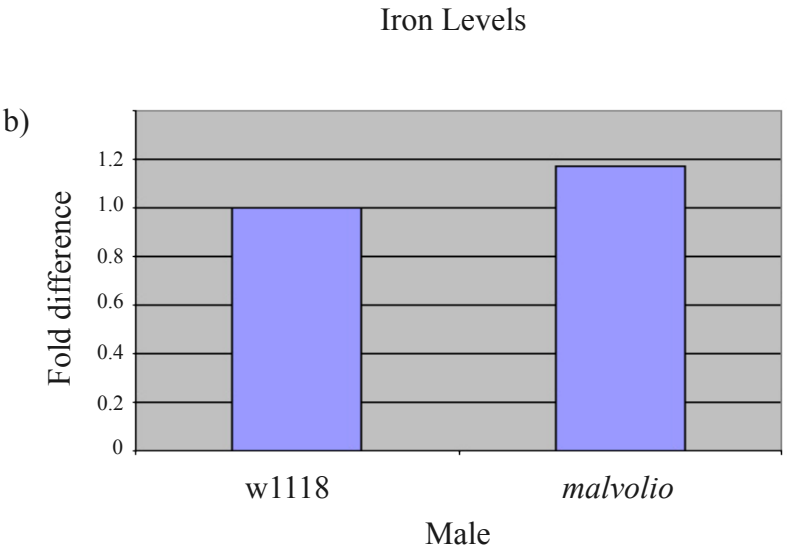
Iron Levels
b)
Fold difference
1.2
1.0
0.8
0.6
0.4
0.2
0
w1118
malvolio
Male

images showed that iron in *malvolio* was evenly distributed in the head, thorax, and abdomen (Figure 16). The wildtype male accumulated iron in the thorax when fed normal diet. Since beamtime was limited, only one image of each fly was collected. ICP-MS data confirmed that iron levels were about the same in *malvolio* and wildtype.

Resolution of rapid-scanning XRF was only 50 microns, and structures in the head were difficult to distinguish. XRF microprobe imaging was used to localize iron to specific regions of the head in these flies. In both males and females more iron was seen in the wildtype than in *malvolio* (Figure 17 a, b); whereas ICP-MS showed that *malvolio* had similar iron to wildtype. Localization of iron in female heads of w1118 and *malvolio* were similar. The dorsal-ventral (D-V) view showed that most of the iron was in the antennae and some was in the rostrum (Figure 17 a). Localization of iron in w1118 male head was similar to that of *malvolio* male head. This was done in the anterior-posterior (A-P) view (Figure 17 b). This shows that the orientation of the sample is important in localizing the iron, since our picture is a 2-D image of the whole head. In the D-V view (Figure 17 a), the iron accumulation in the antennae appears to be localized to brain structures, but in the A-P view (Figure 17 b) it is clear that the iron is most likely accumulating in the antennae. Although sample size is small, imaging has been done on several heads not included in this thesis and all heads accumulate most of their iron in the antennae and rostrum (personal communication, Nichol).

4.9 Effect of elevated dietary iron on iron levels in malvolio heads.

Figure 16: Rapid XRF imaging of whole male flies: When both are fed on normal diet, *malvolio* has more iron than w1118. w1118 accumulates iron in the thoracic region (red arrow). *Limited conclusions can be made from these data due to small sample size resulting from limited beamtime. Left: Optical image, Right: Iron Kα fluorescence, Scale bar: 1mm.

Figure 16

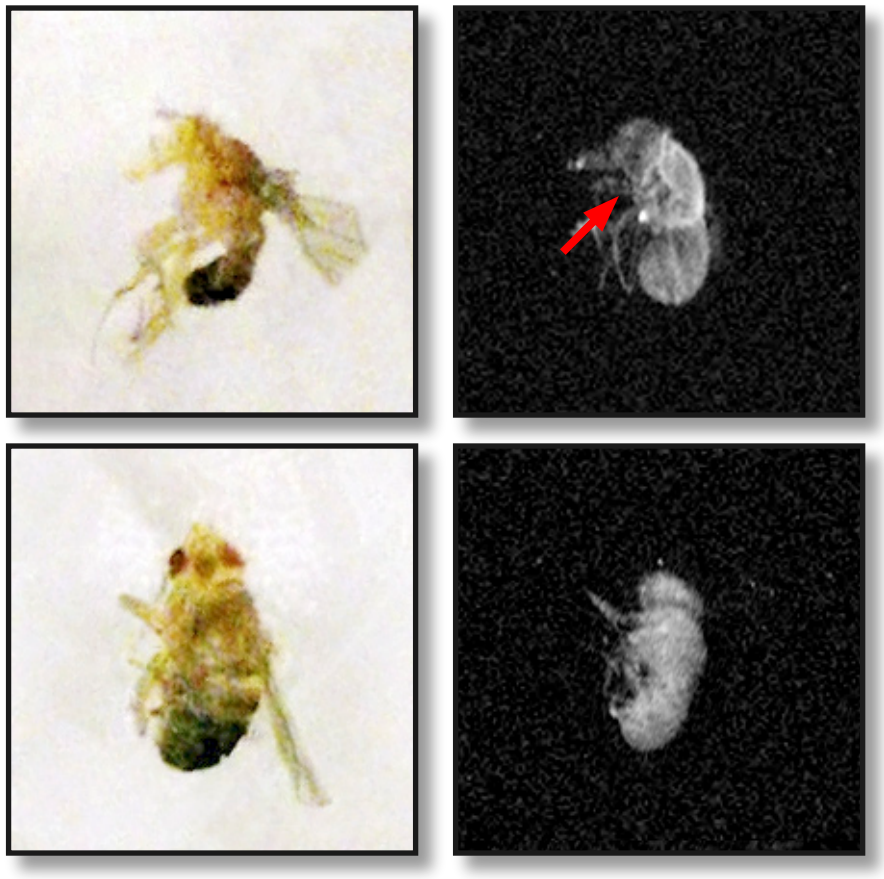
w1118
malvolio
Optical Image
Iron
1 mm
lowest iron
highest iron

Figure 17: a) Iron is more abundant in the antennae and rostrum of w1118 and *malvolio* adults. Iron was spatially mapped with a microprobe with a 15 micron spot size. Iron K_α fluorescence counts were recorded at each pixel and summed over all detector channels and divided by the scatter fluorescence as described in methods. Flies were raised on a normal diet. From left to right: Normalized Iron K_α fluorescence; optical image. From top to bottom: w1118; *malvolio*, isolated female heads, dorsal-ventral view. Iron is more abundant in the antennae and rostrum. These observations are based on a small sample size due to limited beamtime.

Figure 17a

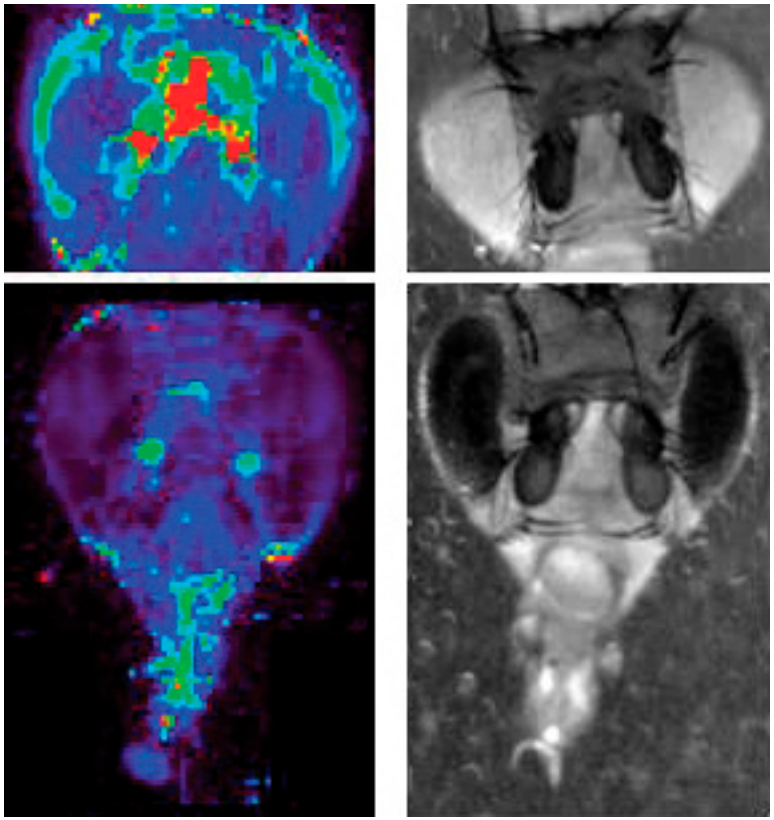

Female w1118 normal diet, dorsal-ventral (D-V) view (top); female *malvolio* normal diet, D-V view (bottom).

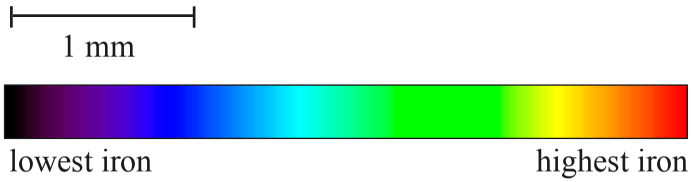

Figure 17: b) Iron is more abundant in the antennae and rostrum of w1118 and *malvolio* adults. Iron was spatially mapped with a microprobe with a 15 micron spot size. Iron K_α fluorescence counts were recorded at each pixel and summed over all detector channels and divided by the scatter fluorescence as described in methods. Flies were raised on a normal diet. From left to right: Normalized Iron K_α fluorescence; optical image. From top to bottom: w1118; *malvolio*, heads of male whole flies, anterior-posterior view. Iron is more abundant in the antennae and rostrum. These observations are based on a small sample size due to limited beamtime.

Figure 17b

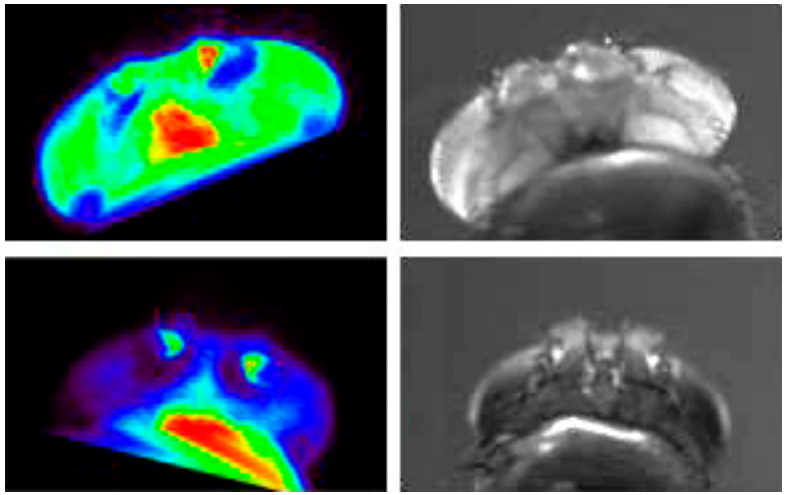

Male w1118 normal diet, anterior-posterior (A-P) view (top); male *malvolio* normal diet, A-P view (bottom).

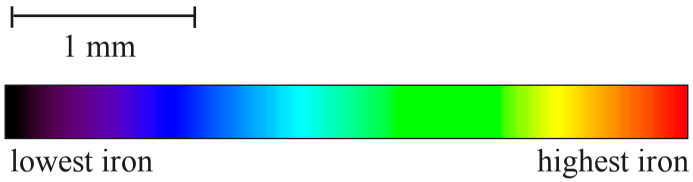

Iron supplementation did not affect iron levels in the heads of male or female *malvolio* flies (Figure 18 a, b). All the *malvolio* had about 70 ng/mg iron in the heads irrespective of diet. XRF mapping was performed on whole male *malvolio* flies fed on normal diet or iron-supplemented diet and no visible differences were seen (Figure 19). Although few images were collected, this data agrees with the ICP-MS data that shows no effect of iron supplementation on iron levels in the heads of *malvolio*.

To determine if iron supplementation affects the localization of iron in the head of the *malvolio* mutant we did XRF microprobe imaging (Figure 20). Both *normal* diet and iron-supplemented *malvolio* accumulated iron in the antennae. The iron-supplemented *malvolio* had slightly more iron in the antennae than the normal diet *malvolio* but this can be attributed to individual fly differences because ICP-MS did not show differences in iron levels between normal and iron supplemented *malvolio*.

4.10 Effect of dietary iron on iron levels in w1118 wildtype heads.

Since *malvolio* has a non-functional MVL transporter iron uptake should be impaired. Since increasing dietary iron by 20% did not result in elevated iron in the head of MVL we next examined the effect of dietary iron on its wildtype (Figure 21). Both female and male wildtype flies reared on either control or iron-supplemented diet contained about 75 ng/mg iron. We were unable to attribute unchanged iron levels in *malvolio* to impaired iron absorption since both *malvolio* and the wildtype fly did not accumulate iron.

Figure 18: Dietary iron supplementation does not affect iron levels in *malvolio* adult heads. Iron levels in whole adult heads measured by ICP-MS are expressed as the fold difference between flies reared on iron supplemented (Fe +) relative to normal diet. (a) Females; (b) Males. Differences do not exceed the intrinsic error of ICP-MS.

Figure 18

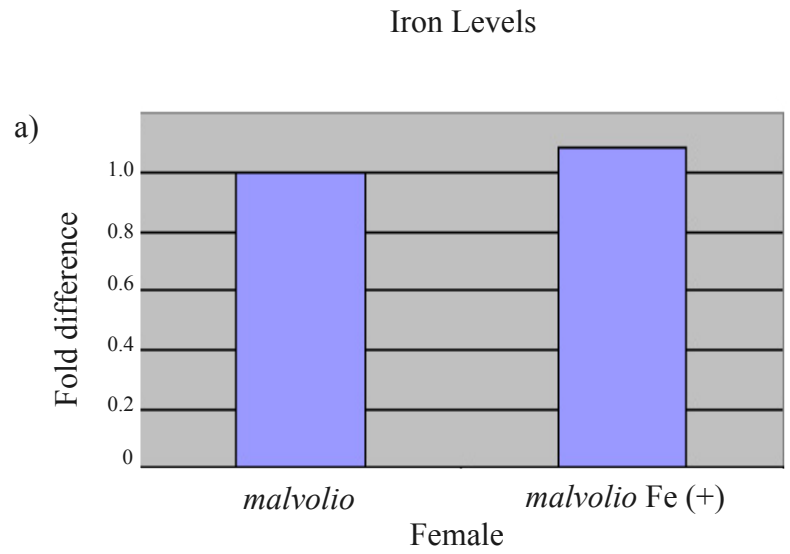
Iron Levels
a)
Fold difference
1.0
0.8
0.6
0.4
0.2
0
malvolio
malvolio Fe (+)
Female

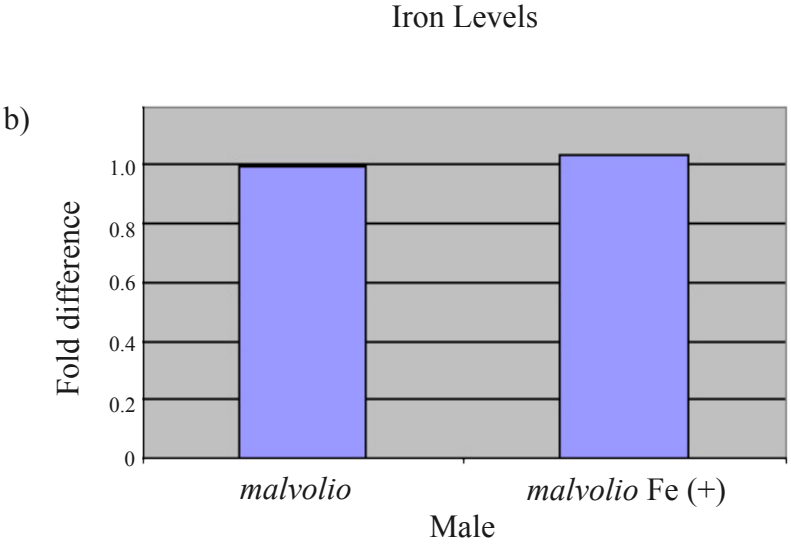
Iron Levels
b)
Fold difference
1.0
0.8
0.6
0.4
0.2
0
malvolio
malvolio Fe (+)
Male

Figure 19: Rapid XRF imaging of whole male flies: There are no visible differences between *malvolio* fed on normal diet and *malvolio* fed on iron supplemented diet (Fe +). *Limited conclusions can be made from these data due to small sample size resulting from limited beamtime. Left: Optical image, Right: Iron Kα fluorescence, Scale bar: 1mm.

Figure 19

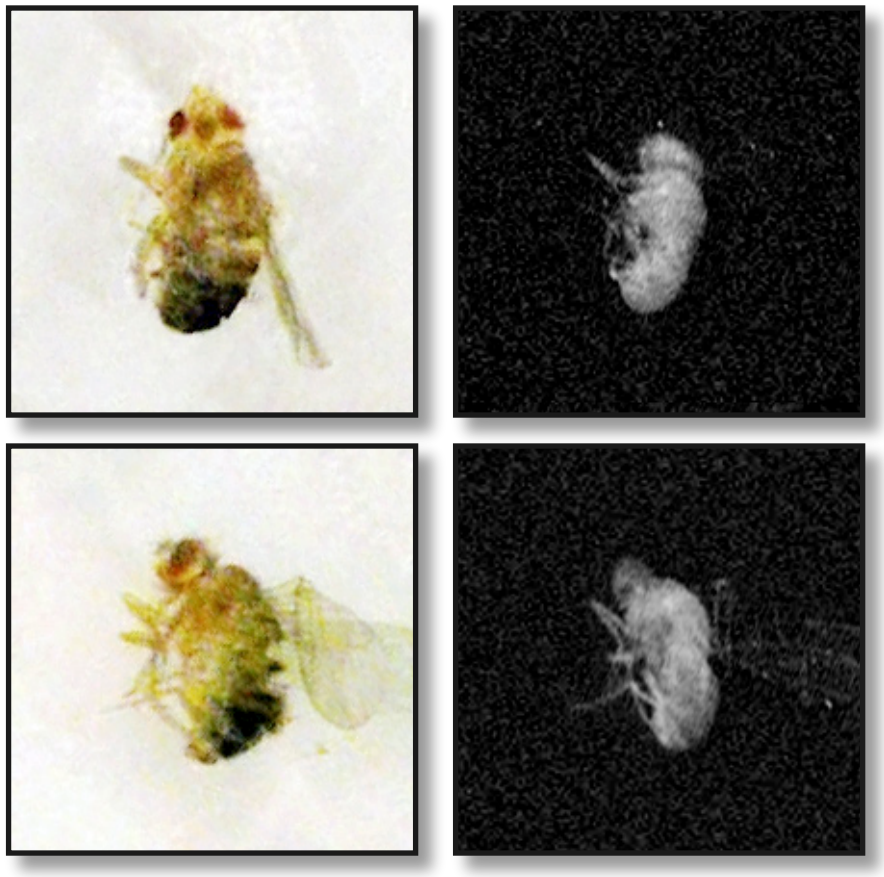
malvolio
malvolio
Fe (+)
Optical Image
Iron
1 mm
lowest iron
highest iron

Figure 20: A 20% increase in dietary iron supplementation does not affect the location of iron in the heads of *malvolio* adults. Iron was spatially mapped with a microprobe with a 10 micron spot size. Iron K_α fluorescence counts were recorded at each pixel and summed over all detector channels and divided by the scatter fluorescence as described in methods. Dorsal-ventral view of isolated *malvolio* heads is shown. From left to right: Iron K_α fluorescence; optical image. From top to bottom: normal diet; iron-supplemented diet. Iron is more abundant in the antennae and rostrum in both normal and iron-fed *malvolio* flies. These observations are based on a small sample size due to limited beamtime.

Figure 20

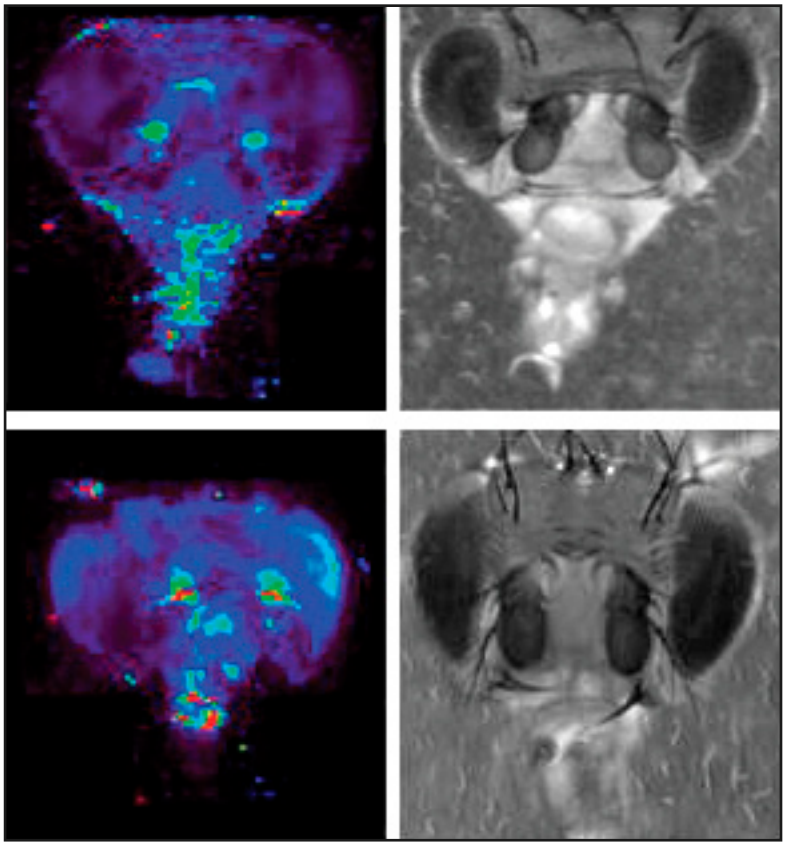

malvolio female normal diet, D-V view (top); *malvolio* female Iron-fed, D-V view (bottom).

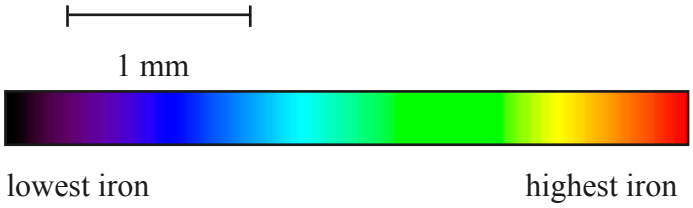

Figure 21: Dietary iron supplementation does not affect iron levels in wildtype (w1118) adult heads. Iron levels in whole adult heads measured by ICP-MS are expressed as the fold difference between flies reared on iron supplemented (Fe +) relative to normal diet. (a) Females; (b) Males. Differences do not exceed the intrinsic error of ICP-MS.

Figure 21

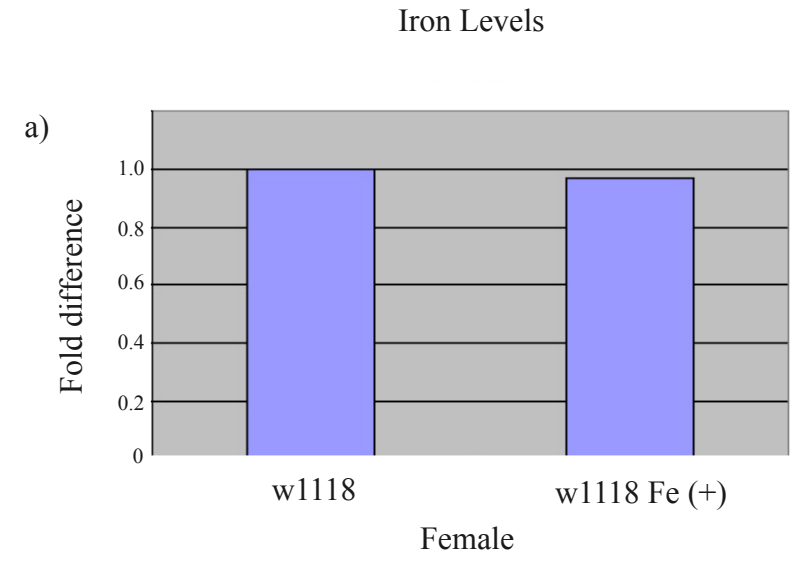
Iron Levels
a)
Fold difference
1.0
0.8
0.6
0.4
0.2
0
w1118
w1118 Fe (+)
Female

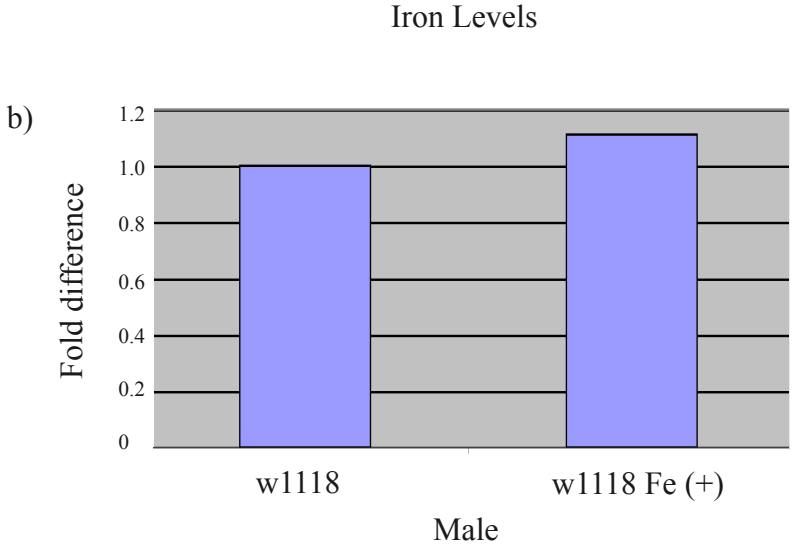
Iron Levels
b)
Fold difference
1.2
1.0
0.8
0.6
0.4
0.2
0
w1118
w1118 Fe (+)
Male

Although there were no differences in the iron levels in the heads of iron-supplemented wildtype flies, XRF mapping was done to see if iron accumulates in specific regions of the flies. In the iron fluorescence image of male wildtype flies fed on normal diet or iron-supplemented diet there is more iron in the abdomen with iron-supplementation than normal diet (Figure 22). This is probably excess dietary iron in the gut lumen, as seen in the iron-supplemented Oregon R images. No differences were seen in the heads of the wildtype males on iron-supplemented diet compared to normal diet in agreement with ICP-MS data.

4.11 Ferritin expression in the heads of the fumble mutant relative to wildtype.

Ferritin stores iron in a non-toxic, soluble form in the body. Excess iron in the cells is expected to require increased ferritin expression to sequester increased iron. To determine whether the excess iron in the heads of the *fumble* mutant causes a change in ferritin expression, ferritin levels were examined by Western blots. Ferritin expression was unchanged in *fumble* (Figure 23) and excess iron in *fumble* does not lead to increased ferritin expression.

4.12 Effect of elevated dietary iron on ferritin expression in fumble heads.

Since dietary iron increases the levels of iron in the heads of the *fumble* mutant, this excess iron should increase ferritin synthesis. However, western blot analysis

Figure 22: Rapid XRF imaging of whole male flies: Iron can be visualized within the abdomen of w1118 fed on iron supplemented diet (Fe +) but not in w1118 normal diet (red arrows). *Limited conclusions can be made from these data due to small sample size resulting from limited beamtime. Left: Optical image, Right: Iron Kα fluorescence, Scale bar: 1mm.

Figure 22

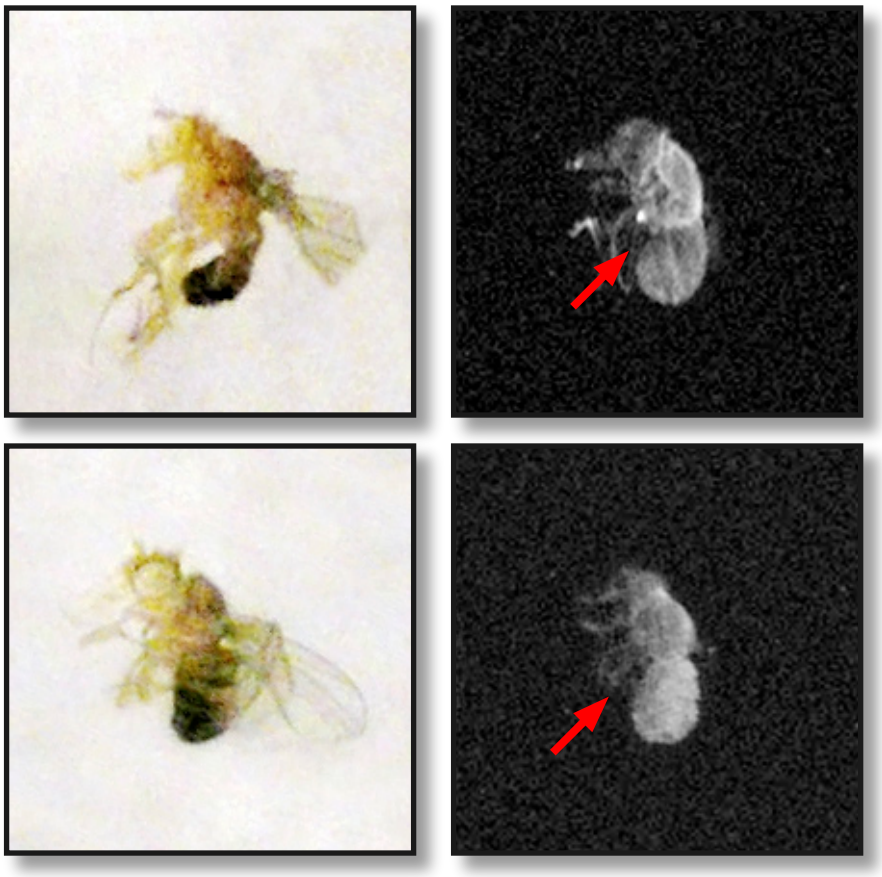
w1118
w1118
Fe (+)
Optical Image
Iron
1 mm
lowest iron
highest iron

Figure 23: Ferritin expression is unchanged in *fumble* female heads relative to parental strain Oregon R. (a) Western blot of protein extracts (5 μg) prepared from whole heads of Oregon R and *fumble* female flies raised on normal diet, probed with polyclonal antiserum raised against native *D. melanogaster* ferritin (Georgieva et al, 2002). (b) Ferritin quantification: Four independent replicates were normalized to actin and averaged. Error bars indicate standard error of the mean. T-test showed no significant difference in ferritin expression.

Figure 23

a)

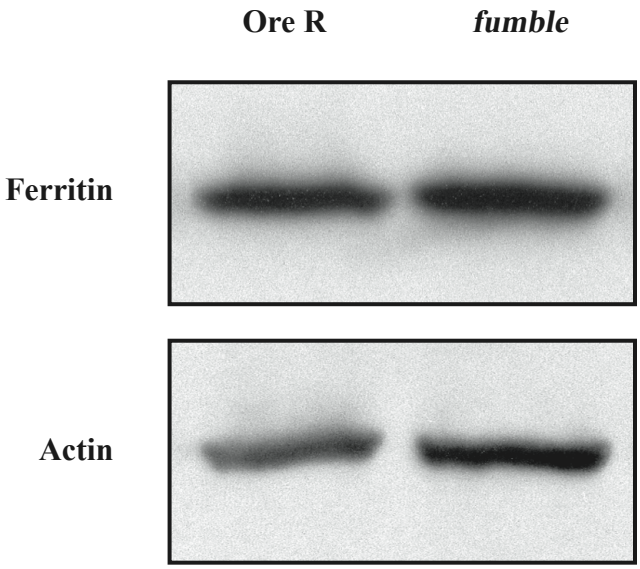
Ore R
fumble
Ferritin
Actin

b)

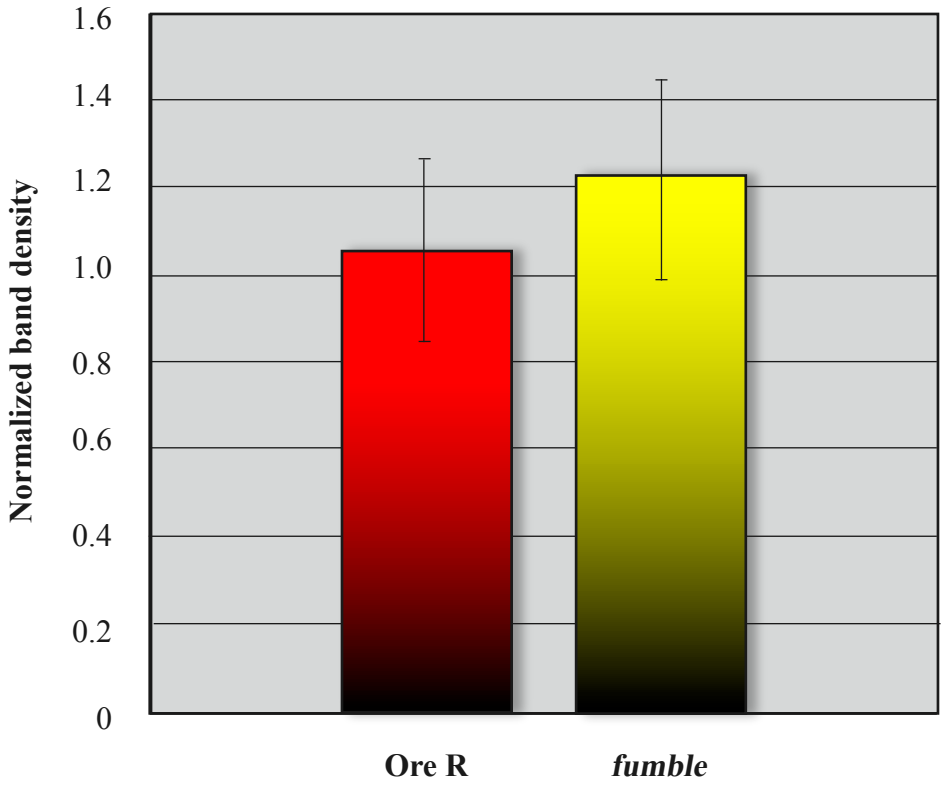
Normalized band density
1.6
1.4
1.2
1.0
0.8
0.6
0.4
0.2
0
Ore R
fumble

showed that dietary iron supplementation does not affect ferritin subunit expression in the heads of *fumble* females (Figure 24).

4.13 Effect of elevated dietary iron on ferritin expression in heads of Oregon R wildtype.

Since dietary iron did not affect ferritin expression in the *fumble* mutant, we examined the effect of dietary iron on ferritin expression in Oregon R since an increase in dietary iron could trigger an increase in ferritin expression. A slight increase in ferritin expression was consistently seen in the iron-supplemented Oregon R, but this difference is not statistically significant (Figure 25). Dietary iron does not affect ferritin expression of Oregon R female flies in an appreciable way.

4.14 Ferritin expression in the heads of malvolio relative to wildtype.

Since the MVL transporter is involved in iron uptake, a non-functional transporter may affect iron metabolism and ferritin expression in the mutant. The western blot of heads of w1118 wildtype and *malvolio* females showed that ferritin expression was slightly lower in *malvolio* flies (Figure 26). Although the difference is not visually apparent, a consistent decrease of 20% was measured by densitometry. Since this was reproduced in 4 independent replicates and a t-test showed a statistically significant difference. *Malvolio* expresses less ferritin in the heads than wildtype.

Figure 24: A 20% increase in dietary iron does not affect ferritin expression in heads of *fumble* female flies. (a) Western blot of protein extracts (5 μg) prepared from whole heads of *fumble* female flies raised on normal or iron supplemented (Fe +) diet, probed with polyclonal antiserum raised against native *D. melanogaster* ferritin (Georgieva et al, 2002). (b) Ferritin quantification: Four independent replicates were normalized to actin and averaged. Error bars indicate standard error of the mean. T-test showed no significant difference in ferritin expression.

Figure 24

a)

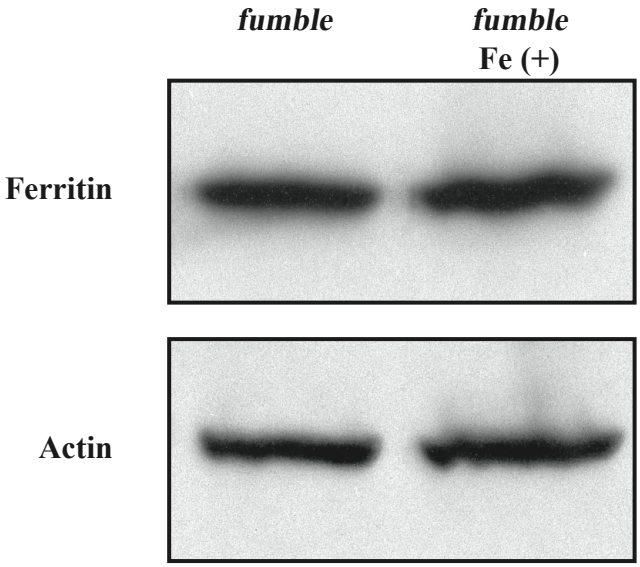
fumble
fumble
Fe (+)
Ferritin
Actin

b)

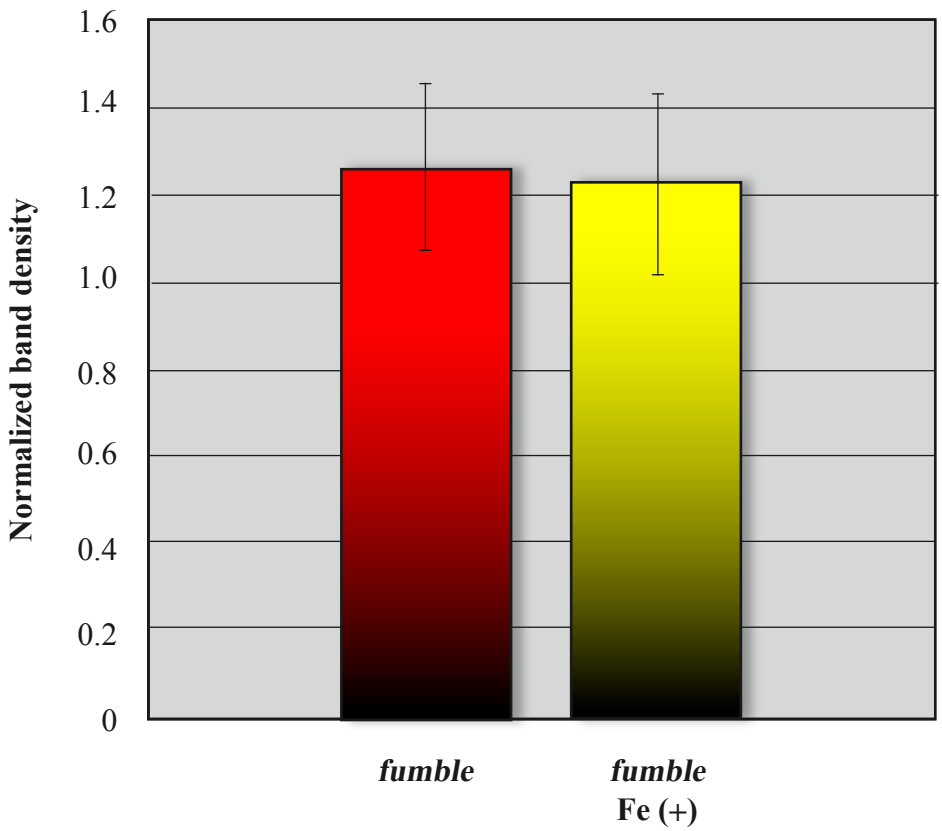
Normalized band density
1.6
1.4
1.2
1.0
0.8
0.6
0.4
0.2
0
fumble
fumble
Fe (+)

Figure 25: A 20% increase in dietary iron does not affect ferritin expression in heads of Oregon R female flies. (a) Western blot of protein extracts (5 μg) prepared from whole heads of Oregon R female flies raised on normal or iron supplemented (Fe +) diet, probed with polyclonal antiserum raised against native D. *melanogaster* ferritin (Georgieva et al, 2002). (b) Ferritin quantification: Four independent replicates were normalized to actin and averaged. Error bars indicate standard error of the mean. T-test showed no significant difference in ferritin expression.

Figure 25

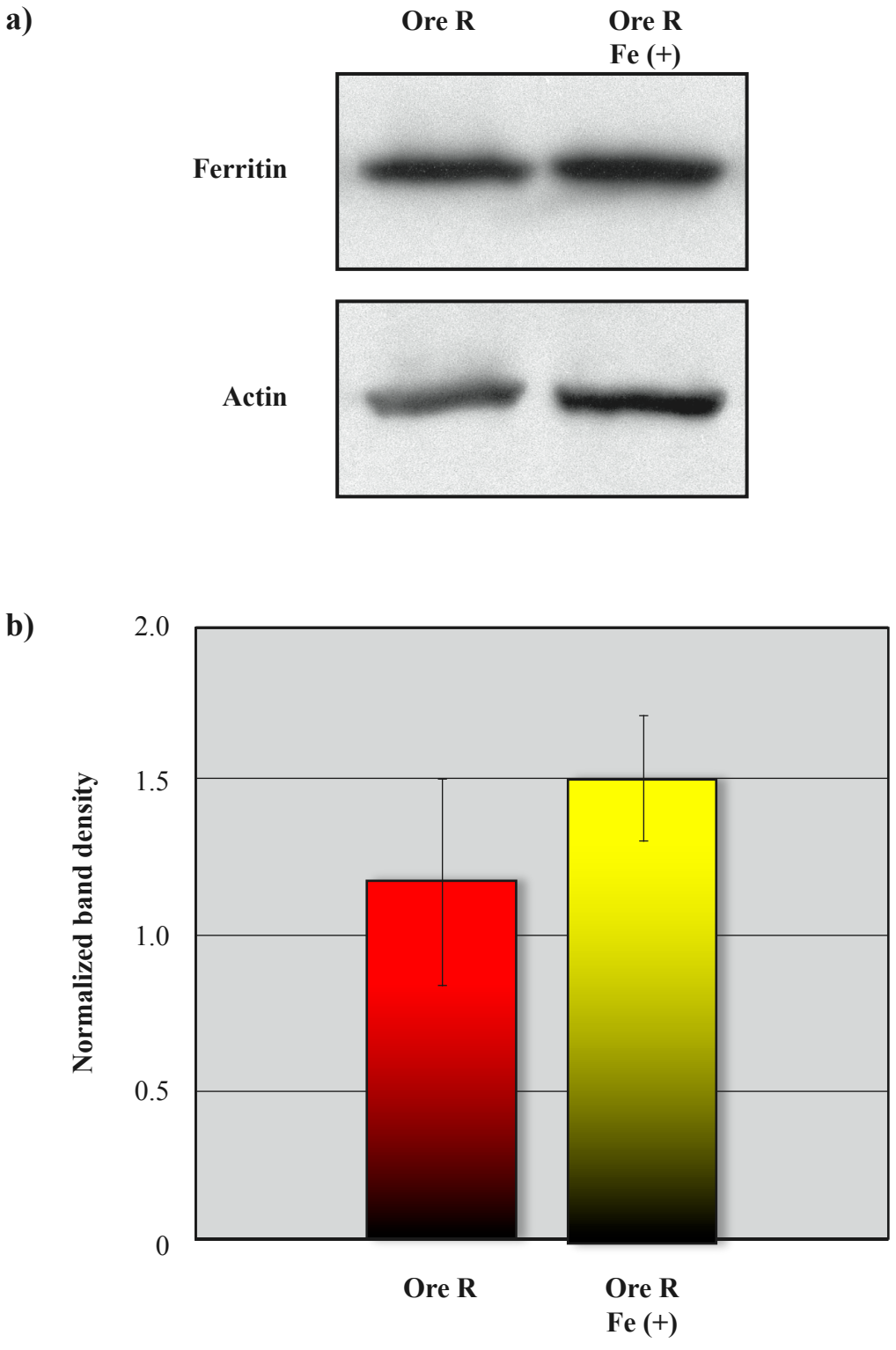
a)
Ore R
Ore R
Fe (+)
Ferritin
Actin
b)
Normalized band density
2.0
1.5
1.0
0.5
0
Ore R
Ore R
Fe (+)

Figure 26: Ferritin expression is lower in *malvolio* female heads relative to parental strain w1118. (a) Western blot of protein extracts (5 μg) prepared from whole heads of w1118 and *malvolio* female flies raised on control diet, probed with polyclonal antiserum raised against native *D. melanogaster* ferritin (Georgieva et al, 2002). (b) Ferritin quantification: Four independent replicates were normalized to actin and averaged. Error bars indicate standard error of the mean. * indicates significant difference, $p<0.05$.

Figure 26

a)

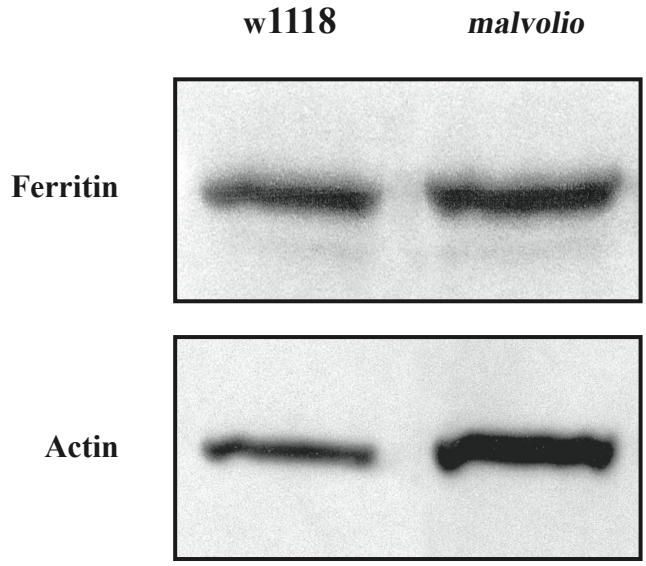
w1118
malvolio
Ferritin
Actin

b)

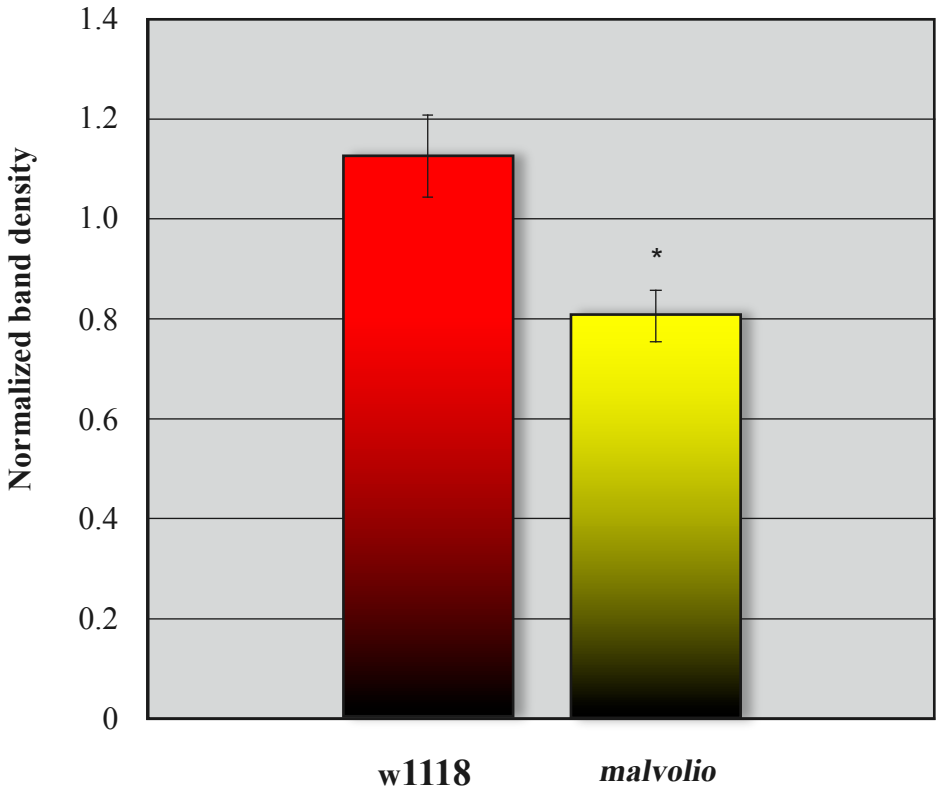
Normalized band density
1.4
1.2
1.0
0.8
0.6
0.4
0.2
0
*
w1118
malvolio

4.15 Effect of elevated dietary iron on ferritin expression in malvolio heads.

Ferritin expression in the *malvolio* mutant was examined by Western blot to see if iron supplementation affects iron storage in *malvolio* (Figure 27). A 20% increase in ferritin expression was measured by densitometry. The standard error between replicates did not exceed the difference between means and this was reproduced in 4 independent replicates. A t-test showed this difference is statistically significant. Iron supplementation causes a slight increase in ferritin expression in *malvolio* heads.

4.16 Effect of elevated dietary iron on ferritin expression in w1118 wildtype heads.

Dietary iron supplementation decreased ferritin expression by about 30% in the heads of w1118 females as determined by densitometry (Figure 28). This result was reproducible in 4 independent replicates and the standard error was less than the difference between the means. A t-test showed this decrease in ferritin expression is statistically significant.

4.17 Rationale for XAS.

We are interested in the role of iron in the pathogenicity of PKAN-type neurodegeneration. Although iron is elevated in *fumble*, there were no major differences in ferritin expression in the heads of the flies. This indicates that either the ferritin in *fumble* contains more iron than that of wildtype, or that iron in *fumble* is in a chemical

Figure 27: A 20% increase in dietary iron increases ferritin expression in heads of *malvolio* female flies. (a) Western blot of protein extracts (5 µg) prepared from whole heads of *malvolio* female flies raised on normal or iron supplemented (Fe +) diet, probed with polyclonal antiserum raised against native *D. melanogaster* ferritin (Georgieva et al, 2002). (b) Ferritin quantification: Four independent replicates were normalized to actin and averaged. Error bars indicate standard error of the mean. * indicates significant difference, $p<0.05$.

Figure 27

a)

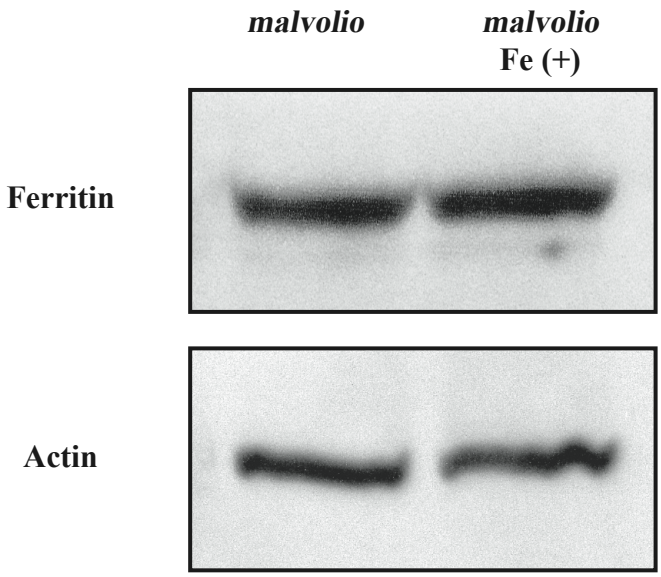
malvolio
malvolio
Fe (+)
Ferritin
Actin

b)

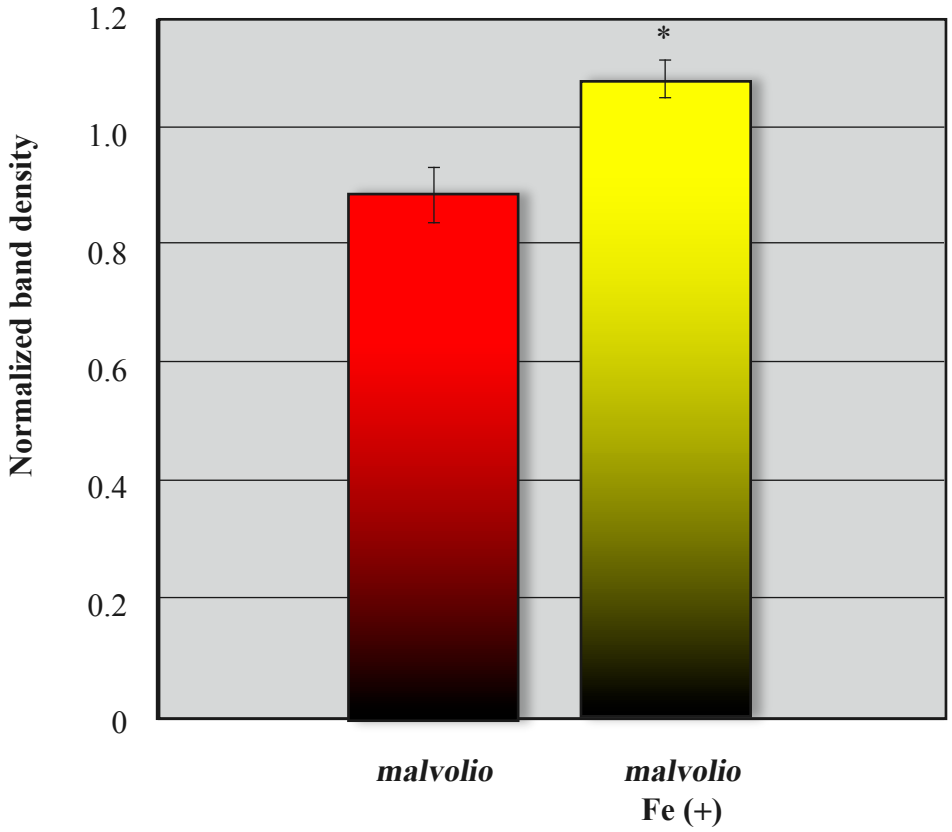
Normalized band density
1.2
1.0
0.8
0.6
0.4
0.2
0
*
malvolio
malvolio
Fe (+)

Figure 28: A 20% increase in dietary iron decreases ferritin expression in heads of w1118 female flies. (a) Western blot of protein extracts (5 μg) prepared from whole heads of w1118 female flies raised on normal or iron supplemented (Fe +) diet, probed with polyclonal antiserum raised against native *D. melanogaster* ferritin (Georgieva et al, 2002). (b) Ferritin quantification: Four independent replicates were normalized to actin and averaged. Error bars indicate standard error of the mean. * indicates significant difference, $p<0.05$.

Figure 28

a)

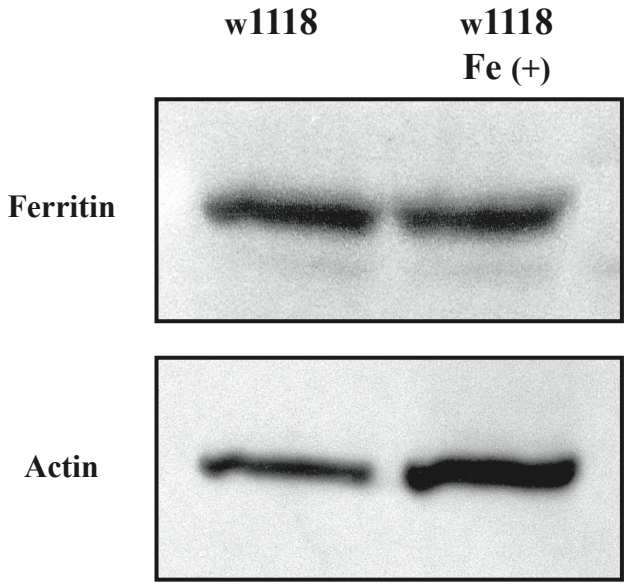
w1118
w1118
Fe (+)
Ferritin
Actin

b)

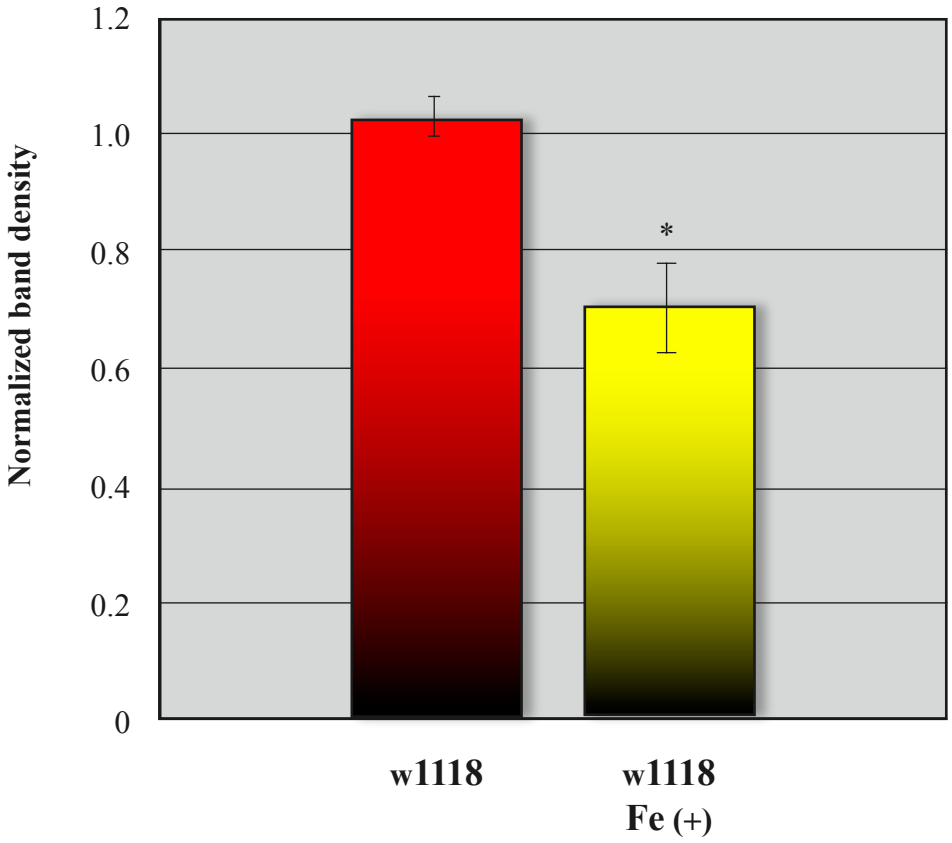
Normalized band density
1.2
1.0
0.8
0.6
0.4
0.2
0
*
w1118
w1118
Fe (+)

form not associated with ferritin. We used X-ray absorption spectroscopy to determine if the *malvolio* or *fumble* mutants have other non-ferritin forms of iron in the head. Pooled samples of approximately 50 whole heads of mixed sexes were tightly packed in the center of Lucite sample cells. An iron K-edge spectrum was collected from whole heads of Oregon R, *fumble*, and *malvolio* reared on either normal diet or iron-supplemented diet (Figure 29). All spectra were fitted with 21 iron-containing model compounds (Table 1). The fit and percent of model compounds contributing to each spectrum are shown in Table 2.

4.18 Chemical form of iron in heads of fumble relative to wildtype.

Although there was increased iron in the heads of the *fumble* mutants relative to Oregon R, ferritin expression was not affected in the *fumble* flies. If iron is in ferrihydrite, the form of iron stored in ferritin, it is in a soluble, non-toxic form. If iron is in a more labile form it may be free to react and cause oxidative damage to cells. If the *fumble* mutant is a model for human PKAN, abnormal iron species in the heads of the fly may be relevant to the human disease. Iron K-edge spectra were collected from whole heads of Oregon R and *fumble* flies fed on normal diet (Figure 29 A, B). Iron oxides are the most abundant chemical form of iron in Oregon R heads (58% goethite) followed by iron--sulfur clusters (32 %) and transferrin (10%) (Figure 29 A). The main chemical form of iron in the heads of *fumble* was also iron oxides (48% goethite, 41% frataxin) followed by 11% iron-sulfur clusters (Figure 29 B). Most of the iron in the *fumble* mutant is in the storage form of iron, as ferrihydrite and iron oxides. The major differences between

Figure 29: A 20 % increase in dietary iron supplementation changes the proportion of iron species in *Drosophila* adult heads. Iron K-edge spectra taken from whole heads of flies fed on normal diet or iron-supplemented diet were fitted with a linear series of model compounds. Fit (——), data (•••••), Ferrous species (• — • — •), horse-spleen ferritin (— — – — —), Rubredoxin (reduced) (— – —), Ferrochelatase (·····), ferric phosphate (----), ferric pyrophosphate (— — —), goethite (–••–••–), frataxin (— • • • —), transferrin (••• – – •••), hemin (— • – • —). Panel A) Oregon R, normal diet; B) *fumble,* normal diet; C) *malvolio,* normal diet; D) Oregon R, Iron diet; E) *fumble*, Iron diet; F) *malvolio*, Iron Diet.

Figure 29

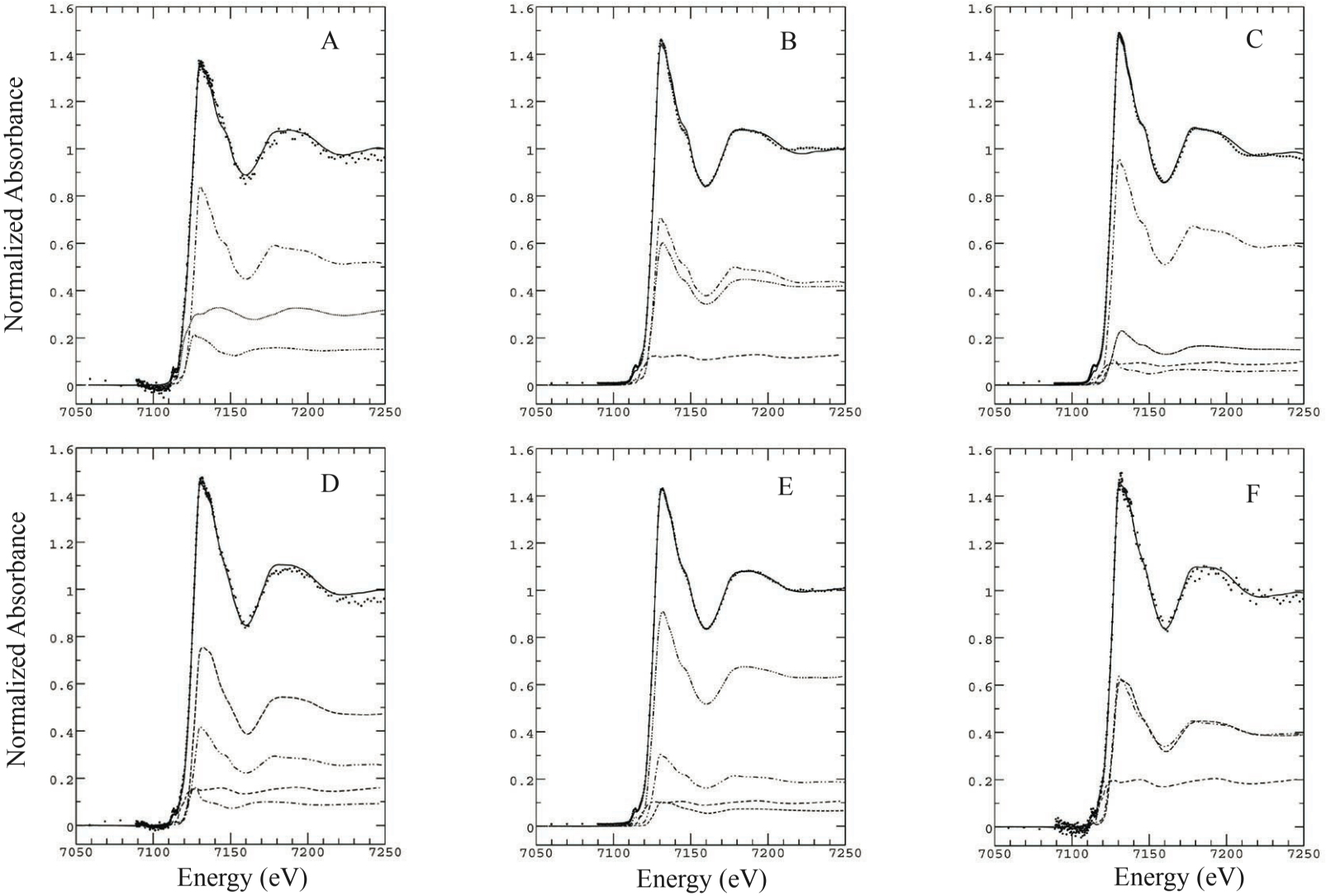
A
B
C
D
E
F
Normalized Absorbance
Normalized Absorbance
Energy (eV)
Energy (eV)
Energy (eV)
1.6
1.4
1.2
1
0.8
0.6
0.4
0.2
0
7050
7100
7150
7200
7250

Table 2: Percent of Iron Species in Whole Heads: Control or Iron Supplemented Diet.

Percentage Contributions from Spectra of Iron Compounds and Metalloproteins[a]							
Sample	Iron Oxides	Ferrous Species[b]	Iron sulfur clusters	Transferrin	Iron Phosphates	Hemin	Fit-error[c] x 10^{-4}
Oregon R – Normal Diet	58 (3)[d]		32 (3)[g]	10 (3)			3.757
Oregon R – Iron fed	27 (9)[d]	9 (1)	14 (2)[h]		50 (8)[i]		2.033
Fumble – Normal Diet	48 (9)[d] 41 (9)[e]		11 (1)[h]				1.704
Fumble – Iron Fed	62 (5)[e] 21 (4)[d]		10 (1)[h]		7 (4)[j]		0.377
Malvolio – Normal Diet	62 (7)[d] 23 (7)[f]	6 (1)	9 (1)[h]				0.983
Malvolio – Iron Diet	33 (9)[d]		15 (2)[h]		37 (7)[j]	15 (7)	3.203

[a] Values derived from the percentage contributions of spectra of iron compounds and metalloproteins to the best fit of spectra taken from whole heads plotted in Figure 10. Precisions, shown in parenthesis, are calculated as three times the estimated standard deviation, as derived from the diagonal elements of the covariance matrix; Best fit using all model spectra in Table 1; [b] $[Fe(H_2O)_6](NH_4)_2(SO_4)_2$; [c] Fit error (x 10^{-4}) or residual is the average of the sum of the squares of the differences between the observed and calculated signals for all data points in the spectrum; [d] goethite; [e] frataxin; [f] ferritin; [g] ferrochelatase; [h] reduced rubredoxin; [i] ferric pyrophosphate; [j] ferric phosphate.

wildtype and *fumble* were the absence of transferrin in *fumble* and the presence of frataxin-like ferrihydrite (Nichol et al 2003) in *fumble*. The absence of transferrin and presence of frataxin needs to be confirmed by Western blot analysis. This could not be performed at this time due to unavailability of antibodies cross-reacting with *Drosophila* transferrin and frataxin.

4.19 Effect of elevated dietary iron on chemical form of iron in fumble heads.

If dietary iron alters the chemical form of iron in the heads of the *fumble* mutant, this may be relevant to excess dietary iron in neurodegenerative disease. Iron K-edge spectra were compared between heads of *fumble* reared on either normal diet or iron-supplemented diet (Figure 29 B, E). The most abundant form of iron in the heads of *fumble* reared on iron-supplemented diet were iron oxides (62% frataxin, 21% goethite) with 7% ferric phosphate and 10% iron-sulfur clusters. The proportion of frataxin relative to goethite increased in iron fed *fumble* (Figure 29 E). Ferric phosphate was not present in the fit of *fumble* fed on a normal diet, but a small amount of ferric phosphate was seen under conditions of iron supplementation in *fumble*.

4.20 Effect of dietary iron on chemical form of iron in wildtype heads.

Iron supplementation induces ferric phosphate in *fumble* but it is not clear if this is pathological. Therefore, iron K-edge spectra were collected from whole heads of Oregon R flies fed on either normal or iron supplemented diet (Figure 29A, D). The most

abundant chemical form of iron in the heads of Oregon R is iron oxides (58% goethite), and then iron-sulfur clusters (32%) and transferrin (10%) when reared on normal diet (Figure 29 A). Dietary iron changes the proportions of iron species to ferric phosphates (50%), iron oxides (27% goethite), iron-sulfur clusters (14%), and ferrous species (9%) in wildtype (Figure 29 D). There is a shift from a high percentage of goethite, which is an iron oxide, to ferric phosphates which is a more labile form of iron with dietary iron supplementation. These data suggest that ferric phosphates in the iron-supplemented *fumble* are not pathological, but are a normal response to dietary iron.

4.21 Chemical form of iron in heads of malvolio relative to wildtype.

Since MVL is an iron transporter, the non-functional transporter in the *malvolio* mutant may alter the location of iron in the cell and have an effect on whether the iron is stored in ferritin, or in a more labile form in the cell. There was a decrease in ferritin expression detected in the heads of *malvolio* flies by Western blot (Figure 26). Although there is less ferritin in the heads of *malvolio*, ferritin levels do not always reflect iron levels. Ferritin can be found in the iron poor form, apoferritin, as well as the iron rich form, holoferritin. The expression of ferritin determined by western blotting does not distinguish whether the ferritin is iron loaded or not. Therefore, iron K-edge spectra were taken from whole heads of Oregon R and *malvolio* flies (Figure 29 A, C). The chemical form of iron in the heads of *malvolio* were mostly iron oxides (62% goethite, 23% ferritin), then iron-sulfur clusters (9%) and ferrous species (6%) (Figure 29 C). The heads of *malvolio* flies have a greater proportion of ferric oxides and the chemical form

of iron typically found in ferritin than the heads of Oregon R wildtype (Figure 29 A). This may indicate that the ferritin in *malvolio* is richer in iron or that there is less goethite in *malvolio* than wildtype.

4.22 Effect of dietary iron on chemical form of iron in malvolio heads.

Since there was no change in iron levels in the heads of *malvolio* fed on diet supplemented with an additional 20% iron, and the change in ferritin expression was minimal, we did not expect the chemical form of iron to change in the heads of *malvolio* fed on this diet. Iron K-edge spectra of *malvolio* flies reared on normal diet or iron-supplemented diet (Figure 29 C, F) showed that the most abundant form of iron in the heads of *malvolio* was ferric phosphates (37%) when reared on iron-supplemented diet (Figure 29 F). Goethite (33%), iron-sulfur clusters (15%) and hemin (15%) made up the rest of the fit. Iron supplementation leads to the presence of a high proportion of ferric phosphates in the heads of *malvolio* flies. As we saw with *fumble* and wildtype, ferric phosphates were not present in the *malvolio* flies reared on normal diet. An iron species with iron coordination similar to hemin also appeared in iron-fed *malvolio* that was not seen with a normal diet (Figure 29 C).

Ferric phosphates are present in the fits of Oregon R, *fumble*, and *malvolio* when reared on iron-supplemented diet, but not present in any when reared on normal diet. This seems to be a response to iron loading common to all flies. While the proportion of ferric phosphates in the heads of *fumble* is much less than in Oregon R and *malvolio* the

amount of iron in *fumble* is much greater and so if the actual amount of ferric phosphate is the same it will be a smaller proportion of the total. Therefore the response to iron supplementation with respect to ferric phosphate is probably similar in *fumble*, *malvolio* and wildtype.

5.0 Discussion.

5.1 General Discussion.

Iron metabolism is complex and poorly understood in *Drosophila*. This thesis examines the amount, location, and chemical form of iron in two *Drosophila* mutants, *fumble* and *malvolio* that are believed to have abnormal iron metabolism, and their respective wildtypes. The expression of two key proteins involved in iron transport and storage, MVL and ferritin respectively, are examined to determine how the abnormal iron metabolism affects their expression. For the purposes of this discussion, unless otherwise stated, we are referring to iron and protein in whole heads of adult female *Drosophila* aged 12-20 days. The *fumble* mutant has a defect in mitochondrial PANK and only the females exhibit a movement disorder that characterizes *fumble* (Afshar et al 2001). The movement disorder may be related to elevated iron levels in females (Figures 4, 5).

5.2 Iron in the fumble mutant.

ICP-MS was used to screen mutants for differences in iron levels in the heads. Oregon R fed on iron supplemented diet had higher iron levels and this observation was consistent with previous studies done in our lab (Nichol, unpublished). *Fumble* had higher iron levels than wildtype and this increased with iron supplementation. These data

also agreed with previous studies done in our lab (Nichol, unpublished). Unfortunately batch to batch differences and the high cost of ICP-MS precluded the collection of the number of replicates that would be required to establish statistical significance between groups.

The XAS imaging of whole flies showed increased iron in the heads of *fumble* compared to wildtype, which agreed with the ICP-MS data. To summarize, the *fumble* mutant has a defective PANK isoform that is predicted to be targeted to mitochondria (MitoProt, Expasy Tools), the iron is elevated in the heads, and the females show a movement disorder (Afshar et al 2001). Together the ICP-MS and XAS imaging data support the use of the *fumble* mutant as a relevant model system to study the mechanism of iron overload in human PKAN. Although more research is needed, the observation that dietary iron supplementation increases iron levels in *fumble* indicates that a reduction in dietary iron could benefit human PKAN patients.

5.3 The function of MVL in Drosophila.

There are three isoforms of MVL. The two largest (molecular weight 65.5 kDa) have identical protein coding sequences and differ only in the length of the 5'UTR (Flybase). The third isoform is truncated at the C terminus and has a molecular weight of 53.3 kDa. Truncation of the C-terminus removes several putative YXXΦ internalization motifs (Lam-Yuk-Tseung et al 2006). We are detecting the 53.3 kDa isoform (Appendix A). Although the antibody recognizes a stretch of amino acids common to all isoforms,

only the small isoform is seen in the whole head. The larger isoform may be expressed in other tissues, but I have no other evidence of tissue specific expression. It is possible that the three isoforms are regulated differently, respond differently to iron, have different subcellular locations, or are expressed in different tissues. Given these uncertainties, MVL could be functioning in the following ways (Figure 30):

1. MVL may transport iron from the endosome to the cytosol.

MVL could function like NRAMP2 in an endosome (Gruenheid et al 1999, Tabuchi et al 2000). In this model, MVL transports iron from the endosome to the cytosol. In mammals, NRAMP2 transports iron into the cytosol where it can be stored in cytosolic ferritin (Gruenheid et al 1999, Tabuchi et al 2000, Touret et al 2003), but there is no cytosolic ferritin in flies (Nichol et al 2002, Nichol & Locke 1990) so iron entering the cell by this route would be bound by citrate, phosphate, and other low molecular weight compounds until it can be sequestered in the vacuolar compartment. Elevated cytosolic iron should trigger the synthesis of HCH ferritin through IRE/IRP interactions. More extreme iron loading induces ferritin synthesis in wildtype flies (Georgieva et al 2002, Georgieva et al 1999). If MVL were acting to restrict iron transport into the brain, it should be downregulated in wildtype flies with dietary iron supplementation. MVL is upregulated in response to dietary iron, so MVL may be functioning in another way. Downregulation of MVL in response to dietary iron supplementation is seen only in *fumble*. This indicates that the response to iron in *fumble* is abnormal.

Figure 30: Proposed model of intracellular iron trafficking. Pink – iron; red – ferritin; orange - mitochondria; blue – endosomes; yellow - Tf; purple- TfR. The black arrows represent MVL in the direction of iron transport. The hemolymph contains ferritin, Tf, Tf-Fe, and NTBI. Tf could be bound to the PM by a GPi anchor, or possibly bind to a TfR to be endocytosed. Ferritin is secreted into the hemolymph through the vacuolar system. (1) MVL transports iron from the endosome to the cytosol. (2) MVL transports iron directly into mitochondria from the endosome. (3) MVL transports iron into the vacuolar system where it can be incorporated into ferritin. (4) MVL transports iron out of the vacuolar compartment into the cytosol. (5) MVL transports iron directly from the endosome into the ER where it can be incorporated into ferritin. (6) MVL transports iron directly from the hemolymph to the cytosol. * Adapted from Locke and Nichol, 1992.

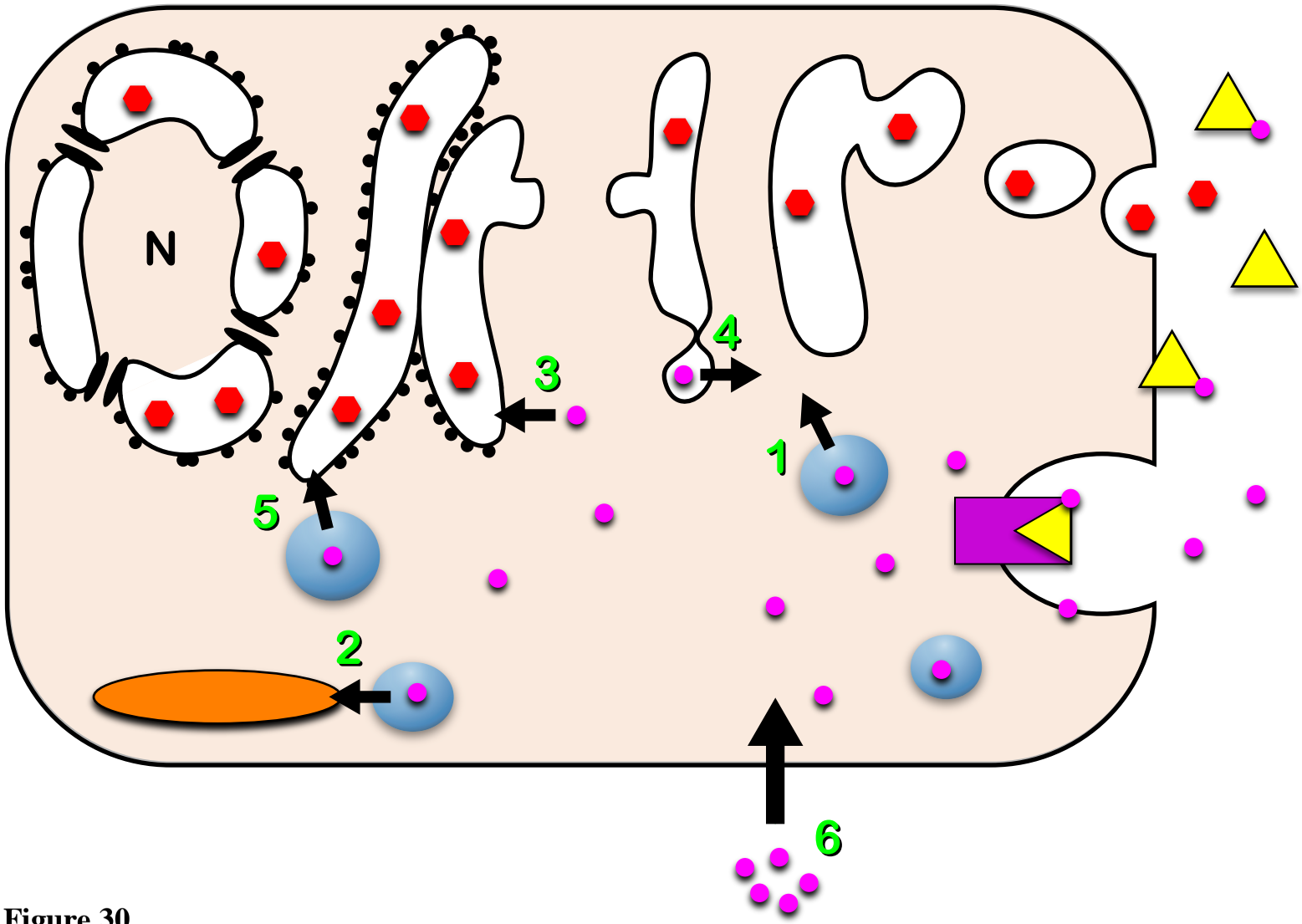

Figure 30

2. MVL may transport iron directly from the endosome to the mitochondria.

MVL could function like NRAMP2 in the endosomes of reticulocytes, to move iron directly between the endosome and the mitochondria so there is no free cytosolic iron intermediary (Sheftel et al 2007). In the fly brain, iron would be transported directly from the endosome to the mitochondria. Upregulation of MVL would result in increased mitochondrial iron. Mitochondrial dysfunctions through mutations in PANK cause human PKAN and are expected to be involved in the *fumble* phenotype (Johnson et al 2004, Yang et al 2005). If MVL is shuttling iron to the mitochondria, *fumble* should exhibit mitochondrial iron overload and this would be interesting to explore further. XAS provides some evidence of an increase in mitochondrial iron since ferrihydrite as seen in frataxin is seen in *fumble* but not in wildtype or *malvolio* (Figure 29). There may also be feedback mechanisms that enable mitochondria to limit iron under certain conditions, such as oxidative stress. If such mechanisms exist, excessive mitochondrial iron could downregulate MVL. Perhaps such mitochondrial feedback could be triggered in iron supplementation of *fumble* leading to downregulation of MVL.

3. MVL could transport iron from the cytosol to the vacuolar compartment.

MVL could function like NRAMP1 in mammalian macrophages that pump iron into the phagosome/lysosome compartment to kill microorganisms (Zwilling et al 1999). In the fly, MVL could transport iron from the cytosol into the vacuolar system for storage or export from the cell. Upregulation would result in movement of iron out of the cytosol

and into either vacuolar iron storage and/or secretion of ferritin. This seems a likely scenario for MVL function. Paradoxically, MVL upregulation could result in more iron being secreted from the cell. In wildtype flies, dietary iron would induce ferritin secretion, while in *fumble*, downregulation of MVL would induce iron overload.

4. MVL could transport iron from the vacuolar system to the cytosol.

It has also been proposed that NRAMP1 can remove iron from the phagosome to starve microorganisms of iron or that NRAMP1 can move iron bidirectionally (Jabado et al 2000, Nevo & Nelson 2006, Zwilling et al 1999). If MVL were moving iron from the vacuolar system to the cytosol, then upregulation would result in the movement of iron out of the vacuolar system where it is safely stored, into the cytosol, nucleus, or mitochondria. While this is a likely way for compartmentalized iron to be used by normal cells during times of iron starvation, in *fumble*, excessive movement of iron out of storage could result in oxidative stress. This is particularly likely given that cytosolic ferritin is absent in flies.

5. MVL may transport iron from the endosome to the ER.

MVL may transport iron directly from the endosome to the ER, where it can be incorporated into ferritin and then secreted into the hemolymph. Upregulation of MVL would be protective in high iron conditions. The upregulation of MVL in *fumble* could increase transport of iron into the ER and promote ferritin secretion. The upregulation of

MVL in the iron-supplemented wildtype also favors this mechanism. Ferritin secretion could account for the lack of change in ferritin found in *fumble* and in iron supplemented wildtype. The downregulation of MVL could account for the increased iron levels in the heads of iron supplemented *fumble*, since a reduction in MVL would lead to iron accumulation in the cell, whether it remains in the endosome, or ends up in the cytosol, mitochondria, or other compartment.

6. MVL transports iron directly from the hemolymph to the cytosol.

NRAMP2 is expressed in the plasma membrane of mammalian cells (Forbes & Gros 2003, Picard et al 2000). There is evidence that MVL may localize to the plasma membrane in flies as well (Folwell et al 2006). MVL may transport iron directly from the hemolymph to the cytosol, similar to iron uptake at the gut epithelium in mammals (Garrick et al 1999, Picard et al 2000). An upregulation in MVL could lead to increased iron uptake into cells, which is consistent with the increased iron levels and upregulation of MVL seen in *fumble* and in iron supplemented wildtype. The downregulation of MVL in iron supplemented *fumble* and high iron levels suggest this is not the only mechanism of iron transport at the plasma membrane.

The function of MVL is likely a combination of those described previously. Our model suggests this transporter transports iron from the endosome to the ER where it can be sequestered in ferritin and then secreted into the hemolymph. MVL may also transport iron from the endosome to the mitochondria. This model explains the lack of

ferritin induction with increased iron in the heads of the *fumble* mutant and in iron supplemented wildtype flies. The increased expression of MVL in the *fumble* mutant as well as the iron loaded wildtype flies may function to get rid of excess cellular iron and decrease the oxidative damage caused by iron intermediates in the cytosol. MVL would seem to be protective in iron overload in the wildtype flies. The induction of MVL could provide a mechanism to transport the excess iron to the ER for incorporation into ferritin.

A decrease in MVL expression caused by iron supplementing the diet in the *fumble* fly is an unexpected result. Since the iron fed *fumble* still accumulates more iron than *fumble* fed normal diet, another pathway may also be involved in the accumulation of iron in *fumble*. It also suggests that iron has some role in regulating MVL expression, possibly at the transcriptional level. If MVL is upregulated with dietary iron in the wildtype flies to compensate for the excess iron so more can be transported from the endosome to the ER, the greater concentration of iron in *fumble* fed on iron-supplemented diet could lead to a disruption in the normal MVL expression. The excess iron in *fumble* fed iron-supplemented diet could disrupt MVL expression, leading to less iron secretion through the ferritin pathway and thus accumulation of iron in the cells. This may be related to MVL transport of iron to the mitochondria. Mitochondria may have mechanisms to compensate for excess iron and oxidative stress as previously discussed. Further studies are needed to understand the regulation of MVL expression in *Drosophila*.

5.4 MVL expression in fumble.

To probe the mechanism of iron overload in *fumble*, we examined the iron transporter, MVL. Nothing is known about the regulation of MVL expression in flies. Since an IRE has not been found in the mRNA of *mvl*, it is presumed to be transcriptionally regulated.

We found a startling increase in the expression of MVL in *fumble* (Figure 12). This increased MVL expression is of significant interest because no other proteins involved in iron metabolism have been associated with PANK deficiency so far. In mammals, the MVL homologue NRAMP2 is downregulated when dietary iron is high (Martini et al 2002, Zoller et al 1999). Therefore the increased expression of MVL (Figure 12) when iron is in excess (Figures 4,5) suggests that the transporter is dysregulated in *fumble* since *fumble* has 2 fold more iron than wildtype.

Iron supplementation of the diet in wildtype flies increased iron levels (Figure 4, 9) and the expression of MVL (Figure 12, 14), suggesting that MVL may be induced by dietary iron. Both the iron supplemented wildtype and the *fumble* have high iron levels and high MVL expression and we postulate that MVL may transport iron from the endosome directly to the ER where it can be loaded into ferritin, then secreted to the hemolymph (Figure 30). This enables the fly to keep iron outside of its cells where it may do less damage. *In vitro*, transcription of NRAMP1 is increased in response to oxidative stress (Yeung et al 2004). Oxidative stress could play a role in the induction of MVL in the *fumble* mutant and in iron supplemented wildtype (Figure 12, 14), since iron is known to contribute to oxidative stress (Blokhina et al 2003).

Surprisingly, the expression of MVL was decreased in the heads of *fumble* reared on iron supplemented diet (Figure 13). Since dietary iron induced MVL expression in the wildtype heads, this suggests that MVL regulation is altered in the *fumble* mutant. If MVL is responsible for importing some of the excess iron in the heads of the *fumble* mutant, there is likely another pathway contributing to the iron overload. Cellular iron uptake in mammals can occur directly through the plasma membrane through NRAMP2, or through receptor-mediated endocytosis through the transferrin receptor. The excess iron in the *fumble* could be taken up by a transferrin-related mechanism, although no transferrin receptor has yet been found in the *Drosophila* genome. Of the three transferrins found in *Drosophila*, two are GPI anchored and resemble melanotransferrin (Dunkov & Georgieva 2006). Melanotransferrin does not require a transferrin receptor to take in iron (Food & Richardson 2002, Food et al 2002, Kennard et al 1995, Richardson 2000, Richardson & Morgan 2004), and *Drosophila* transferrins may operate in a similar manner (Dunkov & Georgieva 2006). Although no transferrin receptor has been found in the *Drosophila* genome, a new transferrin receptor has recently been described in mammals (Raje et al 2007), but further work needs to be done to determine if GAPDH acts similarly in flies.

5.5 Ferritin expression in fumble.

No consistent changes were seen in ferritin expression between wildtype and *fumble* (Figure 23) or after iron loading of wildtype and *fumble* (Figures 24, 25). There may be several reasons for the lack of change in ferritin expression.

The dietary iron supplementation was low at only 20% above normal dietary iron levels, and this may be insufficient to affect ferritin expression. Dietary iron supplementation has been shown to increase ferritin message levels, but this was at 5mM $FeCl_3$ supplementation, about 500X the level used in these experiments (Georgieva et al 2002, Georgieva et al 1999).

There could be sufficient apoferritin present in the ER to take up all the new iron, since apoferritin has the capacity to store up to 4500 atoms of iron in each polymer (Theil 1990). New synthesis of ferritin may not be required at low level dietary supplementation. However, XAS analysis did not show an elevated proportion of ferritin-like ferrihydrite, but rather ferric phosphate.

If new ferritin had been synthesized, it may have been secreted to the hemolymph to decrease the iron load in the flies. The tissue to hemolymph ratio in the heads is high, so changes in ferritin levels in the hemolymph would not be as apparent in the heads as opposed to whole flies.

There may have been an increase in HCH expression, but this is not visible due to the dominance of LCH. The ferritin antibody we used detects both LCH and HCH ferritin subunits, but the LCH subunit was so abundant on Western blots that the HCH subunit could not be resolved. LCH is the predominant subunit in all life stages of the Oregon R strain of *Drosophila* (Georgieva et al 2002), and was the predominant subunit in all 4 strains that were used in these experiments. LCH does not contain the ferroxidase

residues that are present in HCH and does not share strong sequence identity with mammalian L chain ferritin, but is highly expressed in *Drosophila* (Georgieva et al 2002). Should antibodies become available that can distinguish between the HCH and LCH subunits, it would be of interest to determine if iron supplementation increases the expression of HCH.

Expression of mitochondrial ferritin in the *fumble* mutant would also be of interest since a deficiency in mitochondrial PANK would be expected to affect iron metabolism in the mitochondria. A custom antibody made to *Drosophila* mitochondrial ferritin did not detect mitochondrial ferritin on western blots. Preliminary data show no increase in mitochondrial ferritin mRNA in *fumble* (Nichol, personal communication).

This may indicate that some iron may not be stored in ferritin, but it could be in the cytosol as low molecular weight iron complexes, in the hemolymph as non-transferrin bound iron (NTBI), or it could be bound to transferrin in the hemolymph (see section 5.6).

XAS imaging showed iron localizes to antennae and rostrum in *Drosophila* (see section 5.8). These structures contain sensory neurons which may utilize iron or they may store iron in goethite rather than ferritin in wildtype and *fumble* flies as discussed in section 5.6.

5.6 Iron chemistry in fumble.

The chemical form of iron in *fumble* heads is mostly ferritin (ferrihydrite) and goethite (Figure 29 B and D). Goethite has been found in the haemosiderin cores of human patients with thalassemia. Haemosiderin is formed by lysosomal degradation of ferritin and contains particles of hydrated iron (III) oxyhydroxide associated with organic components (Ward, 1994; Hackett, 2007). Goethite has a more ordered structure than ferrihydrite (Chasteen & Harrison 1999). XAS fits of the flies show that goethite forms in the head. The goethite may occur as a type of extracellular haemosiderin, or perhaps in *Drosophila* ferritin. The iron core of horse spleen ferritin was shown to contain a mixture of iron oxides, including hematite and magnetite, as well as highly disordered material, but not goethite (Cowley et al 2000). However, there could be differences in the structure of the ferritin iron core since insects assemble the core in the ER or hemolymph rather than the cytosol as in mammals. The iron core of ferritin for bacteria has been shown to contain phosphate, which is not seen in mammalian ferritin (Mann et al 1986). Goethite has a more crystalline, more highly ordered structure than ferrihydrite and has a needle-like appearance (St. Pierre et al 1986). Rod-like, electron dense particles have been observed by electron-microscopy in fly heads (Nichol, personal communication). This could account for the presence of goethite in the XAS fits.

Iron coordination seen in transferrin is present in the wildtype but not the *fumble* K-edge (Figure 29 A, B). Transferrin message levels are decreased with iron supplementation of 5 mM $FeCl_3$ in *Drosophila* (Yoshiga et al 1999). The reduction in transferrin levels could be a mechanism of decreasing the transferrin-dependant iron uptake when iron is abundant. The presence of transferrin-bound iron in wildtype flies

fed on normal diet, which have low iron levels, and the absence of transferrin-bound iron in the *fumble* and wildtype flies fed on iron-supplemented diet, which have high iron levels, are supported by the findings of Yoshiga et al (1999). Down-regulation of Tf in *fumble* needs to be confirmed by Western blotting.

The presence of ferric phosphates in the iron supplemented flies suggests that dietary iron changes the iron chemistry in the heads (Figure 29 D, E). Since there was no ferric phosphate present in wildtype or the mutants fed on control diet, the presence of iron phosphates is linked to increased iron uptake. If transferrin expression is decreased with dietary iron (Yoshiga et al 1999), there may be insufficient transferrin to bind iron in the hemolymph. This could result in iron phosphates in the hemolymph. XAS of whole heads does not distinguish if the ferric phosphates are in the tissue or hemolymph, but a decreased expression of transferrin with increased dietary iron could lead to more labile iron in the hemolymph. It is also of note that some forms of haemosiderin in diseased patients have phosphate in the iron core (Ward et al 1994).

Much of the iron in the normal diet comes from yeast, in organic form bound to proteins or citrate. The ferric chloride used to supplement the diet would be dissociated in the low pH of the midgut to Fe^{3+} and Cl^{-}. Absorption of this free iron could disrupt normal homeostasis and possibly lead to ferric phosphate accumulation. There are no published papers available concerning the differences in organic vs. inorganic iron uptake in *Drosophila.*

5.7 Iron in the malvolio mutant.

.

Iron levels in *malvolio* were similar with or without iron supplementation using ICP-MS and XAS imaging of whole flies (Figures 18, 19). Although more replicates of these data would have been ideal, the data supports the hypothesis that the *malvolio* mutant does not absorb dietary iron effectively. However, dietary iron also did not affect the iron levels in w1118 (Figures 21, 22), the parental strain for *malvolio,* indicating that reduced iron absorption cannot be attributed to the *malvolio* mutation. The mvl^{97f} mutation does not affect overall iron concentration. Since the *malvolio* mutation is not detrimental to the mutant and does not affect viability, *malvolio* must be absorbing enough iron from another pathway. Because the w1118 wildtype did not accumulate iron in the heads when reared on iron supplemented diet and the Oregon R wildtype did accumulate iron (Figures 9, 21), further studies should be done on iron accumulation in wildtypes. There is no published information on differences in metal levels or metal metabolism in wildtype flies of different genetic background.

5.8 Localization of iron in malvolio heads.

The *malvolio* mutant has previously been shown to have defective taste perception that can be corrected by dietary iron supplementation with either $FeCl_2$ or $MnCl_2$ (Orgad et al 1998). The role of Fe and Mn in taste perception is unclear, it has been speculated that divalent metals may be involved in signal transduction involved in taste perception (Orgad et al 1998, Rodrigues et al 1995). Our data shows that the

malvolio mutant has similar iron levels to its parental strain (Figures 15, 16). This suggests that MVL is not the main iron uptake pathway in *Drosophila* and there must be redundant iron uptake mechanisms. The XAS microprobe imaging showed that the antennae and rostrum had a higher concentration of iron relative to the rest of the regions of the head in all of the images (Figures 17, 20). The presence of iron in the rostrum could be iron accumulating in neurons which run from gustatory receptor neurons and olfactory neurons through the rostrum to the brain (Gao et al 2000). The antennae function as near-field sound receptors and contain neurons that convert mechanical signals to electrochemical responses in the peripheral nervous system (Todi et al 2004). The antennae contain primary olfactory sensory neurons, approximately 1200 neurons per antenna (Gao et al 2000). The maxillary palps also contain olfactory sensory neurons, about 120 per palp (Gao et al 2000). Gustatory receptor neurons are found on the labial palps, tarsis, wings, and genitalia of *Drosophila* (Ishimoto & Tanimura 2004). Both the maxillary palps and labial palps appear to accumulate iron in the images, it may be that these sensory receptors use metals in signal transduction. The images show that these structures accumulate iron in both *malvolio* and wildtype. The significance of the iron in the antennae is unknown. To the best of my knowledge, there are no publications concerning iron in the antennae of *Drosophila*.

5.9 Ferritin expression in the malvolio mutant.

While no significant changes in ferritin expression were observed in the heads of *fumble* and its wildtype on normal or iron supplemented diet, we were able to detect changes in ferritin expression in the heads of *malvolio* and its wildtype. Ferritin

expression was slightly lower in *malvolio* compared to wildtype (Figure 26). This suggests that iron metabolism is dysregulated in the *malvolio* mutant, but the physiological relevance of a small change in ferritin expression is unknown. It is possible that the *malvolio* gustatory defect results in reduced food intake or has other uncharacterized effects on fly physiology.

If the iron content of the ferritin is on average the same, then there may be less storage iron in *malvolio* and more ferritin already made in wildtype to deal with fluxes of iron. Since the *malvolio* mutant may have decreased iron transport, the basal level of ferritin expression may be lower because the mutant would not have to compensate for the iron fluxes that occur in the wildtype. Tissue specific expression of ferritin in *malvolio* could give more insight to this finding.

When *malvolio* is raised on iron supplemented diet, an increase of ferritin expression is observed (Figure 27) and this is linked with an increased proportion of ferrihydrite of the ferritin types seen in fits of the iron K-edge. This indicates that some of the dietary iron is sequestered in ferritin (Figure 29). This is consistent with other studies that show upregulation of ferritin expression in *Drosophila* with dietary iron supplementation of 5 mM $FeCl_3$ (Georgieva, 2002). Iron supplementation in this experiment is at a lower level than the 5mM $FeCl_3$ used by Georgieva et al, but it is a more physiologically relevant level of dietary iron and less likely to produce a stress response. The increased ferritin (Figure 27) and ferrihydrite (Figure 29) may therefore be involved in the correction of signal transduction in gustatory neurons.

A decrease in ferritin expression was observed in the heads of w1118 wildtype flies fed on iron supplemented diet (Figure 28). The effect of iron supplementation on ferritin expression in the heads of the *malvolio* mutant differs with that of its wildtype, indicating that ferritin expression in the heads of *malvolio* is abnormal. As stated previously, this could be due to *malvolio* having less ferritin and therefore less iron storage capacity. This could also be a result of defective intracellular iron transport through the MVL pathway. Increased iron in the cytosol should lead to ferritin synthesis either by IRE/IRP interaction or transcriptional regulation. However, a defect in MVL transport into the ER could lead to ineffective iron storage in newly synthesized vacuolar ferritin and holoferritin secretion would not decrease iron in the tissue. Wildtype flies could have efficient intracellular trafficking of iron to the ER which would promote incorporation of iron into ferritin, and thus promote holoferritin secretion into the hemolymph, and excretion of ferritin from the gut to the gut lumen.

If MVL is involved in transport of iron into the cytosol through the plasma membrane, it is not likely the only pathway involved. Perhaps iron entering the cell through MVL is bound and handled differently than iron entering by other routes. Changes in bound iron may be reflected in X-ray absorption spectra at the iron K-edge (see section 5.10).

5.10 Iron chemistry in the malvolio mutant.

The iron K-edge analysis of the *malvolio* mutant showed that the iron was predominantly in the form of goethite and ferritin (Figure 29 C and F). *Malvolio* contained almost three times more goethite than ferritin. Since goethite was prominent in most fits of the *Drosophila* heads, it is likely not pathological. However, goethite is associated with haemosiderin in human diseases such as haemochromatosis, Alzheimer's disease, and β-thalassemia (Chasteen & Harrison 1999, Quintana et al 2006, Ward et al 1994). Although goethite has not been found in ferritin (Cowley et al 2000), the structure of the iron cores of bacterial, plant, and mammalian ferritins are known to be different (Mann et al 1986, St Pierre et al 1986), and it is possible that this is also the case for *Drosophila* ferritin.

Interestingly, when *malvolio* is reared on iron supplemented diet, there is a shift in the proportion of iron species in the heads. The most prominent form of iron is ferric phosphates. Phosphates have been associated with the iron cores of haemosiderin in human disease (Chasteen & Harrison 1999, Quintana et al 2006, Ward et al 1994). Bacterial ferritin also contains phosphates in the iron core (Mann et al 1986, St Pierre et al 1986). Dietary iron caused ferric phosphates to be present in both mutants and the wildtype flies. To better understand the biological significance of the phosphate in the heads of iron loaded flies, the structure of the iron core of ferritin should be determined.

Also of note is the presence of an iron species with coordination similar to hemin in the iron fed *malvolio* heads (Figure 29F). Hemin is the highly reactive oxidized form of heme and has been associated with iron-dependant oxidative injury to neuron-like cells

(Goldstein et al 2003). Only iron-supplemented *malvolio* contained hemin, and this is of interest because of the implications for oxidative damage caused by hemin in cells. This also supports the idea that iron metabolism is dysregulated in the *malvolio* mutant. If MVL transports iron into the ER, as suggested in the model (Figure 30), a disruption in the MVL transport pathway could lead to excess free iron in the cytosol which could be responsible for the iron phosphates and the hemin-like reactive iron compounds in the K-edge fits. Excess iron in the cytosol could trigger increased synthesis of HCH ferritin by IRE-IRP interaction.

The ferric phosphate could be non-transferrin bound iron. Iron in the tissue can not be distinguished from iron in the hemolymph by XAS of whole heads. Iron phosphates, as well as the hemin-like iron, could be accumulating in the hemolymph. Excess dietary iron decreases the message levels of transferrin in *Drosophila* (Yoshiga et al 1999). The excess iron could form low molecular weight complexes in the hemolymph if there is not enough transferrin to bind the iron.

6.0 Conclusions and Future Directions.

6.1 Expression of 53 kDa MVL isoform in Drosophila heads.

Only the 53.3 kDa isoform of MVL is observed in western blots of whole heads. This implies that this isoform is important in the heads of *Drosophila*. This is the first finding of tissue specific expression of an isoform of MVL in *Drosophila*. Subcellular localization of MVL needs to be determined. MVL could be expressed in the plasma membrane and be involved in iron uptake from extracellular fluid, as well as expressed in endosomes and participate in intracellular iron trafficking. This could be done using differential ultra-centrifugation or density centrifugation to look at nuclear, mitochondrial, microsomal, and plasma membrane fractions. Also of interest would be to determine if the 3 isoforms of MVL are expressed in different subcellular membranes or in different tissues. Custom antibodies would have to be made to identify each isoform.

6.2 MVL responds to iron.

MVL appears to be regulated by iron transcriptionally, rather than translationally regulated by iron since no IRE is found in the mRNA. This is of interest because NRAMP2 expression is regulated by iron in mammals. NRAMP1 is regulated by oxidative stress, which can be caused by iron and could play a role in the regulation

of MVL as well. MVL may be induced by iron in the cell to increase transport to the vacuolar system where it can be incorporated in ferritin. Extensive analysis has not been done of the *mvl* gene, so regulation at the transcriptional level is poorly understood. Only the 53 kDa isoform of MVL is observed in this study; the larger isoforms may be seen in other tissues and the effect of iron supplementation on MVL should be examined here. It would be of interest to determine if dietary iron changes MVL expression in the gut, since MVL is likely the main transport mechanism for dietary iron uptake.

6.3 MVL is upregulated in fumble.

Little research has been done in the area of PKAN, since a good model system has not been fully established. The mouse model for human PKAN that lacks the mitochondrially targeted PANK isoform does not show a neurodegenerative phenotype. It does however show retinal degeneration and azoospermia (Kuo et al 2005). Recently, pantothenic acid deficiency was found to induce a movement disorder, similar to dystonia, in the mouse model of PKAN. Dietary supplementation of pantothenic acid restored the mice to normal (Kuo et al 2007), but since the mice do not accumulate iron it is not known what effect this might have on reducing iron overload in humans.

The *Drosophila* mutant *fumble* is the first model for human PKAN to exhibit a similar phenotype, have a similar PANK mutation, and as we have shown, have abnormal iron accumulation. The finding of MVL dysregulation in the *fumble* mutant gives reason

to pursue further studies in this area. The expression of NRAMP1 and NRAMP2 should be looked at in human PKAN patients. Since the *fumble* mutant also had increased iron levels and decreased MVL expression in the heads with dietary iron supplementation, other iron uptake pathways should also be considered for a role in iron uptake in the mutant. Currently there is no antibody available for *Drosophila* transferrin, but this would be of interest to examine in *fumble*. Transferrin may be responsible for iron uptake at the plasma membrane and could be involved in the excess iron in the *fumble* mutant. NRAMP1 is believed to be protective against oxidative stress (Yeung et al 2004). Induction of MVL with dietary iron supplementation of wildtype and in *fumble* could be a mechanism of reducing oxidative stress by removing excess iron from the cytoplasm; this appears to be disrupted in *fumble.*

6.4 Iron accumulates in sense organs.

The observation of iron accumulating in the antennae and the rostrum of the heads indicates that iron may play an important role in these structures, which contain sensory neurons. This is the first observation of this in *Drosophila* and suggests that iron may be important in the function of the neurons in the antennae, maxillary palps, and labial palps. MVL may contribute to the iron accumulation in these organs (Rodrigues et al 1995). Very high resolution microprobe imaging may be useful to localize iron to the sensory neurons in these structures.

6.5 Dietary iron changes the chemical form of iron in the heads.

For the first time a change in iron chemistry has been seen with iron supplementation of the diet in *Drosophila*. The ferric phosphates are likely in the hemolymph as non-transferrin bound iron, but this needs to be confirmed. Transferrin expression should be examined by western blotting in these flies to determine if a reduction in Tf is contributing to the presence of ferric phosphates. The ferric phosphates could be an intermediary between iron being transported into the cell and stored in ferritin. This cannot be localized by bulk XAS of whole heads. Further investigation is needed to determine if phosphates occur in the hemolymph, cytosol, ER, or mitochondria. Iron has been observed in the ER of insects that is not stored in ferritin (Locke & Leung 1984). Ferric phosphates may be present in the ER prior to iron incorporation into ferritin, in the cytosol before transport into the mitochondria and vacuolar system, or in the mitochondria. Pyrophosphate has previously been found to increase iron accumulation in mitochondria. Ferric pyrophosphate has been found bound to mitochondria, and is also implicated in cytosolic iron transport (Konopka & Romslo 1981, Nilsen & Romslo 1984a, Nilsen & Romslo 1984b, Popescu et al 2007).

The diet was supplemented with inorganic iron in these experiments. The mechanism of dietary iron uptake for inorganic and organic iron differs in mammals (Dunn et al 2007). The chemistry of iron should be examined after dietary iron supplementation with an organic form of iron, such as ferritin. Protein bound iron may be handled differently than inorganic iron. All literature concerning iron supplementation of *Drosophila* uses inorganic iron.

We used ferric chloride, not ferrous chloride, which was used in the taste perception restoration study (Orgad et al 1998). We could look at differences in iron uptake using ferrous iron. While it is assumed that iron absorption occurs mainly in the iron region of the gut, which has a low pH, some iron may be absorbed anterior or posterior to this region. Anterior to the iron region the gut pH is higher and ferrous iron is more soluble than ferric iron at a higher pH.

6.6 Ferritin expression in Drosophila.

Ferritin expression was unchanged in *fumble* and wildtype flies. The expression of LCH was the only ferritin subunit observed. Although technically difficult, looking at changes in ferritin expression in hemolymph may show differences between the mutants and their wildtypes. Also of interest would be to look at expression of HCH and Fer3HCH in the mutants. HCH is known to be regulated by iron levels, and little is known about the regulation of Fer3HCH. The expression of these ferritins could be altered in the mutants. This study was the first to examine ferritin expression in *Drosophila* using physiologically relevant levels of iron supplementation.

References.

Abouhamed M, Gburek J, Liu W, Torchalski B, Wilhelm A, et al. 2006. Divalent metal transporter 1 in the kidney proximal tubule is expressed in late endosomes/lysosomal membranes: implications for renal handling of protein-metal complexes. *Am J Physiol Renal Physiol* 290: F1525-33

Afshar K, Gonczy P, DiNardo S, Wasserman SA. 2001. fumble encodes a pantothenate kinase homolog required for proper mitosis and meiosis in Drosophila melanogaster. *Genetics* 157: 1267-76

Arosio C, Fossati L, Vigano M, Trombini P, Cazzaniga G, Piperno A. 1999. Hereditary hyperferritinemia cataract syndrome: a de novo mutation in the iron responsive element of the L-ferritin gene. *Haematologica* 84: 560-1

Asenjo A. 1968. Cytosiderosis and iron deposits in ventrolateral nucleus of the thalamus in Parkinson's disease. Clinical and experimental study. *Johns Hopkins Med J* 122: 284-94

Bannon DI. 2003. Effect of DMT1 knockdown on iron, cadmium, and lead uptake in Caco-2 cells. *American Journal of Physiology. Cell Physiology* 284: 53-61

Basclain KA, Jeffrey GP. 1999. Coincident increase in periportal expression of iron proteins in the iron-loaded rat liver. *Journal of Gastroenterology and Hepatology* 14: 659-68

Blackwell JM. 1998. Genetics of host resistance and susceptibility to intramacrophage pathogens: a study of multicase families of tuberculosis, leprosy and leishmaniasis in north-eastern Brazil. *Int J Parasitol* 28: 21-8

Blackwell JM, Searle S, Mohamed H, White JK. 2003. Divalent cation transport and susceptibility to infectious and autoimmune disease: continuation of the Ity/Lsh/Bcg/Nramp1/Slc11a1 gene story. *Immunol Lett* 85: 197-203

Blokhina O, Virolainen E, Fagerstedt KV. 2003. Antioxidants, oxidative damage and oxygen deprivation stress: a review. *Ann Bot (Lond)* 91 Spec No: 179-94

Bonilla E, Estevez J, Suarez H, Morales LM, Chacin de Bonilla L, et al. 1991. Serum ferritin deficiency in Huntington's disease patients. *Neurosci Lett* 129: 22-4

Brooks DG, Manova-Todorova K, Farmer J, Lobmayr L, Wilson RB, et al. 2002. Ferritin crystal cataracts in hereditary hyperferritinemia cataract syndrome. *Invest Ophthalmol Vis Sci* 43: 1121-6

Camaschella C, Roetto A, Cali A, De Gobbi M, Garozzo G, et al. 2000. The gene TFR2 is mutated in a new type of haemochromatosis mapping to 7q22. *Nat Genet* 25: 14-5

Campanella A, Isaya G, O'Neill HA, Santambrogio P, Cozzi A, et al. 2004. The expression of human mitochondrial ferritin rescues respiratory function in frataxin-deficient yeast. *Hum Mol Genet* 13: 2279-88

Canonne-Hergaux F, Fleming MD, Levy JE, Gauthier S, Ralph T, et al. 2000. The Nramp2/DMT1 iron transporter is induced in the duodenum of microcytic anemia mk mice but is not properly targeted to the intestinal brush border. *Blood* 96: 3964-70

Canonne-Hergaux F, Gros P. 2002. Expression of the iron transporter DMT1 in kidney from normal and anemic mk mice. *Kidney Int* 62: 147-56

Canonne-Hergaux F, Gruenheid S, Ponka P, Gros P. 1999. Cellular and subcellular localization of the Nramp2 iron transporter in the intestinal brush border and regulation by dietary iron. *Blood* 93: 4406-17

Canonne-Hergaux F, Levy JE, Fleming MD, Montross LK, Andrews NC, Gros P. 2001. Expression of the DMT1 (NRAMP2/DCT1) iron transporter in mice with genetic iron overload disorders. *Blood* 97: 1138-40

Casey JL, Hentze MW, Koeller DM, Caughman SW, Rouault TA, et al. 1988. Iron-responsive elements: regulatory RNA sequences that control mRNA levels and translation. *Science* 240: 924-8

Castrillon DH, Gonczy P, Alexander S, Rawson R, Eberhart CG, et al. 1993. Toward a molecular genetic analysis of spermatogenesis in Drosophila melanogaster: characterization of male-sterile mutants generated by single P element mutagenesis. *Genetics* 135: 489-505

Caughman SW, Hentze MW, Rouault TA, Harford JB, Klausner RD. 1988. The iron-responsive element is the single element responsible for iron-dependent translational regulation of ferritin biosynthesis. Evidence for function as the binding site for a translational repressor. *J Biol Chem* 263: 19048-52

Cazzola M, Bergamaschi G, Tonon L, Arbustini E, Grasso M, et al. 1997. Hereditary hyperferritinemia-cataract syndrome: relationship between phenotypes and specific mutations in the iron-responsive element of ferritin light-chain mRNA. *Blood* 90: 814-21

Cazzola M, Foglieni B, Bergamaschi G, Levi S, Lazzarino M, Arosio P. 2002. A novel deletion of the L-ferritin iron-responsive element responsible for severe hereditary hyperferritinaemia-cataract syndrome. *Br J Haematol* 116: 667-70

Cazzola M, Invernizzi R, Bergamaschi G, Levi S, Corsi B, et al. 2003. Mitochondrial ferritin expression in erythroid cells from patients with sideroblastic anemia. *Blood* 101: 1996-2000

Charlesworth A, Georgieva T, Gospodov I, Law JH, Dunkov BC, et al. 1997. Isolation and properties of Drosophila melanogaster ferritin--molecular cloning of a cDNA that encodes one subunit, and localization of the gene on the third chromosome. *Eur J Biochem* 247: 470-5

Chasteen ND. 1998. Ferritin. Uptake, storage, and release of iron. *Met Ions Biol Syst* 35: 479-514

Chasteen ND, Harrison PM. 1999. Mineralization in ferritin: an efficient means of iron storage. *J Struct Biol* 126: 182-94

Cheah JH, Kim SF, Hester LD, Clancy KW, Patterson SE, 3rd, et al. 2006. NMDA receptor-nitric oxide transmission mediates neuronal iron homeostasis via the GTPase Dexras1. *Neuron* 51: 431-40

Chen H, Su T, Attieh ZK, Fox TC, McKie AT, et al. 2003. Systemic regulation of Hephaestin and Ireg1 revealed in studies of genetic and nutritional iron deficiency. *Blood* 102: 1893-9

Claros MG. 1995. MitoProt, a Macintosh application for studying mitochondrial proteins. *Comput Appl Biosci* 11: 441-7

Claros MG, Vincens P. 1996. Computational method to predict mitochondrially imported proteins and their targeting sequences. *Eur J Biochem* 241: 779-86

Cornell RM, Giovanoli Rudolf, Schneider Walter 1989. Review of the hydrolysis of iron(III) and the crystallization of amorphous iron(III) hydroxide hydrate. *Journal of Chemical Technology & Biotechnology* 46: 115-34

Corsi B, Cozzi A, Arosio P, Drysdale J, Santambrogio P, et al. 2002. Human mitochondrial ferritin expressed in HeLa cells incorporates iron and affects cellular iron metabolism. *J Biol Chem* 277: 22430-7

Cowley JM, Janney DE, Gerkin RC, Buseck PR. 2000. The structure of ferritin cores determined by electron nanodiffraction. *J Struct Biol* 131: 210-6

Cozzi A, Santambrogio P, Corsi B, Campanella A, Arosio P, Levi S. 2006. Characterization of the l-ferritin variant 460InsA responsible of a hereditary ferritinopathy disorder. *Neurobiol Dis* 23: 644-52

Cragg SJ, Wagstaff M, Worwood M. 1981. Detection of a glycosylated subunit in human serum ferritin. *Biochem J* 199: 565-71

Crichton RR, Charloteaux-Wauters M. 1987. Iron transport and storage. *Eur J Biochem* 164: 485-506

Crichton RR, Wilmet S, Legssyer R, Ward RJ. 2002. Molecular and cellular mechanisms of iron homeostasis and toxicity in mammalian cells. *J Inorg Biochem* 91: 9-18

Crompton DE, Chinnery PF, Bates D, Walls TJ, Jackson MJ, et al. 2005. Spectrum of movement disorders in neuroferritinopathy. *Mov Disord* 20: 95-9

Crompton DE, Chinnery PF, Fey C, Curtis AR, Morris CM, et al. 2002. Neuroferritinopathy: a window on the role of iron in neurodegeneration. *Blood Cells Mol Dis* 29: 522-31

Curtis AR, Fey C, Morris CM, Bindoff LA, Ince PG, et al. 2001. Mutation in the gene encoding ferritin light polypeptide causes dominant adult-onset basal ganglia disease. *Nat Genet* 28: 350-4

D'Souza J, Cheah PY, Gros P, Chia W, Rodrigues V. 1999. Functional complementation of the malvolio mutation in the taste pathway of Drosophila melanogaster by the human natural resistance-associated macrophage protein 1 (Nramp-1). *J Exp Biol* 202: 1909-15

De Domenico I, Ward DM, Langelier C, Vaughn MB, Nemeth E, et al. 2007. The Molecular Mechanism of Hepcidin-mediated Ferroportin Down-Regulation. *Mol Biol Cell* 18: 2569-78

Dorner MH, Silverstone A, Nishiya K, de Sostoa A, Munn G, de Sousa M. 1980. Ferritin synthesis by human T lymphocytes. *Science* 209: 1019-21

Drysdale J, Arosio P, Invernizzi R, Cazzola M, Volz A, et al. 2002. Mitochondrial ferritin: a new player in iron metabolism. *Blood Cells Mol Dis* 29: 376-83

Drysdale J, Dugast I, Papadopoulos P, Zappone E. 1991. Intracellular iron metabolism. *Curr Stud Hematol Blood Transfus*: 148-52

Dunkov B, Georgieva T. 2006. Insect iron binding proteins: insights from the genomes. *Insect Biochem Mol Biol* 36: 300-9
Dunkov BC, Georgieva T. 1999. Organization of the ferritin genes in Drosophila melanogaster. *DNA Cell Biol* 18: 937-44
Dunkov BC, Georgieva T, Yoshiga T, Hall M, Law JH. 2002. Aedes aegypti ferritin heavy chain homologue: feeding of iron or blood influences message levels, lengths and subunit abundance. *J Insect Sci* 2: 7
Dunn LL, Rahmanto YS, Richardson DR. 2007. Iron uptake and metabolism in the new millennium. *Trends Cell Biol* 17: 93-100
Evans CA, Harbuz MS, Ostenfeld T, Norrish A, Blackwell JM. 2001. Nramp1 is expressed in neurons and is associated with behavioural and immune responses to stress. *Neurogenetics* 3: 69-78
Feder JN, Penny DM, Irrinki A, Lee VK, Lebron JA, et al. 1998. The hemochromatosis gene product complexes with the transferrin receptor and lowers its affinity for ligand binding. *Proc Natl Acad Sci U S A* 95: 1472-7
Ferguson CJ, Wareing M, Ward DT, Green R, Smith CP, Riccardi D. 2001. Cellular localization of divalent metal transporter DMT-1 in rat kidney. *Am J Physiol Renal Physiol* 280: F803-14
Ferreira C, Bucchini D, Martin ME, Levi S, Arosio P, et al. 2000. Early embryonic lethality of H ferritin gene deletion in mice. *J Biol Chem* 275: 3021-4
Fleming MD, Romano MA, Su MA, Garrick LM, Garrick MD, Andrews NC. 1998. Nramp2 is mutated in the anemic Belgrade (b) rat: evidence of a role for Nramp2 in endosomal iron transport. *Proc Natl Acad Sci U S A* 95: 1148-53
Fleming MD, Trenor CC, 3rd, Su MA, Foernzler D, Beier DR, et al. 1997. Microcytic anaemia mice have a mutation in Nramp2, a candidate iron transporter gene. *Nat Genet* 16: 383-6
Fleming RE, Ahmann JR, Migas MC, Waheed A, Koeffler HP, et al. 2002. Targeted mutagenesis of the murine transferrin receptor-2 gene produces hemochromatosis. *Proc Natl Acad Sci U S A* 99: 10653-8
Fleming RE, Migas MC, Holden CC, Waheed A, Britton RS, et al. 2000. Transferrin receptor 2: continued expression in mouse liver in the face of iron overload and in hereditary hemochromatosis. *Proc Natl Acad Sci U S A* 97: 2214-9
Folwell JL, Barton CH, Shepherd D. 2006. Immunolocalisation of the D. melanogaster Nramp homologue Malvolio to gut and Malpighian tubules provides evidence that Malvolio and Nramp2 are orthologous. *J Exp Biol* 209: 1988-95
Food MR, Richardson DR. 2002. Iron uptake by melanoma cells from the soluble form of the transferrin homologue, melanotransferrin. *Redox Rep* 7: 279-82
Food MR, Sekyere EO, Richardson DR. 2002. The soluble form of the membrane-bound transferrin homologue, melanotransferrin, inefficiently donates iron to cells via nonspecific internalization and degradation of the protein. *Eur J Biochem* 269: 4435-45
Forbes JR, Gros P. 2003. Iron, manganese, and cobalt transport by Nramp1 (Slc11a1) and Nramp2 (Slc11a2) expressed at the plasma membrane. *Blood* 102: 1884-92
Galatro A, Puntarulo S. 2007. Mitochondrial ferritin in animals and plants. *Front Biosci* 12: 1063-71
Ganz T. 2005. Cellular iron: ferroportin is the only way out. *Cell Metab* 1: 155-7

Ganz T, Nemeth E. 2006. Regulation of iron acquisition and iron distribution in mammals. *Biochim Biophys Acta* 1763: 690-9

Gao Q, Yuan B, Chess A. 2000. Convergent projections of Drosophila olfactory neurons to specific glomeruli in the antennal lobe. *Nat Neurosci* 3: 780-5

Garate MA, Nunez MT. 2000. Overexpression of the ferritin iron-responsive element decreases the labile iron pool and abolishes the regulation of iron absorption by intestinal epithelial (Caco-2) cells. *J Biol Chem* 275: 1651-5

Garrick LM, Dolan KG, Romano MA, Garrick MD. 1999. Non-transferrin-bound iron uptake in Belgrade and normal rat erythroid cells. *J Cell Physiol* 178: 349-58

Garrick MD, Singleton ST, Vargas F, Kuo HC, Zhao L, et al. 2006. DMT1: which metals does it transport? *Biol Res* 39: 79-85

Geiser DL, Chavez CA, Flores-Munguia R, Winzerling JJ, Pham DQ. 2003. Aedes aegypti ferritin. *Eur J Biochem* 270: 3667-74

Georgieva T, Dunkov BC, Dimov S, Ralchev K, Law JH. 2002. Drosophila melanogaster ferritin: cDNA encoding a light chain homologue, temporal and tissue specific expression of both subunit types. *Insect Biochem Mol Biol* 32: 295-302

Georgieva T, Dunkov BC, Harizanova N, Ralchev K, Law JH. 1999. Iron availability dramatically alters the distribution of ferritin subunit messages in Drosophila melanogaster. *Proc Natl Acad Sci U S A* 96: 2716-21

Ghosh S, Hevi S, Chuck SL. 2004. Regulated secretion of glycosylated human ferritin from hepatocytes. *Blood* 103: 2369-76

Girelli D, Corrocher R, Bisceglia L, Olivieri O, Zelante L, et al. 1997. Hereditary hyperferritinemia-cataract syndrome caused by a 29-base pair deletion in the iron responsive element of ferritin L-subunit gene. *Blood* 90: 2084-8

Goessling LS, Mascotti DP, Thach RE. 1998. Involvement of heme in the degradation of iron-regulatory protein 2. *J Biol Chem* 273: 12555-7

Goldstein L, Teng ZP, Zeserson E, Patel M, Regan RF. 2003. Hemin induces an iron-dependent, oxidative injury to human neuron-like cells. *J Neurosci Res* 73: 113-21

Gonnet GH, Cohen MA, Benner SA. 1994. Analysis of amino acid substitution during divergent evolution: the 400 by 400 dipeptide substitution matrix. *Biochem Biophys Res Commun* 199: 489-96

Gray NK, Pantopoulos K, Dandekar T, Ackrell BA, Hentze MW. 1996. Translational regulation of mammalian and Drosophila citric acid cycle enzymes via iron-responsive elements. *Proc Natl Acad Sci U S A* 93: 4925-30

Gruenheid S, Canonne-Hergaux F, Gauthier S, Hackam DJ, Grinstein S, Gros P. 1999. The iron transport protein NRAMP2 is an integral membrane glycoprotein that colocalizes with transferrin in recycling endosomes. *J Exp Med* 189: 831-41

Gunshin H, Allerson CR, Polycarpou-Schwarz M, Rofts A, Rogers JT, et al. 2001. Iron-dependent regulation of the divalent metal ion transporter. *FEBS Lett* 509: 309-16

Gunshin H, Fujiwara Y, Custodio AO, Direnzo C, Robine S, Andrews NC. 2005a. Slc11a2 is required for intestinal iron absorption and erythropoiesis but dispensable in placenta and liver. *J Clin Invest* 115: 1258-66

Gunshin H, Mackenzie B, Berger UV, Gunshin Y, Romero MF, et al. 1997. Cloning and characterization of a mammalian proton-coupled metal-ion transporter. *Nature* 388: 482-8

Gunshin H, Starr CN, Direnzo C, Fleming MD, Jin J, et al. 2005b. Cybrd1 (duodenal cytochrome b) is not necessary for dietary iron absorption in mice. *Blood* 106: 2879-83

Han O, Kim EY. 2007. Colocalization of ferroportin-1 with hephaestin on the basolateral membrane of human intestinal absorptive cells. *J Cell Biochem* 101: 1000-10

Harrison PM, Arosio P. 1996. The ferritins: molecular properties, iron storage function and cellular. *Biochimica et biophysica acta* 1275: 161-203

Hayflick SJ. 2003. Unraveling the Hallervorden-Spatz syndrome: pantothenate kinase-associated neurodegeneration is the name. *Curr Opin Pediatr* 15: 572-7

Hentze MW, Caughman SW, Casey JL, Koeller DM, Rouault TA, et al. 1988. A model for the structure and functions of iron-responsive elements. *Gene* 72: 201-8

Hentze MW, Caughman SW, Rouault TA, Barriocanal JG, Dancis A, et al. 1987. Identification of the iron-responsive element for the translational regulation of human ferritin mRNA. *Science* 238: 1570-3

Hentze MW, Kuhn LC. 1996. Molecular control of vertebrate iron metabolism: mRNA-based regulatory circuits operated by iron, nitric oxide, and oxidative stress. *Proc Natl Acad Sci U S A* 93: 8175-82

Hentze MW, Muckenthaler MU, Andrews NC. 2004. Balancing acts: molecular control of mammalian iron metabolism. *Cell* 117: 285-97

Hintze KJ, Theil EC. 2005. DNA and mRNA elements with complementary responses to hemin, antioxidant inducers, and iron control ferritin-L expression. *Proc Natl Acad Sci U S A* 102: 15048-52

Hortnagel K, Prokisch H, Meitinger T. 2003. An isoform of hPANK2, deficient in pantothenate kinase-associated neurodegeneration, localizes to mitochondria. *Hum Mol Genet* 12: 321-7

Hubert N, Hentze MW. 2002. Previously uncharacterized isoforms of divalent metal transporter (DMT)-1: implications for regulation and cellular function. *Proc Natl Acad Sci U S A* 99: 12345-50

Ikuta K, Zak O, Aisen P. 2004. Recycling, degradation and sensitivity to the synergistic anion of transferrin in the receptor-independent route of iron uptake by human hepatoma (HuH-7) cells. *Int J Biochem Cell Biol* 36: 340-52

Ishimoto H, Tanimura T. 2004. Molecular neurophysiology of taste in Drosophila. *Cell Mol Life Sci* 61: 10-8

Iwasaki K, Mackenzie EL, Hailemariam K, Sakamoto K, Tsuji Y. 2006. Hemin-mediated regulation of an antioxidant-responsive element of the human ferritin H gene and role of Ref-1 during erythroid differentiation of K562 cells. *Mol Cell Biol* 26: 2845-56

Jabado N, Jankowski A, Dougaparsad S, Picard V, Grinstein S, Gros P. 2000. Natural resistance to intracellular infections: natural resistance-associated macrophage protein 1 (Nramp1) functions as a pH-dependent manganese transporter at the phagosomal membrane. *J Exp Med* 192: 1237-48

Jeong J, Rouault TA, Levine RL. 2004. Identification of a heme-sensing domain in iron regulatory protein 2. *J Biol Chem* 279: 45450-4

Johnson MA, Kuo YM, Westaway SK, Parker SM, Ching KH, et al. 2004. Mitochondrial localization of human PANK2 and hypotheses of secondary iron accumulation in pantothenate kinase-associated neurodegeneration. *Ann N Y Acad Sci* 1012: 282-98

Johnson MB, Chen J, Murchison N, Green FA, Enns CA. 2007. Transferrin receptor 2: evidence for ligand-induced stabilization and redirection to a recycling pathway. *Mol Biol Cell* 18: 743-54

Kappler C, Meister M, Lagueux M, Gateff E, Hoffmann JA, Reichhart JM. 1993. Insect immunity. Two 17 bp repeats nesting a kappa B-related sequence confer inducibility to the diptericin gene and bind a polypeptide in bacteria-challenged Drosophila. *Embo J* 12: 1561-8

Kawabata H, Germain RS, Ikezoe T, Tong X, Green EM, et al. 2001. Regulation of expression of murine transferrin receptor 2. *Blood* 98: 1949-54

Kawabata H, Yang R, Hirama T, Vuong PT, Kawano S, et al. 1999. Molecular cloning of transferrin receptor 2. A new member of the transferrin receptor-like family. *J Biol Chem* 274: 20826-32

Kennard ML, Richardson DR, Gabathuler R, Ponka P, Jefferies WA. 1995. A novel iron uptake mechanism mediated by GPI-anchored human p97. *Embo J* 14: 4178-86

Kimura M. 1980. A simple method for estimating evolutionary rates of base substitutions through comparative studies of nucleotide sequences. *J Mol Evol* 16: 111-20

Koeller DM, Casey JL, Hentze MW, Gerhardt EM, Chan LN, et al. 1989. A cytosolic protein binds to structural elements within the iron regulatory region of the transferrin receptor mRNA. *Proc Natl Acad Sci U S A* 86: 3574-8

Koningsberger DC, Prins R. 1988. *X-ray Absorption: Principles, Applications, Techniques of EXAFS, SEXAFS and XANES*: John Wiley & Sons, New York. 673 pp.

Konopka K, Romslo I. 1981. Studies on the mechanism of pyrophosphate-mediated uptake of iron from transferrin by isolated rat-liver mitochondria. *Eur J Biochem* 117: 239-44

Kuhn LC, Hentze MW. 1992. Coordination of cellular iron metabolism by post-transcriptional gene regulation. *J Inorg Biochem* 47: 183-95

Kuo YM, Duncan JL, Westaway SK, Yang H, Nune G, et al. 2005. Deficiency of pantothenate kinase 2 (Pank2) in mice leads to retinal degeneration and azoospermia. *Hum Mol Genet* 14: 49-57

Kuo YM, Hayflick SJ, Gitschier J. 2007. Deprivation of pantothenic acid elicits a movement disorder and azoospermia in a mouse model of pantothenate kinase-associated neurodegeneration. *J Inherit Metab Dis* 30: 310-7

Kwak EL, Larochelle DA, Beaumont C, Torti SV, Torti FM. 1995. Role for NF-kappa B in the regulation of ferritin H by tumor necrosis factor-alpha. *J Biol Chem* 270: 15285-93

Laemmli UK. 1970. Cleavage of structural proteins during the assembly of the head of bacteriophage T4. *Nature* 227: 680-5

Lam-Yuk-Tseung S, Govoni G, Forbes J, Gros P. 2003. Iron transport by Nramp2/DMT1: pH regulation of transport by 2 histidines in transmembrane domain 6. *Blood* 101: 3699-707

Lam-Yuk-Tseung S, Gros P. 2006. Distinct targeting and recycling properties of two isoforms of the iron transporter DMT1 (NRAMP2, Slc11A2). *Biochemistry* 45: 2294-301

Lam-Yuk-Tseung S, Picard V, Gros P. 2006. Identification of a tyrosine-based motif (YGSI) in the amino terminus of Nramp1 (Slc11a1) that is important for lysosomal targeting. *J Biol Chem* 281: 31677-88

Landis GN, Abdueva D, Skvortsov D, Yang J, Rabin BE, et al. 2004. Similar gene expression patterns characterize aging and oxidative stress in Drosophila melanogaster. *Proc Natl Acad Sci U S A* 101: 7663-8

Lawson DM, Treffry A, Artymiuk PJ, Harrison PM, Yewdall SJ, et al. 1989. Identification of the ferroxidase centre in ferritin. *FEBS Lett* 254: 207-10

Lebron JA, West AP, Jr., Bjorkman PJ. 1999. The hemochromatosis protein HFE competes with transferrin for binding to the transferrin receptor. *J Mol Biol* 294: 239-45

Lee PL, Gelbart T, West C, Halloran C, Beutler E. 1998. The human Nramp2 gene: characterization of the gene structure, alternative splicing, promoter region and polymorphisms. *Blood Cells Mol Dis* 24: 199-215

Leonardi R, Rock CO, Jackowski S, Zhang YM. 2007. Activation of human mitochondrial pantothenate kinase 2 by palmitoylcarnitine. *Proc Natl Acad Sci U S A* 104: 1494-9

Levi S, Arosio P. 2004. Mitochondrial ferritin. *Int J Biochem Cell Biol* 36: 1887-9

Levi S, Corsi B, Bosisio M, Invernizzi R, Volz A, et al. 2001. A human mitochondrial ferritin encoded by an intronless gene. *J Biol Chem* 276: 24437-40

Levi S, Cozzi A, Arosio P. 2005. Neuroferritinopathy: a neurodegenerative disorder associated with L-ferritin mutation. *Best Pract Res Clin Haematol* 18: 265-76

Levi S, Girelli D, Perrone F, Pasti M, Beaumont C, et al. 1998. Analysis of ferritins in lymphoblastoid cell lines and in the lens of subjects with hereditary hyperferritinemia-cataract syndrome. *Blood* 91: 4180-7

Levi S, Salfeld J, Franceschinelli F, Cozzi A, Dorner MH, Arosio P. 1989. Expression and structural and functional properties of human ferritin L-chain from Escherichia coli. *Biochemistry* 28: 5179-84

Levi S, Santambrogio P, Cozzi A, Rovida E, Corsi B, et al. 1994. The role of the L-chain in ferritin iron incorporation. Studies of homo and heteropolymers. *J Mol Biol* 238: 649-54

Levi S, Yewdall SJ, Harrison PM, Santambrogio P, Cozzi A, et al. 1992. Evidence of H- and L-chains have co-operative roles in the iron-uptake mechanism of human ferritin. *Biochem J* 288 (Pt 2): 591-6

LeVine SM. 1997. Iron deposits in multiple sclerosis and Alzheimer's disease brains. *Brain Res* 760: 298-303

Levy F, Bulet P, Ehret-Sabatier L. 2004. Proteomic analysis of the systemic immune response of Drosophila. *Mol Cell Proteomics* 3: 156-66

Levy JE, Jin O, Fujiwara Y, Kuo F, Andrews NC. 1999. Transferrin receptor is necessary for development of erythrocytes and the nervous system. *Nat Genet* 21: 396-9
Lill R, Diekert K, Kaut A, Lange H, Pelzer W, et al. 1999. The essential role of mitochondria in the biogenesis of cellular iron-sulfur proteins. *Biol Chem* 380: 1157-66
Lill R, Kispal G. 2000. Maturation of cellular Fe-S proteins: an essential function of mitochondria. *Trends Biochem Sci* 25: 352-6
Lill R, Muhlenhoff U. 2005. Iron-sulfur-protein biogenesis in eukaryotes. *Trends Biochem Sci* 30: 133-41
Lin L, Goldberg YP, Ganz T. 2005. Competitive regulation of hepcidin mRNA by soluble and cell-associated hemojuvelin. *Blood* 106: 2884-9
Lind MI, Ekengren S, Melefors O, Soderhall K. 1998. Drosophila ferritin mRNA: alternative RNA splicing regulates the presence of the iron-responsive element. *FEBS Lett* 436: 476-82
Lind MI, Missirlis F, Melefors O, Uhrigshardt H, Kirby K, et al. 2006. Of two cytosolic aconitases expressed in Drosophila, only one functions as an iron-regulatory protein. *J Biol Chem* 281: 18707-14
Locke M, Leung H. 1984. The induction and distribution of an insect ferritin--a new function for the endoplasmic reticulum. *Tissue Cell* 16: 739-66
Lok CN, Loh TT. 1998. Regulation of transferrin function and expression: review and update. *Biol Signals Recept* 7: 157-78
Lok CN, Ponka P. 1999. Identification of a hypoxia response element in the transferrin receptor gene. *J Biol Chem* 274: 24147-52
Lubec G. 1996. The hydroxyl radical: from chemistry to human disease. *J Investig Med* 44: 324-46
Ludwiczek S, Theurl I, Muckenthaler MU, Jakab M, Mair SM, et al. 2007. Ca(2+) channel blockers reverse iron overload by a new mechanism via divalent metal transporter-1. *Nat Med* 13: 448-54
Lytle FW. 1989. *Experimental x-ray absorption spectroscopy, in Applications of Synchrotron Radiation*: Gordon and Breach
Mackenzie B, Ujwal ML, Chang MH, Romero MF, Hediger MA. 2006. Divalent metal-ion transporter DMT1 mediates both H+ -coupled Fe2+ transport and uncoupled fluxes. *Pflugers Arch* 451: 544-58
Mancuso M, Davidzon G, Kurlan RM, Tawil R, Bonilla E, et al. 2005. Hereditary ferritinopathy: a novel mutation, its cellular pathology, and pathogenetic insights. *J Neuropathol Exp Neurol* 64: 280-94
Mann S, Bannister JV, Williams RJ. 1986. Structure and composition of ferritin cores isolated from human spleen, limpet (Patella vulgata) hemolymph and bacterial (Pseudomonas aeruginosa) cells. *J Mol Biol* 188: 225-32
Martini LA, Tchack L, Wood RJ. 2002. Iron treatment downregulates DMT1 and IREG1 mRNA expression in Caco-2 cells. *J Nutr* 132: 693-6
Massie HR, Aiello VR, Williams TR. 1985. Iron accumulation during development and ageing of Drosophila. *Mech Ageing Dev* 29: 215-20
Massie HR, Aiello VR, Williams TR. 1993. Inhibition of iron absorption prolongs the life span of Drosophila. *Mech Ageing Dev* 67: 227-37

Maxfield FR, McGraw TE. 2004. Endocytic recycling. *Nat Rev Mol Cell Biol* 5: 121-32
McKnight GS, Lee DC, Hemmaplardh D, Finch CA, Palmiter RD. 1980a. Transferrin gene expression. Effects of nutritional iron deficiency. *J Biol Chem* 255: 144-7
McKnight GS, Lee DC, Palmiter RD. 1980b. Transferrin gene expression. Regulation of mRNA transcription in chick liver by steroid hormones and iron deficiency. *J Biol Chem* 255: 148-53
Mikulits W, Sauer T, Infante AA, Garcia-Sanz JA, Mullner EW. 1997. Structure and function of the iron-responsive element from human ferritin L chain mRNA. *Biochem Biophys Res Commun* 235: 212-6
Miller LL, Miller SC, Torti SV, Tsuji Y, Torti FM. 1991. Iron-independent induction of ferritin H chain by tumor necrosis factor. *Proc Natl Acad Sci U S A* 88: 4946-50
Missirlis F, Holmberg S, Georgieva T, Dunkov BC, Rouault TA, Law JH. 2006. Characterization of mitochondrial ferritin in Drosophila. *Proc Natl Acad Sci U S A* 103: 5893-8
Muckenthaler M, Gunkel N, Frishman D, Cyrklaff A, Tomancak P, Hentze MW. 1998. Iron-regulatory protein-1 (IRP-1) is highly conserved in two invertebrate species--characterization of IRP-1 homologues in Drosophila melanogaster and Caenorhabditis elegans. *Eur J Biochem* 254: 230-7
Nemeth E, Roetto A, Garozzo G, Ganz T, Camaschella C. 2005. Hepcidin is decreased in TFR2 hemochromatosis. *Blood* 105: 1803-6
Nemeth E, Tuttle MS, Powelson J, Vaughn MB, Donovan A, et al. 2004. Hepcidin regulates cellular iron efflux by binding to ferroportin and inducing its internalization. *Science* 306: 2090-3
Nevo Y, Nelson N. 2006. The NRAMP family of metal-ion transporters. *Biochim Biophys Acta* 1763: 609-20
Nichol H, Gakh O, O'Neill HA, Pickering IJ, Isaya G, George GN. 2003. Structure of frataxin iron cores: an X-ray absorption spectroscopic study. *Biochemistry* 42: 5971-6
Nichol H, Law JH, Winzerling JJ. 2002. Iron metabolism in insects. *Annu Rev Entomol* 47: 535-59
Nichol H, Locke M. 1990. The localization of ferritin in insects. *Tissue and Cell* 22: 767-77
Nichol H, Locke M. 1999. Secreted ferritin subunits are of two kinds in insects molecular cloning of cDNAs encoding two major subunits of secreted ferritin from Calpodes ethlius. *Insect Biochem Mol Biol* 29: 999-1013
Nichol H, Winzerling J. 2002. Structured RNA upstream of insect cap distal iron responsive elements enhances iron regulatory protein-mediated control of translation. *Insect Biochem Mol Biol* 32: 1699-710
Nicolas G, Bennoun M, Devaux I, Beaumont C, Grandchamp B, et al. 2001. Lack of hepcidin gene expression and severe tissue iron overload in upstream stimulatory factor 2 (USF2) knockout mice. *Proc Natl Acad Sci U S A* 98: 8780-5
Nicolas G, Bennoun M, Porteu A, Mativet S, Beaumont C, et al. 2002. Severe iron deficiency anemia in transgenic mice expressing liver hepcidin. *Proc Natl Acad Sci U S A* 99: 4596-601

Nie G, Sheftel AD, Kim SF, Ponka P. 2005. Overexpression of mitochondrial ferritin causes cytosolic iron depletion and changes cellular iron homeostasis. *Blood* 105: 2161-7
Nilsen T, Romslo I. 1984a. Pyrophosphate as a ligand for delivery of iron to isolated rat-liver mitochondria. *Biochim Biophys Acta* 766: 233-9
Nilsen T, Romslo I. 1984b. Transferrin as a donor of iron to mitochondria. Effect of pyrophosphate and relationship to mitochondrial metabolism and heme synthesis. *Biochim Biophys Acta* 802: 448-53
Oates PS. 2007. The role of hepcidin and ferroportin in iron absorption. *Histol Histopathol* 22: 791-804
Ohgami RS, Campagna DR, Greer EL, Antiochos B, McDonald A, et al. 2005. Identification of a ferrireductase required for efficient transferrin-dependent iron uptake in erythroid cells. *Nat Genet* 37: 1264-9
Ohgami RS, Campagna DR, McDonald A, Fleming MD. 2006. The Steap proteins are metalloreductases. *Blood* 108: 1388-94
Okubo M, Yamada K, Hosoyamada M, Shibasaki T, Endou H. 2003. Cadmium transport by human Nramp 2 expressed in Xenopus laevis oocytes. *Toxicol Appl Pharmacol* 187: 162-7
Orgad S, Nelson H, Segal D, Nelson N. 1998. Metal ions suppress the abnormal taste behavior of the Drosophila mutant malvolio. *J Exp Biol* 201: 115-20
Pantopoulos K, Mueller S, Atzberger A, Ansorge W, Stremmel W, Hentze MW. 1997. Differences in the regulation of iron regulatory protein-1 (IRP-1) by extra- and intracellular oxidative stress. *J Biol Chem* 272: 9802-8
Parkkila S, Niemela O, Britton RS, Fleming RE, Waheed A, et al. 2001. Molecular aspects of iron absorption and HFE expression. *Gastroenterology* 121: 1489-96
Petrak J, Myslivcova D, Halada P, Cmejla R, Cmejlova J, et al. 2007. Iron-independent specific protein expression pattern in the liver of HFE-deficient mice. *Int J Biochem Cell Biol* 39: 1006-15
Petrak J, Vyoral D. 2005. Hephaestin--a ferroxidase of cellular iron export. *Int J Biochem Cell Biol* 37: 1173-8
Pham DQ, Douglass PL, Chavez CA, Shaffer JJ. 2005. Regulation of the ferritin heavy-chain homologue gene in the yellow fever mosquito, Aedes aegypti. *Insect Mol Biol* 14: 223-36
Picard V, Govoni G, Jabado N, Gros P. 2000. Nramp 2 (DCT1/DMT1) expressed at the plasma membrane transports iron and other divalent cations into a calcein-accessible cytoplasmic pool. *J Biol Chem* 275: 35738-45
Pickering IJ, Prince RC, Divers T, George GN. 1998. Sulfur K-edge X-ray absorption spectroscopy for determining the chemical speciation of sulfur in biological systems. *FEBS Letters* 441: 11-4
Ponka P. 1997. Tissue-specific regulation of iron metabolism and heme synthesis: distinct control mechanisms in erythroid cells. *Blood* 89: 1-25
Ponka P. 1999. Cellular iron metabolism. *Kidney Int Suppl* 69: S2-11
Popescu BF, Pickering IJ, George GN, Nichol H. 2007. The chemical form of mitochondrial iron in Friedreich's ataxia. *J Inorg Biochem* 101: 957-66
Quintana C, Bellefqih S, Laval JY, Guerquin-Kern JL, Wu TD, et al. 2006. Study of the localization of iron, ferritin, and hemosiderin in Alzheimer's disease

hippocampus by analytical microscopy at the subcellular level. *J Struct Biol* 153: 42-54

Raje CI, Kumar S, Harle A, Nanda JS, Raje M. 2007. The macrophage cell surface glyceraldehyde-3-phosphate dehydrogenase is a novel transferrin receptor. *J Biol Chem* 282: 3252-61

Restifo LL. 2005. Mental retardation genes in drosophila: New approaches to understanding and treating developmental brain disorders. *Ment Retard Dev Disabil Res Rev* 11: 286-94

Richardson DR. 2000. The role of the membrane-bound tumour antigen, melanotransferrin (p97), in iron uptake by the human malignant melanoma cell. *Eur J Biochem* 267: 1290-8

Richardson DR, Morgan EH. 2004. The transferrin homologue, melanotransferrin (p97), is rapidly catabolized by the liver of the rat and does not effectively donate iron to the brain. *Biochim Biophys Acta* 1690: 124-33

Richardson DR, Ponka P. 1997. The molecular mechanisms of the metabolism and transport of iron in normal and neoplastic cells. *Biochim Biophys Acta* 1331: 1-40

Rock CO, Calder RB, Karim MA, Jackowski S. 2000. Pantothenate kinase regulation of the intracellular concentration of coenzyme A. *J Biol Chem* 275: 1377-83

Rodrigues V, Cheah PY, Ray K, Chia W. 1995. malvolio, the Drosophila homologue of mouse NRAMP-1 (Bcg), is expressed in macrophages and in the nervous system and is required for normal taste behaviour. *Embo J* 14: 3007-20

Roetto A, Totaro A, Piperno A, Piga A, Longo F, et al. 2001. New mutations inactivating transferrin receptor 2 in hemochromatosis type 3. *Blood* 97: 2555-60

Rouault TA. 2005. The intestinal heme transporter revealed. *Cell* 122: 649-51

Rouault TA. 2006. The role of iron regulatory proteins in mammalian iron homeostasis and disease. *Nat Chem Biol* 2: 406-14

Rouault TA, Hentze MW, Caughman SW, Harford JB, Klausner RD. 1988. Binding of a cytosolic protein to the iron-responsive element of human ferritin messenger RNA. *Science* 241: 1207-10

Shaw GC, Cope JJ, Li L, Corson K, Hersey C, et al. 2006. Mitoferrin is essential for erythroid iron assimilation. *Nature* 440: 96-100

Shayeghi M, Latunde-Dada GO, Oakhill JS, Laftah AH, Takeuchi K, et al. 2005. Identification of an intestinal heme transporter. *Cell* 122: 789-801

Sheftel AD, Zhang AS, Brown CM, Shirihai OS, Ponka P. 2007. Direct interorganellar transfer of iron from endosome to mitochondrion. *Blood* 110: 125-32

Shulman JM, Shulman LM, Weiner WJ, Feany MB. 2003. From fruit fly to bedside: translating lessons from Drosophila models of neurodegenerative disease. *Curr Opin Neurol* 16: 443-9

St Pierre TG, Bell SH, Dickson DP, Mann S, Webb J, et al. 1986. Mossbauer spectroscopic studies of the cores of human, limpet and bacterial ferritins. *Biochim Biophys Acta* 870: 127-34

St. Pierre TGS, Mann S, Webb J, Dickson DPE, Runham NW, Williams RJP. 1986. Iron Oxide Biomineralization in the Radula Teeth of the Limpet Patella vulgata; Mossbauer Spectroscopy and High Resolution Transmission Electron

Microscopy Studies. *Proceedings of the Royal Society of London. Series B, Biological Sciences* 228: 31-42
Su MA, Trenor CC, Fleming JC, Fleming MD, Andrews NC. 1998. The G185R mutation disrupts function of the iron transporter Nramp2. *Blood* 92: 2157-63
Tabuchi M, Yoshimori T, Yamaguchi K, Yoshida T, Kishi F. 2000. Human NRAMP2/DMT1, which mediates iron transport across endosomal membranes, is localized to late endosomes and lysosomes in HEp-2 cells. *J Biol Chem* 275: 22220-8
Tandy S, Williams M, Leggett A, Lopez-Jimenez M, Dedes M, et al. 2000. Nramp2 Expression Is Associated with pH-dependent Iron Uptake across the Apical Membrane of Human Intestinal Caco-2 Cells. *J Biol Chem* 275: 1023-9
Theil EC. 1990. The ferritin family of iron storage proteins. *Adv Enzymol Relat Areas Mol Biol* 63: 421-49
Theil EC. 1993. The IRE (iron regulatory element) family: structures which regulate mRNA translation or stability. *Biofactors* 4: 87-93
Theil EC. 2000. Targeting mRNA to regulate iron and oxygen metabolism. *Biochem Pharmacol* 59: 87-93
Theil EC. 2006. Integrating iron and oxygen/antioxidant signals via a combinatorial array of DNA - (antioxidant response elements) and mRNA (iron responsive elements) sequences. *J Inorg Biochem* 100: 2074-8
Theil EC. 2007. Coordinating responses to iron and oxygen stress with DNA and mRNA promoters: The ferritin story. *Biometals* 20: 513-21
Todi SV, Sharma Y, Eberl DF. 2004. Anatomical and molecular design of the Drosophila antenna as a flagellar auditory organ. *Microsc Res Tech* 63: 388-99
Touret N, Furuya W, Forbes J, Gros P, Grinstein S. 2003. Dynamic traffic through the recycling compartment couples the metal transporter Nramp2 (DMT1) with the transferrin receptor. *J Biol Chem* 278: 25548-57
Touret N, Martin-Orozco N, Paroutis P, Furuya W, Lam-Yuk-Tseung S, et al. 2004. Molecular and cellular mechanisms underlying iron transport deficiency in microcytic anemia. *Blood* 104: 1526-33
Towbin H, Staehelin T, Gordon J. 1979. Electrophoretic transfer of proteins from polyacrylamide gels to nitrocellulose sheets: procedure and some applications. *Proc Natl Acad Sci U S A* 76: 4350-4
Tran TN, Eubanks SK, Schaffer KJ, Zhou CY, Linder MC. 1997. Secretion of ferritin by rat hepatoma cells and its regulation by inflammatory cytokines and iron. *Blood* 90: 4979-86
Trinder D, Baker E. 2003. Transferrin receptor 2: a new molecule in iron metabolism. *Int J Biochem Cell Biol* 35: 292-6
Trinder D, Zak O, Aisen P. 1996. Transferrin receptor-independent uptake of differic transferrin by human. *Hepatology* 23: 1512-20
Truscott KN, Brandner K, Pfanner N. 2003. Mechanisms of protein import into mitochondria. *Curr Biol* 13: R326-37
Tsiftsoglou AS, Tsamadou AI, Papadopoulou LC. 2006. Heme as key regulator of major mammalian cellular functions: molecular, cellular, and pharmacological aspects. *Pharmacol Ther* 111: 327-45

Tsuji Y. 2005. JunD activates transcription of the human ferritin H gene through an antioxidant response element during oxidative stress. *Oncogene* 24: 7567-78
Tsuji Y, Ayaki H, Whitman SP, Morrow CS, Torti SV, Torti FM. 2000. Coordinate transcriptional and translational regulation of ferritin in response to oxidative stress. *Mol Cell Biol* 20: 5818-27
Tuil D, Vaulont S, Levin MJ, Munnich A, Moguilewsky M, et al. 1985. Transient transcriptional inhibition of the transferrin gene by cyclic AMP. *FEBS Lett* 189: 310-4
Viatte L, Lesbordes-Brion JC, Lou DQ, Bennoun M, Nicolas G, et al. 2005. Deregulation of proteins involved in iron metabolism in hepcidin-deficient mice. *Blood* 105: 4861-4
Viatte L, Nicolas G, Lou DQ, Bennoun M, Lesbordes-Brion JC, et al. 2006. Chronic hepcidin induction causes hyposideremia and alters the pattern of cellular iron accumulation in hemochromatotic mice. *Blood* 107: 2952-8
Vierstraete E, Verleyen P, Sas F, Van den Bergh G, De Loof A, et al. 2004. The instantly released Drosophila immune proteome is infection-specific. *Biochemical and Biophysical Research Communications* 317: 1052-60
Vulpe CD, Kuo YM, Murphy TL, Cowley L, Askwith C, et al. 1999. Hephaestin, a ceruloplasmin homologue implicated in intestinal iron transport, is defective in the sla mouse. *Nat Genet* 21: 195-9
Wagstaff M, Worwood M, Jacobs A. 1978. Properties of human tissue isoferritins. *Biochem J* 173: 969-77
Ward RJ, Ramsey M, Dickson DP, Hunt C, Douglas T, et al. 1994. Further characterisation of forms of haemosiderin in iron-overloaded tissues. *Eur J Biochem* 225: 187-94
Wareing M, Ferguson CJ, Delannoy M, Cox AG, McMahon RF, et al. 2003. Altered dietary iron intake is a strong modulator of renal DMT1 expression. *Am J Physiol Renal Physiol* 285: F1050-9
West AP, Jr., Bennett MJ, Sellers VM, Andrews NC, Enns CA, Bjorkman PJ. 2000. Comparison of the interactions of transferrin receptor and transferrin receptor 2 with transferrin and the hereditary hemochromatosis protein HFE. *J Biol Chem* 275: 38135-8
West AP, Jr., Giannetti AM, Herr AB, Bennett MJ, Nangiana JS, et al. 2001. Mutational analysis of the transferrin receptor reveals overlapping HFE and transferrin binding sites. *J Mol Biol* 313: 385-97
Wienk KJ, Marx JJ, Beynen AC. 1999. The concept of iron bioavailability and its assessment. *European Journal Of Nutrition* 38: 51-75
Winterbourn CC. 1995. Toxicity of iron and hydrogen peroxide: the Fenton reaction. *Toxicol Lett* 82-83: 969-74
Worwood M. 1990. Ferritin. *Blood Rev* 4: 259-69
Wu KJ, Polack A, Dalla-Favera R. 1999. Coordinated regulation of iron-controlling genes, H-ferritin and IRP2, by c-MYC. *Science* 283: 676-9
Xu H, Jin J, DeFelice LJ, Andrews NC, Clapham DE. 2004. A spontaneous, recurrent mutation in divalent metal transporter-1 exposes a calcium entry pathway. *PLoS Biol* 2: E50

Yang J, Tiong J, Kennard M, Jefferies WA. 2004. Deletion of the GPI pre-anchor sequence in human p97--a general approach for generating the soluble form of GPI-linked proteins. *Protein Expr Purif* 34: 28-48

Yang Y, Wu Z, Kuo YM, Zhou B. 2005. Dietary rescue of fumble--a Drosophila model for pantothenate-kinase-associated neurodegeneration. *J Inherit Metab Dis* 28: 1055-64

Yeung IY, Phillips E, Mann DA, Barton CH. 2004. Oxidant regulation of the bivalent cation transporter Nramp1. *Biochem Soc Trans* 32: 1008-10

Yoshiga T, Georgieva T, Dunkov BC, Harizanova N, Ralchev K, Law JH. 1999. Drosophila melanogaster transferrin. Cloning, deduced protein sequence, expression during the life cycle, gene localization and up-regulation on bacterial infection. *Eur J Biochem* 260: 414-20

Youdim MB, Riederer P. 1993. The role of iron in senescence of dopaminergic neurons in Parkinson's disease. *J Neural Transm Suppl* 40: 57-67

Zecca L, Youdim MB, Riederer P, Connor JR, Crichton RR. 2004. Iron, brain ageing and neurodegenerative disorders. *Nat Rev Neurosci* 5: 863-73

Zhang YM, Rock CO, Jackowski S. 2006. Biochemical properties of human pantothenate kinase 2 isoforms and mutations linked to pantothenate kinase-associated neurodegeneration. *J Biol Chem* 281: 107-14

Zhou B, Westaway SK, Levinson B, Johnson MA, Gitschier J, Hayflick SJ. 2001. A novel pantothenate kinase gene (PANK2) is defective in Hallervorden-Spatz syndrome. *Nat Genet* 28: 345-9

Zoller H, Pietrangelo A, Vogel W, Weiss G. 1999. Duodenal metal-transporter (DMT-1, NRAMP-2) expression in patients with hereditary haemochromatosis. *Lancet* 353: 2120-3

Zou S, Meadows S, Sharp L, Jan LY, Jan YN. 2000. Genome-wide study of aging and oxidative stress response in Drosophila melanogaster. *Proc Natl Acad Sci U S A* 97: 13726-31

Zwilling BS, Kuhn DE, Wikoff L, Brown D, Lafuse W. 1999. Role of iron in Nramp1-mediated inhibition of mycobacterial growth. *Infect Immun* 67: 1386-92

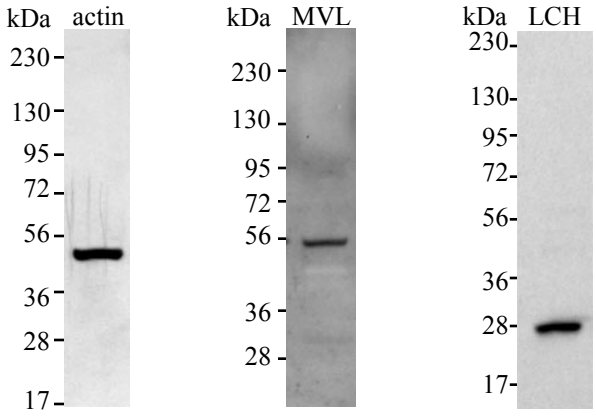

Appendix A: Antibody Specificity Testing. Western blot of lysates of whole wildtype (w1118) *Drosophila* heads showing actin ~42 kDa, MVL ~53.3 kDa, and LCH ~28 kDa.